Internal Surface Coating and Photochemical Modification of Polypropylene Microfiltration Membrane

by

Li Wang, B.Sc., M.Eng.

A Thesis

Submitted to the School of Graduate Studies

in Partial Fulfillment of the Requirements

for the Degree

Doctor of Philosophy

McMaster University

TITLE: Internal Surface Coating and Photochemical Modification of Polypropylene Microfiltration Membranes

AUTHOR: Li Wang, B.Sc. and M. Eng. (East China University of Sci. and Tech.).

SUPERVISOR: Professor J.M. Dickson

NUMBER OF PAGES: xx, 217

ABSTRACT

Membrane surface modification is of interest to most membrane scientists because the surface properties of most commercial membranes are often nonoptimal for particular applications. This thesis focuses on the further development of a thin film coating on the internal surface of polypropylene microfiltration membrane. A modified interfacial polymerization of 1,6-naphthalene disulfonylchloride containing a photoactive diazoketone (DK) group on the side chain and 1,8-octanediamine is studied. Various fabrication conditions including concentration of monomers, organic solvent selection, crosslinking agent, selection of an acid acceptor and reaction time were investigated. The choice of organic solvent was found to be critical for obtaining an even, smooth coating layer without significantly changing the membrane morphology. Mass of the polysulfonamide coating layer was typically 10-15 wt% of the base membrane. The coating layer at the membrane internal surface demonstrated a high stability to Soxhlet extracting using $CHCl_3$ for 48 hours.

A mechanism of this new type of interfacial polymerization is qualitatively proposed, and investigated experimentally. The first reported study of end-group analysis and molecular weight measurement of coating polysulfonamide provided a solid ground to evaluate the hypothesis. Most results from experiments either strongly support the proposed mechanism or can be reasonably interpreted by the proposed mechanism. The mechanistic study defines the most important principles of this new type of interfacial polymerization which can be varied to control the coating process, and gives a better understanding of this new coating technology.

General applicability of this coating technology was tested by applying this technology to polyester and polyamide. The results indicate that this new technology is generally applicable and can be used to coat condensation polymers to the internal

membrane surface as an even thin layer, without significantly changing the morphology of the polyolefin microfiltration membranes.

The chemical functionality of polysulfonamide coated membrane surface could be further modified *via* photochemical transformation of the diazoketone group contained in the coating polysulfonamide, in the presence of an appropriate medium. Thus, membranes containing indene acid, glycolic acid, bromoethyl ester, and polyethylene glycol ester functionalities were obtained. The photochemical reaction conversion was found to be approximately 80%. The highest charge density (0.097 meq/g) could be achieved on the glycolic acid ester membrane. The hydrophilicity of the membrane surface is increased by polysulfonamide coating and further increased by photochemical functionalization.

The microfiltration flux and separation performance of these membranes with polystyrene latex (PSL) and carboxylate modified latex (CML) spheres, was examined. The extent of fouling of the membranes was studied by SEM. A lower separation of PSL and a higher pure buffer flux were found for the functionalized membrane compared to the polysulfonamide coated control (DK) membrane. Pure buffer flux was increased after photochemical modification. These results suggest that the increase of hydrophilicity of the photochemically modified membranes was the dominant factor affecting the membrane separation performance. The degree of fouling of the functionalized membranes was significantly decreased which would presumably lead to an improvement of membrane effective life-time.

A remarkable change of polypropylene microfiltration membrane performance was found after the addition of Triton X-100 to the PSL feed solution. This phenomenon was explained in terms of the change of membrane surface properties. Polyethylene glycol ester membranes were introduced to mimic the membrane physically adsorbed Triton X-100. The results suggested that the Triton X-100 in the testing solution not only temporarily modified the membrane surface properties to be more hydrophillic, but also prevented the PSL particles from aggregating, particularly in the membrane pores.

ACKNOWLEDGEMENTS

I would like to express my sincere gratitude to my research supervisors, Drs J.M. Dickson and R.F. Childs, for their continued guidance, patience, encouragement and support during my study at McMaster and during my writing of this thesis.

I would like to thank Drs J. Brash and R. Pelton, my supervisory committee members, for their valuable advice and encouragement over these years.

To all members of the McMaster Membrane Research Group, thank you so much for your help and friendship. I would particularly like to thank Dr. A. Mika for her valuable suggestions and help during my study, B. Trushinski for his all technical support, and Dr. J. Ji for his suggestions, help and friendship.

Thank you also, to the Chair of Chemical Engineering Department, Dr. P.E. Wood, and staff members, Sara Gallo-O'Toole and Barb Owen for their assistance through many years.

I am very grateful to the members of the Electron Microscopy unit in the Biology Department, Mr. K. Schultes and D. Flannigan for their assistance. I would also like to acknowledge Dr. D. Gagnon (3M) for his valuable discussion during these five years.

I wish to thank The Natural Sciences and Engineering Research Council Canada (NSERC), 3M Canada Inc., and the University Research Incentive Fund (URIF) for their financial support.

Finally, I sincerely thank my wife, Ping An, for her constant support and encouragement during these years, and my parents for their moral support.

Table of Contents

List of Figures

Chapter 3

Chapter 4

List of Tables

List of Schemes

List of Abbreviations

DK	Diazoketone
NTSC	Naphthalene trisulfonyl chloride
PEG	Polyethylene glycol
PP	Polypropylene
TIPS	Thermal Induced Phase Separation
PSL	Polystyrene Latex
CML	Carboxylate Modified Latex
EDS	Energy Dispersive Spectroscopy
FTIR	Fourier Transform Infrared
NAA	Nuclear Activation Analysis
MF	Microfiltration
UF	Ultrafiltration
SEM	Scanning Electron Microscopy
TFC	Thin Film Composite
UV	Ultraviolet
B-Ester	Bromo ester
G-Acid	Glycolic Acid
I-Acid	Indene Acid
G-CON	Glycolic acid Control
I-CON	Indene acid Control
PBP	Pure Buffer Permeation
CMC	Critical Micelle Concentration

List of Symbols

Mn	Molecular weight
C_i	Initial feed concentration
C_f	Final feed concentration
C_{af}	The average of initial and final feed concentration
C_e	Permeate concentration
R_t	Total resistance
R_m	Membrane resistance
R_{if}	Internal fouling resistance
R_{ef}	External fouling resistance
γ_w	Wetting surface energy

Chapter 1

INTRODUCTION

Pressure-driven membrane processes have experienced dramatic growth in the last 30 years. The current worldwide market demand for membrane is estimated to be $1.5-2 billion, in which the demand for the three most common membrane processes, reverse osmosis, ultrafiltration, and microfiltration, is estimated to be in excess of $1.2 billion annually. Microfiltration has the largest share, approximately 30%, of this total market.

Microfiltration (MF) is an unit operation capable of removing microsize particles, typically in the range of 0.1 to 10 μm. MF can be distinguished from reverse osmosis (up to 1 nm) and ultrafiltration (1 to 100 nm) by the size of the retained particles. Further, since microfiltration membranes have no retention for salt, there is no osmotic pressure to be overcome, and filtration can be carried out at relatively low pressure, often below 350 kPa (50 psi).

Microfiltration is widely used in industry in both dead-end and crossflow modes. Dead-end MF is applied extensively in clarification, sterilisation, in laboratories etc., while the use of cross flow is increasing used in large scale industrial applications. Selection of appropriate microfiltration systems depends on the particular application and the final ultimate goal required by the user. Several examples of microfiltration in pharmaceutical, food, semiconductor and in wastewater treatment industries are briefly described, as follows.

In the pharmaceutical industry, a range of filtration and microfiltration membranes are employed to maintain product purity and product quality. Microfiltration membrane filters coupled with depth filters or surface filters provide a complete removal of all particles (including microorganisms) to a pre-established

size. By suitably combining either a depth filter or a surface filter upstream of a membrane filter, an optimum performance of retention efficiency, high dirt capacity and process economics is achievable.

Microfiltration processes are indispensable techniques in the food and beverage industry; applications where high product quality and long shelf life are required. It is estimated that over 1.3×10^5 m^2 of membrane area for microfiltration and ultrafiltration is in use world wide in the beverage industry. The use of microfiltration is generally for the retention of cellular components, microorganism and other solids from alcoholic or non-alcoholic beverages; ie., clarification and sterilisation. A wide range of materials are processed including milk, beer, wine, soft drinks, potable water, syrups and vinegar.

In the wastewater treatment industry, microfiltration is being increasingly used to treat various wastewater, such as recycle of water in the paint industry, car wash water recycling, waste effluent from olive oil production and from pulp mills. The requirement of the membranes for treatment of wastewater should include heat-resistance, a high degree of resistance to organic solvents, good cleaning potential, high mechanical strength, applicable in a wide pH range, and a long life cycle; ceramic membranes have been developed for some of these applications.

1.1 Microfiltration Membrane Material, Structure and Fabrication

Microfiltration membranes can be classified as to pore configuration into two generic types: tortuous-pore and capillary-pore. The membrane structure with tortuous-pores resembles that of a sponge with a tortuous labyrinth of pores. The membrane with capillary-pores has a well-defined, uniform pore size and low porosity. These capillary-pore membranes have found niches in specialized laboratory applications. However, most of the large-scale industrial applications

are better served by the more common type of tortuous-pore membranes. Such membranes can be fabricated by several methods: phase-inversion technology, sintering and stretching processes. Phase-inversion membranes can be solution-cast from a variety of polymers including cellulose esters, polyvinylchloride (PVC), PVC-acrylonitrile copolymer, polyamide, etc. Controlled evaporation of solvents in a humid atmosphere precipitates the polymer around residual solvents creating the open-cell porous structures. The mechanism of phase-inversion membrane has been reviewed by Kesting [1].

The sintering process to produce microporous membranes involves the pressing of a given size of particles and then heating to an elevated temperature [2]. With the correct temperature of sintering, the interface between the particles disappears to produce a porous structure. The pore size produced depends on the particle size and size distribution. The porosity of the membrane is relatively low, in the range of 10 to 20% for polymers. The sintering process is largely restricted to a polymer with a flexible configuration, and generally to substances for which alternative processes are not available.

In a stretching process [3], semicrystalline films or fibers are extruded from the melt and porosity induced by simply stretching the film/membrane in the solid state. No solvent is required. This stretching process is usually restricted to polyolefins. Polypropylene membranes made by the stretching process are among the lowest-cost membranes and are available in a large number of specialty grades.

A significant development in the technology of phase-inversion membranes (1981) was the invention of the thermal process by Castro [4], called thermal-induced phase separation (TIPS). This process is applicable to a wide range of polymers. TIPS is distinguished from the familiar non-solvent-induced phase separation in at least one important way. The homogenous solution from which

the membrane is formed is converted to a two-phase mixture *via* the removal of thermal energy rather than by the slower exchange of non-solvent for solvent [1]. The thermal process utilizes a latent solvent, a substance which is a solvent at elevated temperature and a nonsolvent at lower temperature. The reason for the incompatibility of solvent to polymer is the reduction of solvent power at the lower temperature. Most latent solvents are nonvolatile; they are removed from the final gel by extraction with a liquid which is a solvent for the latent solvent and a nonsolvent for the polymer.

The polypropylene nascent membrane studied in this thesis is manufactured by 3M *via* the TIPS method. A homogenous solution is formed by melt-blending the polypropylene and mineral oil, and the solution is casted into the desired shape. The cast solution is cooled rapidly to induce phase separation and solidification of the polymer. The mineral oil is removed by solvent extraction and then the solvents evaporated. The formed membrane is further stretched mechanically to give the desired pore size. These membranes are inexpensive and available in various pore size grades.

Polypropylene materials are hydrophobic and exhibit excellent to good chemical stability. When such materials are formed into membranes, their hydrophobic nature prevents or inhibits "wetting" by water. These membranes are easily fouled by an adsorption mechanism. Solute adsorption has the effect of reducing flux and can lead to difficulties in membrane cleaning. Most hydrophobic membranes suffer from fouling *via* the adsorption of suspended particles or colloids during the microfiltration process. Therefore, despite the low cost of preparation of such hydrophobic materials in the form of porous membranes, such membranes are not useful as membranes in aqueous systems. As well, lack of functional groups makes the polyolefin membrane less attractive in certain specialized

applications such as affinity membrane processes [5] and membrane chromatography [6]. Surface modification of such commercial polyolefin membranes can lead to increased market for the membrane and also add extra value to these inexpensive polyolefin membranes.

As a result, various modification technologies have been developed to date, such as dip-coating, plasma polymerization, radiation grafting, or *in situ* polycondensation. In a dip-coating process [7], a microporous support is immersed into a polymer or an oligomer solution. After removal from the immersion bath, a thin adherent layer is left on the membrane. Exposure of the membrane to an oven evaporates solvent and causes crosslinking which fixes the thin layer to the sublayer. Cure-treatment in an oven is not suitable for polypropylene microporous membranes, because the membrane structure can be destroyed at an elevated temperature ($\geq$ 90°C) [8]. Treatment of the surface of a hydrophobic microporous membranes made from polyolefin has been attempted using surfactant coating such as a silicone glycol copolymer or a nonionic alkyphenoxy poly(ethyleneoxy)ethanol surfactant [9]. Unfortunately, surfactant treatment to the surface of the hydrophobic material may not be permanent due to the washing away of such surface coating by water or various organic solvents. In plasma polymerization, a thin polymer layer at the external surface is generated by ionisation of gas in an electrical discharge [10]. Plasma polymerization is restricted to modifying the top surface of the membrane because of the difficulty of the plasma to penetrate into the membrane pores; similarly for most types of radiation grafting. For radiation grafting [11], the polymer membrane is immersed into a monomer bath and polymerization is initiated at radical sites which are generated by radiation. Photoinitiated grafting has been developed to fill the inside pores of microporous membranes with grafted polyelectrolytes [12]. Interfacial polymerization can

produce a thin layer at the interface of two immiscible solvents [13]. This technology has been adapted to form a thin layer *in situ* deposited on the surface of microporous support membranes [14]. *In situ* polymerized composite membranes have proven to be one of the most successful types of surface-modified membranes for reverse osmosis applications [15,16]. Such composite membranes have advantages over single-material membranes, such as cellulose acetate asymmetric membranes, because materials used for the microporous support film and for the top layer can be optimized separately to provide improved membrane performance.

1.2 Separation Mechanisms of Microfiltration Membranes

At least four different mechanisms can contribute to the performance of a MF membrane, as follows [17]: (1) particles of radius larger than the rated pore radius are "intercepted" by steric retention, (2) some particles are adsorbed on the internal and external surface due to physical attractions, (3) the particles smaller than the rated pore size may be captured by "inertial impaction" and (4) electric charge on the membrane medium can also have a profound effect on retention of charged particles due to electrostatic interactions.

All the mechanisms mentioned above could result in fouling of the membrane on the internal and external surface. A typical scenario involves the deposition of dissolved and suspended solutes on the membrane surface during the microfiltration process. These phenomena usually result in a decrease in permeation flow rate, through pore constriction and plugging and build-up of a secondary layer on the membrane surface. Membrane fouling is ultimately dependent on the membrane surface chemistry, the solute, and hydrodynamic

mixing. In order to attain technical goals, knowledge has to be combined from two separate areas: surface chemistry and membrane technology. A great deal remains to be done in the development of membranes which reduce solute adhesion. Unfortunately, information from industry is often kept confidential.

The most important criteria affecting the selection of surface properties of membrane materials are as follows [18]:

(1) Electric charge

(2) Hydrophilicity/hydrophobicity

(3) Mechanical strength

(4) Sterilizability

(5) Pore size distribution

(6) Porosity and tortuosity of membrane

(7) Cost

(8) Post-modification ability.

As a rule of thumb, hydrophillic and/or negatively charged membrane are better suited for separation of suspended and dissolved solutes from solutions because most suspended particles have a hydrophobic surface and/or a negatively charged surface. Therefore, hydrophobic membranes, such as polyolefin membranes, are particularly susceptible to fouling and should be modified before use in aqueous separation processes.

1.3 Objectives of This Thesis

For tortuous microporous membranes, such as the polypropylene TIPS microfiltration membranes, the challenge is to develop a simple technology to modify the entire membrane surface, not only the external but also internal surface, with a thin layer of the desired polymer without significantly changing the physical

structure of the membrane. A new type of internal surface coating technology, named modified interfacial polymerization, has been developed recently to meet this propose [19]. Polysulfonamide coating made from the reaction of a diamine with a photoactive monomer, 3-diazo-4-oxo-3,4-dihydro-1,6-naphthalene disulfonylchloride (DKDSC), have been successfully coated on the internal surface of microporous polypropylene membrane. The difficulty was that the synthesis of DKDSC is complicated, low yield, and time-consuming.

Ji [20] prepared and tested a similar photoactive monomer to DKDSC. The new monomer (monomer I) has a photolabile group separated by a flexible spacer arm from the polymerizable groups, synthesized 6-diazo-5-oxo-5-dihydro-naphthalenesulfonyl-chloride, piperazine and 1,3,6-naphthalene trisulfonylchloride. This synthesis process only needs two steps, and the total yield is high. This new monomer has been used to create photolabile polysulfonamide coatings on the top of polysulfone supports by polycondensation for reverse osmosis applications. [20]

The overall mission of this thesis is to evaluate this new type of internal surface coating technology using the new monomer (monomer I) instead of DKDSC, and to characterize and better understand this coating process. The mechanism involved in this new type of coating technology is hypothesised and investigated experimentally. Further functionalization of the coated membrane surface can be done by photochemical transformation in the presence of an appropriate reagent for different proposes.

According to the overall mission, the main objectives of this thesis can be categorized as follows:

(1) Evaluate the effect of each variable of the modified interfacial polymerization on the coating technology to optimize the reaction conditions for the coating technology using monomer I and octanediamine as a

monomer system.

(2) Investigate the mechanism involved in the coating process. Test all evidence obtained to either support or challenge the proposed mechanism.

(3) Generalize the applicability of the coating technology from polysulfonamide to other polymers, such as polyester and polyamide.

(4) Further functionalize the coated membrane surface with various functional groups by photochemical transformation. Determine the efficiency of each photochemical transformation. Distinguish the change of surface properties of nascent, coated and functionalized membranes.

(5) Measure the membrane separation performance using the model colloid particles with a uniform size. Search for non-specific fouling of the microporous membrane under the individual membrane with different surface properties.

(6) The effect of the surfactant (Triton X-100) involved the testing solution on the separation performance and surface properties of the nascent membrane is investigated.

In the following chapters of this thesis, Chapter 2 is focused on objective 1 which is related to evaluation of the coating technology. Chapter 3 is concentrated on the investigation of the coating mechanism and Chapter 4 is centred to the general applicability of the coating technology, objectives 2 and 3. Chapter 5 is related to photochemical functionalization of the coated membrane and its membrane separation performance which is mainly objectives 4 and 5. Chapter 6 of the thesis is focused on the change of membrane surface properties and performance due to the involvement of the surfactant into the testing solution, objective 6. The final conclusions and recommendations are included in Chapter 7 of this thesis. Chapter 2-6 are written as papers for submission to journals.

References

[1] R.E. Kesting, Synthetic Polymeric Membrane, Second Edition, John Wiley & Sons, New York, 1985.

[2] C. Herring, Effect of change of scale on sintering phenomena, J. Appl. Phys., 21 (1950) 301-306.

[3] R. Gore, U.S. Patent, 3,953,566, 3,962,153 (1976)

[4] A. Castro, U.S. Patent, 4,247,498 (1981)

[5] K.B. Male, A.L. Nguyen, and J.H. Luong, Isolation of urokinase by affinity ultrafiltration, Biotechnology and Bioengineering, 35 (1990) 87-93.

[6] J. Thommes and M.R. Kula, Membrane chromatography-An integrative concept in the downstream processing of proteins, Biotechnology Progress, 11 (1995) 357-367.

[7] H.K. Londale, R.L. Riley, C.R. Lyons and O.P. Carosella, Membrane Process in Industry and Biomedicine, M. Bier (Ed.), Plenum Press, New York, 1971, p. 101.

[8] I. Dolgopolsky, Master Thesis, Department of Chemical Engineering, McMaster University, 1996.

[9] Membrane & Separation Technology News, April 1996.

[10] H. Yasuda and H.C. Marsh, Preparation of composite reverse osmosis membranes by plasma polymerization of organic compounds. IV. Influence of plasma-polymer interaction. J. Appl. Polym. Sci., 20 (1976) 543.

[11] Y. Ogiwara, M. Takumi and H. Kubota, Photointroduced grafting of acrylamide onto polyethlene films by means of two step method, J. Appl. Polym. Sci., 35 (1982) 3743.

[12] A.M. Mika, R.F. Childs, J.M. Dickson, B.E. McCarry and D.R. Gagnon,

A new class of polyelectrolyte-filled microfiltration membranes with environmentally controlled porosity, J. Membrane Sci., 108 (1995) 37-56.

[13] P.W. Morgan and S.L. Kwolek, Interfacial polycondensation. II. Fundamentals of polymer formation at liquid interfaces. J. Polym. Sci., XL (1959) 299-327.

[14] J.E. Cadotte, U.S. Patent, 3,926,798, 1985.

[15] L.T. Rozelle, J.E. Cadotte, K.E. Cobian and C.V. Kopp, Nonpolysaccharide membranes for reverse osmosis: NS-100 membranes for reverse osmosis and synthetic membranes, S. Sourirajan (Ed.), National Research Council Canada, Ottawa, Canada, 1977, p. 249.

[16] J.E. Cadotte, R.J. Petersen, R.E. Larson and E.E. Erickson, A new thin film composite seawater reverse osmosis membrane, Desalination, 32 (1980) 25.

[17] M.C. Porter, Synthetic Membranes. Science, Engineering and Application, P.M. Bungay (Ed.), D. Reidel Publishing, 1986, p. 234.

[18] D. Defrise and V. Gekas, Microfiltration membranes and the problem of microbial adhesion, Process Biochemistry, August 1988.

[19] J.M. Dickson, K. Rilling, R.F. Childs, B.E. McCarry and D.R. Gagnon, Development of a functionalized thin film composite coating for the internal structure of polypropylene microfiltration membrane, to be submitted, J. Membrane Sci., (1997).

[20] J. Ji, B.J. Trushinski, R.F. Childs, J.M. Dickson, and B.E. McCarry, Fabrication of thin film composite membranes with pendant, photoreactive diazoketone functionality, accepted, J. Appl. Polym. Sci., 1996.

Chapter 2

Coating the Internal Surface of Polypropylene Microfiltration Membrane by Modified Interfacial Polymerization. Part I: Coating Technology.

ABSTRACT

By means of a modified interfacial polycondensation, a coating of polysulfonamide containing a pendent photoactive group can be formed on the internal surface of a microporous polypropylene membrane. Various fabrication conditions including concentration of monomers, organic solvent selection, polymerization time, crosslinking agent, and addition of acid acceptors were investigated. The strength of solvent was critical for obtaining good coatings. By adjusting the above parameters, an even, smooth coating was obtained on the internal surface of the polypropylene membrane. Mass gain of the coating layer was around 10 to 12%. Surface morphology of the coated membranes was analyzed by SEM. The coating was stable as demonstrated by Soxhlet extraction of the coated membrane. The chemical composition of the coating layer was characterized by FT-IR.

Keywords: Modified interfacial polymerization, Coating, Polysulfonamide, Internal surface, Microfiltration membrane.

Introduction

Membrane surface modification is of interest to membrane scientists because the surface properties of most commercial membranes are often nonoptimal for particular applications. General methods for membrane surface modification have been reviewed by Cadotte [1]. Interfacial polymerization of reactive monomers on the surface of the support layer has already proven to be a good approach to making composite reverse osmosis membranes [2].

A variety of efforts have been made on surface modification by interfacial polymerization. For example, Whitfield [3-5] pointed out that an ultrathin coating of polyamide and various copolymers can be formed on the surface of wool fibre by interfacial polymerization to protect the wool fibre from shrinkage through scouring. Instead of placing the two immiscible solutions in direct contact, they first applied one solution to the surface of the substrate, then dipped the substrate into the second solution, forming an ultrathin film of the polymer on the surface of the substrate. Various polymers including polyamide, polyester, polyurea and polyurethane were investigated. The improvement of fiber resistance to felting shrinkage during laundering was achieved with as little as 1% or 2% polymer coating. Recently, Loh [6] reported that a microporous polypropylene membrane can be coated by an intrinsically conducting polymer, such as polyaniline or polypyrrole, using a similar coating process. They successfully demonstrated the ability to obtain a stable conductivity with the coated polymer membrane. The weight gain of the coated membranes varied from 2 to 17% depending on the coating conditions.

The polypropylene microfiltration membranes used in this work were formed by the thermally induced phase separation (TIPS) process [7], followed by biaxial stretching. The physical structure of the membrane consists of nodules and fibrils of the polymer material separated by large void spaces. Such membranes are mechanically strong. Modification of the internal surface of this kind of membrane without a significant change in the physical structure is difficult due to the incompatibility of the polyolefin base with most coating materials.

In previous work [8,9] of our research group, modified interfacial polymerization has been employed to coat the internal surface of polypropylene microfiltration membranes using the monomer system, 1,5-naphthalene disulfonylchloride and octanediamine. Optimum reaction conditions of the coating process for this monomer system were found by fractional factorial design [8]. The coating polymer, a diamine with 3-diazo-4-oxo-3,4-dihydro-1,6-naphthalene disulfonyl chloride (DKDSC), containing a photoactive group (diazoketone) attached to the polymer backbone was developed for use as a top surface coating on a microporous support membrane [10]. This photoactive polymer was also coated on the internal surface of polypropylene MF membranes by modified interfacial polymerization [8,9]. Further functionalization of this photoactive coated polymer was done by photochemically converting the diazoketone to various functional groups in the presence of various reagents. The simplest functionalized membrane was a carboxylic acid-modified membrane (ACID) made by irradiating the DKDSC coated membrane in water. Flux and separation performance of these membranes were evaluated using polystyrene latex (PSL) or carboxylate modified latex (CML) as probe solutes. Significant differences between the nascent and modified membrane were observed [9]. The ACID membrane with carboxylic acid

functionality was not found to have a greater rejection of CML due to electrostatic repulsion than the DKDSC coated membrane.

The objectives in this chapter are to further investigate this internal surface coating technology based on another monomer system, octanediamine and monomer I (see Scheme 1), which contains a pendent photoactive group (diazoketone) [11]. The reason to replace DKDSC with monomer I is that synthesis of monomer I is less complicated than DKDSC and has a higher yield (around 90%). Analogous to the previous work [8,9], a membrane coated by these polysulfonamides can be photochemically modified to different functionalities. Since one of the monomers is changed, all reaction parameters should be reevaluated. Reaction conditions for the new monomers are optimized to obtain a thin, smooth coating layer which modified the internal surface of the polypropylene microfiltration membranes without significantly changing the physical structure. Also, the stability and the chemical composition of the new coating polymer were examined by Soxhlet extraction and FT-IR, respectively.

2.1 Experimental

2.1.1 Materials

Chemicals

Monomer I (disulfonyl chloride) was synthesised in our laboratory according to the method described elsewhere [11]. Monomer I can have three isomers (see Appendix 1). Scheme 1 shows one of the three possible monomer I isomers. Octanediamine, methanol, dichloromethane, carbon tetrachloride, pyridine, and triethylamine were purchased from Aldrich Co.; all reagents were analytical grade. 1,3,6-naphthalene trisulfonylchloride (NTSC) was synthesised as stated previously [12].

Microfiltration membrane

The polypropylene (PP) microfiltration membrane, from 3M Company, has good mechanical properties, chemical stability, and symmetric pore structure. The porosity of the membrane is around 80 % and the maximum pore size is around 1 μm, measured by the bubble point method [8].

2.1.2 Modified interfacial polymerization/coating process

The membrane was immersed in octanediamine solution (20 wt%) for five minutes, dried for 60 minutes at room temperature, and then soaked in a 1.4 mmol/L (1 g/L) monomer I solution for 1 h at 30°C. The experimental details are presented in Appendix A-3. Reaction and polymerization (see Scheme 1) occurred inside the pores of the membrane and in the bulk solution. Finally, the membrane was washed in dichloromethane and methanol for three cycles of three minutes each. The whole process is summarized in Figure 1.

2.1.3 Mass gain and surface morphology

Mass gain is defined as follows:

$$Mass\ Gain = \frac{(wt.\ of\ coated\ memb.) - (wt.\ of\ nascent\ memb.)}{(wt.\ of\ nascent\ memb.)} \times 100\%$$

The surface morphology of the coating layer was studied by scanning electron microscopy (SEM). Any changes of the membrane microporous structure and surface morphology caused by the modified interfacial polymerization could be observed *via* SEM. The SEM studies were conducted on a ISI-DS300 (PGT Model System 4000). The experimental details are in Appendix A-4.

2.1.4 Coating layer compositions

The chemical composition of the coating layer was evaluated using FT-IR (Biorad-Digilab FTS-40) after squeezing a piece of membrane to a thin, dense film in a die. The details of FT-IR analysis see Appendix A-5. The Sulphur elemental concentration profile on the membrane cross section was analyzed using energy dispersive analyzer (EDS), PGT Model System 4000. The experimental details see Appendix A-4.

2.1.5 Stability

Durability of the coating layer was estimated by performing Soxhlet extraction on the membrane for 48 h using $CHCl_3$, which is a good solvent for the unreacted monomer and the low molecule weight polymer formed in the coating process. The details of stability study are presented in Appendix A-6.

2.2 Results and Discussion

Monomer concentrations, selection of solvent, polymerization time, crosslinking agent and acid acceptors, are the main factors affecting conventional interfacial polymerization [13] and also affecting the fabrication of thin film composite reverse osmosis membranes [14]. The major difference between conventional and modified interfacial polymerization is as follows. In conventional interfacial polycondensation, two immiscible liquid phases are brought into contact directly. In modified interfacial polymerization, as previously described [8,9], one monomer is dried as a solid layer covering the internal surface of the polypropylene support membrane and the second monomer is in an organic phase.

The membrane with dried diamine coated layer is brought into contact with the organic phase. The reaction mechanism, at the molecular level, for these two methods may be totally different. To optimize reaction conditions to obtain a good coating on the membrane internal surface, and to better understand the mechanism of the coating polymerization process, the effects of factors mentioned above upon modified interfacial polymerization were studied in this Chapter. All data presented in the following sections are the average of three membrane samples. These three nascent membrane samples were cut at same size from one roll of PP microfiltration membrane, and coated individually by polysulfonamide under identical coating polymerization conditions within one day. The same coating polymerization performed on the membrane samples cut from other section of same roll of PP membrane on another day has been observed with a deviation of mass gain of coated polysulfonamide of approximately 1-1.5%. The detailed experimental results are presented in Appendix B.

2.2.1 Effect of concentration of monomer I.

Monomers used in this chapter were monomer I and octanediamine (see Scheme 1). The mass gain of octanediamine loaded on the membrane surface was dependent on the diamine concentration. Approximately 20% mass gain of octanediamine loading was achieved after a nascent membrane was dipped into the octanediamine solution (20 g/L) for 5 minutes. The mass gain of coating polymer was increased by increasing the concentration of monomer I in CH_2Cl_2 (Figure 2). With increasing monomer I concentration, more polymer was produced within a certain time leading to a larger mass gain of coating polymer probably due to an increased reaction rate. A maximum of approximately 22% mass gain was obtained when the concentration of monomer I was 0.014 mol/L (10 g/L). The

morphologies of the corresponding coated membranes were investigated by SEM, as illustrated in Figure 3. The SEMs presented in this chapter or the following chapters are the top view of the membrane surface since there is no significant difference between the top and bottom surfaces of the coated membrane. Rather than a smooth, even coating as desired, the coating surface resembled small spherical particles fused together sticking on the fibrils and nodules. The number of small particles increased with increasing monomer I concentration forming a multilayer of fused particles. Consistent with the general coating principles found previously [8,9], there were two effects which caused such a behaviour. (1) Diamine solubility was increased by the increased strength of the organic solvent. The good solvent extracted the diamine loaded on the fibrils rapidly into the organic phase so that the polymerization occurred mostly in the bulk solution. (2) The oligomer (growing polymer) was more soluble in a strong (polar) solvent, and a polymer with higher molecular weight was produced [15]. Because dichloromethane is a good solvent for both monomer I and oligomer [16,17], polymer was formed away from the fibril surface and was dispersed rather than precipitated onto the fibrils and nodules. When precipitation occurred in a strong solvent, polymer, which was already as large as a small bead, adhered to the fibril or nodule surface at random and the layer built up, as depicted in Figure 3. To prevent this bulk polymerization and massive precipitation, weaker solvents were investigated.

2.2.2 Selection of solvent

Solvent strength was reduced by adding CCl_4 into CH_2Cl_2. The results, illustrated in Figure 4, indicated that the mass gain slowly increased with an increased volume percentage of CCl_4 in the solvent mixture. When the ratio was

greater than 45/55 (CCl_4/CH_2Cl_2), mass gain increased more rapidly until 60/40, where it reached a plateau. The highest mass gain could be achieved at the volume ratio 60/40 (CCl_4/CH_2Cl_2). However, the coating layer obtained under this condition appeared to be uneven (Figure 5h). The optimum coating layer should be a smooth, even coating with a relative high (>10%) mass gain. All membranes plotted in Figure 4 were examined by SEM (Figure 5). When the polymerization medium was pure CH_2Cl_2, the surface coating layer morphology was rough, with many small beads formed by polymerization sticking on the membrane nodules and fibrils, and the membrane internal surface was only partially covered by coating polymer (Figure 5b). When CCl_4 was added to the medium to at the volume ratio 30/70 (CCl_4/CH_2Cl_2), the surface coating layer became smooth with no small beads. The membrane surface appeared to be completely covered by the coating polymer (Figure 5c). Upon further increase of the volume ratio to 40/60 and 45/55, the coating layer became more even and smooth, Figures 5d and 5e, respectively. At the volume ratio range from 50/50 to 60/40, surface coating layer morphologies became less uniform and some lumps formed by coating polymer were observed (Figures 5f, 5g, 5h). When the volume ratio reached 80/20, the membrane coating surface presented a messy morphology with fine powders scattered all over the membrane internal surface. According to Figures 4 and 5, the membrane with smoothest coating and relative high mass gain was attained at 45/55 (CCl_4/CH_2Cl_2) solvent ratio. These results indicated that solvent strength was critical to obtaining a smooth, tailored coating layer. The mechanism of this new type of interfacial polymerization is discussed in Chapter 3.

2.2.3 Effect of diamine concentration

After a suitable solvent for this coating process was selected, the effect of

the amount of diamine loaded on the membrane internal surface was investigated. The first step of the coating process, deposition of octanediamine on the polypropylene support membranes as shown in Figure 1, is important for the modified interfacial polymerization because this step determines how much diamine is available for polymerization. Methanol as a solvent quickly wetted the polypropylene membrane surface and delivered octanediamine into the membrane pores instantaneously. After drying the wetted membrane at room temperature, the SEM, presented in Figure 6, illustrated that the deposition layer of octanediamine on the membrane internal surface was homogenous and smooth, since there was little difference found between the surface morphology of the nascent membrane and the octanediamine deposited membrane. Also, the mass gain of octanediamine deposition was proportional to the diamine concentration in methanol, as revealed in Figure 7. The effect of diamine on the coating process is studied based on the mass gain of diamine deposition on the membrane surface.

The dependence of the mass gain of coating polysulfonamide on the amount of octanediamine deposition, in the absence of crosslinking agent, where excess diamine acts as an acid acceptor to neutralize the HCl produced during the reaction, is illustrated in Figure 8. Since the acid acceptor reaction is faster than sulfonamide formation, no more than one half of the amine groups could be acylated. The mass gain of coating polysulfonamide initially increases significantly with an increase in the amount of octanediamine loaded on the membrane internal surface. When the mass gain of octanediamine deposition exceeded approximately 27 wt% (Figure 8), the mass gain of coating polymer levelled off at 14-15 wt%. Examining the SEM's (Figure 9) revealed that the coating surface morphology was even and smooth at a lower diamine deposition (10-20 wt%). When the diamine deposition reached approximately 36 wt%, the coating surface became moderately

rough with agglomerated polymer sticking on the membrane surface. A similar behaviour was found by Varelidis et al. [18] for coating a polyamide on the carbon fiber using interfacial polymerization. They claimed that the mass of polymer coating is very sensitive to the diamine concentration in a coating process in which poly(hexamethyleneadipamide) was deposited on carbon fibers by interfacial polymerization techniques. The possible explanation for this increase of coating polymer is that the increase of the amount of octanediamine deposition layer on the internal surface of polypropylene membrane can provide more diamine for polymerization.

In order to obtain a smooth surface coating layer and achieve a relatively high mass gain, 20 g/L diamine concentration, which leads to approximately 18-20% diamine mass loading, was selected as a standard coating polymerization condition for the remainder of this study.

2.2.4 Effect of polymerization time

The mass gain of coating polymer initially increased with increasing the polymerization time as shown in Figure 10. As the reaction proceeded, more octanediamine dissolved into the organic phase and participated in the polymerization, producing more coating polysulfonamide. Figure 10 shows that the mass of coating polysulfonamide slightly increases within the first 20 minutes and then significantly increases from 20 minutes to 60 minutes. Thereafter, the mass of coating polymer gradually increases and the trend eventually levels off. SEMs, presented in Figure 11, taken at different polymerization times show that the coating surface morphologies became rough when the polymerization time exceeded one hour. "Fish scale" coating surface found at a reaction time of two hours indicates precipitation of agglomerated segments of polymer formed in the

bulk organic phase. The results suggested that the polymerization time for this new type of polysulfonamide interfacial polymerization should be no longer than 120 minutes. On the other hand, polymerization time of less than 60 minutes produced the membrane with too low mass gain.

2.2.5 Effect of crosslinking agents

The effect of adding 1,3,6-naphthalene trisulfonylchloride (NTSC), as a crosslinking agent, is illustrated in Figure 12. Raising the amount of NTSC relative to monomer I slightly increased the mass gain of coating polymer, from 10% to 13%, with a NTSC/monomer I mole ratio of 9 mol% (9 moles NTSC in 100 moles monomer I). The surface morphology of the coating layer, illustrated by SEM (Figure 13), did not show any marked difference compared with an uncrossliked membrane (Figure 3a). According to conventional polycondensation, the addition of crosslinking agent should have dramatically increased the conversion of monomer into polymer product, but, the addition of NTSC into this modified interfacial polymerization did not greatly increase the mass gain. The increase, primarily due to an increase of the total concentration of functional groups (sulfonyl chloride), is consistent with the our previous results presented in the section on "Effect of concentration of monomer I". The other propose of adding a crosslinking agent into coating polymer is to improve the stability of the coating layer. Soxhlet extraction of the coating layer using chloroform as a solvent, presented in Table 1 as percent mass loss of the coating, shows that the crosslinking agent did not appear to significantly improve the stability of the coating layer. A possible explanation for this phenomenon was due in part to the different reactivity of the sulfonyl chloride groups in different positions of NTSC. Okamoto et al. [19-20] found that the reactivity of the second sulfonyl chloride in

naphthalene disulfonylchloride was ten times less than the first one. The reactivity of the third sulfonyl chloride in NTSC may be even less than the second one due to steric effects. Hence, the NTSC might act only as a difunctional monomer, not a trifunctional monomer. So far, evidence was insufficient to clearly explain this behaviour. Further investigations are needed to study the effect of the crosslinking agent on the coating process.

2.2.6 Effect of acid acceptors

In conventional interfacial polymerization [13,15], hydrogen chloride is produced and transferred to the aqueous phase where an acid acceptor, such as sodium hydroxide or sodium carbonate, neutralize hydrogen chloride to a salt. In our case, the acid acceptor was excess diamine in the organic phase. The amine hydrochloride was not an acylatable species and was usually insoluble in the organic phase. Since the acid acceptor reaction was faster than sulfonamide formation, only half of the amine groups could be acylated. Adding an acid acceptor should affect the polymerization process and allow more diamine to be available for polymerization.

The dependence of mass gain on the addition of pyridine or triethylamine as an acid acceptor without a crosslinking agent is illustrated in Figure 14. The mass gain was increased in the presence of triethylamine, but was unchanged when pyridine was added. The difference between the two acid acceptors can be understood in terms of base strength of the organic acid acceptor. Triethylamine (pK_b=3.4) has the same basic strength as the octanediamine (pK_b=3.6), whereas pyridine (pK_b=9.3) is much weaker [21]. Therefore, triethylamine could compete with octanediamine and replace it as an acid acceptor. These results were

consistent with Morgan [22], who claimed that the basic strength of a useful acid acceptor corresponds to a pK_b=6.5 or less.

Based on stoichiometry, the moles of an acid acceptor needed to remove all HCl produced by the reaction should be twice the moles of the disulfonyl chloride. Thus, the maximum moles of triethylamine needed to neutralize all HCl should be twice the moles of monomer I in solution. However, the octanediamine itself can also act as an acid acceptor and may compete with triethylamine in the polymerization process because the base strength of triethylamine is only marginally stronger than that of octanediamine. On the other hand, the octanediamine concentration in the polymerization zone adjacent to the solid-liquid interface is much higher than that of triethylamine since the dissolved octanediamine may need time to diffuse into the organic solvent. Both factors, reactivity and concentration of the acid acceptor, should be considered in the neutralization process [22].

The mass gain was raised from 10% to 14% in the range of triethylamine/monomer I mole ratio from 0 to 2. When the mole ratio was above 2, further increase of the mass gain was insignificant. The result indicates that the reactivity is the dominate factor during the neutralization process even though the base strength of triethylamine marginally exceed the octanediamine. If triethylamine exclusively replaces the octanediamine as an acid acceptor, the amount of octanediamine as a reactant should be doubled. The mass gain of coating polymer in the presence of triethylamine at the range of mole ratio from 2 to 10, approximately 14% to 16%, was consistent to the mass gain of coating polymer (15%) with doubling the loading amount of octanediamine as shown previously in Figure 8. The surface morphology of the coated membrane made in the presence of triethylamine, as presented in Figure 15, is totally different from

that of membrane with doubling the loading amount of octanediamine. A smooth coating with a few very small beads, was observed in the presence of triethylamine at mole ratio of 10. The small beads observed in Figure 15 are probably the precipitated oligomer or polymer sticking on the fibril surface. Addition of the acid acceptor scarcely changes the solvent strength, because the added amount of the acid acceptor is very small compared to the total volume of solvent.

2.3 Evaluation of Coating Layer

The above results focused on two features of coated membranes: mass gain and surface morphology. More evidence was needed to determine if the coating layer was uniform upon the whole internal surface of the membrane. Additional membrane samples fabricated under appropriate conditions were studied to confirm that the whole internal surface was smoothly coated by polysulfonamide. The stability of the coating layer was also evaluated by Soxhlet extraction.

Colour

The visible colour of the nascent membrane and a coated membrane was different. After polymerization, the colour on the top and bottom surfaces of the coated membrane became light yellow, because the coating polymer, containing the diazoketone photoactive group was yellow. The visible change of the membrane colour is a qualitative indication of the coating on the membrane surface.

SEM EDS

In order to confirm that the whole internal surface was being coated by polysulfonamide, the sulphur concentration profile was measured by energy disperse spectra (EDS) on the membrane cross-section (Figure 16). For the

polypropylene nascent membrane, little or no sulphur was detected, as expected. For the polysulfonamide coated membrane, an even sulphur concentration profile was found across the cross-section, which indicated that the polysulfonamide had an uniform distribution across the membrane. Note that the full scale of the Y axis in Figure 16b is ten times greater than in Figure 16a). The SEM of the coated membrane cross-section (Figure 17b) showed that a smooth, even coating was added on the internal surface of the nascent membrane (Figure 17a). Results of EDS, SEM, and mass gain measurements, indicated that the coating polysulfonamide was evenly and smoothly distributed throughout the whole internal surface of the nascent membrane.

Chemical compositions

Chemical compositions of the coating layer was characterized by FT-IR (Figure 18). The IR spectra of the coated membrane showed characteristic twin peaks at 2165 cm^{-1} and 2117 cm^{-1} [10] attributed to the diazoketone group attached to the coating polymer and another peak at 1630 cm^{-1} attributed to the C=O group. None of which existed in the nascent membrane spectrum.

Durability measurement

Soxhlet extraction for 48 h was performed to test the stability of the coating layer, using $CHCl_3$, a good solvent for both monomer I and oligomer. The mass loss of nascent membranes caused by Soxhlet extraction was approximately 2% as background and subtracted from the total mass loss of the coated membrane. The results, listed in Table 1, illustrated that the coating layer was quite stable and mass loss was found to be below 7% of the total mass of the coating layer. The loss of coating layer was probably due to oligomer and/or unreacted monomer I which did

not wash off after polymerization. The addition of a crosslinking agent (NTSC) did not appear to improve the durability of the coating, as presented in Table 1. There are two possible reasons for this lack of effect: (1) the linear polysulfonamide made without crosslinking agent was stable towards $CHCl_3$ extraction since monomer I has a large, rigid molecular structure; (2) the NTSC did not act as a trifunctional monomer due to the lower reactivity of the third sulphonyl chloride group, as previously discussed. No detectable changes in the chemical compositions of the coated membranes without crosslinking was found from FT-IR spectra taken before and after Soxhlet extraction, as shown in Figure 19.

2.4 Novelty of the Coating Process.

The modified interfacial polymerization procedure developed here is different from that reported in the past, and the advantages of this method are as follows: (1) the total internal surface of polypropylene microfiltration membranes is coated with a polysulfonamide containing a pendent photoactive group without significantly changing the physical structure of the support membrane; and (2) the coated membrane with a photoactive group can be further converted by irradiation with long wavelength light into a number of functionalities. This new coating methodology overcomes the difficulties of conventional methods, such as the preparation of different monomers and subsequent interfacial deposition on the membrane surface by various methods. Despite any restrictions, this new coating methodology is useful in extending the knowledge of the coating technology. There is no literature found to deal with the mechanism of such a coating process. So far, we do not clearly understand the mechanism of the coating process. However, some of our findings have a bearing on better understanding of this mechanism, in general. A hypothesis for the mechanism of modified interfacial

polymerization is discussed in Chapter 3 and the general applicability of this coating technology is demonstrated in Chapter 4. The separation performance and surface properties have been changed by both coating polysulfonamide on the internal surface of polypropylene microfiltration membrane and by further functionalizing the membrane surface by converting diazoketone groups to carboxylic or hydroxyl groups *via* photochemical transformation. Those results are presented in Chapter 5.

2.5 Conclusions

This Chapter presents a coating technology for fabrication of a thin-film composite polypropylene microfiltration membrane by modified interfacial polymerization. The results revealed in this paper have shown that a polysulfonamide containing a pendent photoactive group has been successfully coated on the internal surfaces of a polypropylene microfiltration membrane by this coating technology. SEM examinations and mass gain studies of the coated membranes indicate that the morphology and the mass gain of the coating layer are highly dependent upon the strength of the organic solvent. Good reaction conditions: CCl_4/CH_2Cl_2: 45/55; monomer I concentration: 1.4 mmol/L; polymerization time: 60 min; temperature: 30°C, has been found to obtain an even, smooth coating layer on the fibrils and nodules of the nascent membrane. The mass gain of the coating layer is around 10% to 12% under this condition. Addition of triethylamine as an acid acceptor and/or use of NTSC as crosslinking agent can enhance the mass gain without remarkably changing the surface morphology of coating layer. To simplify the variables in the coating process for further study, crosslinking agent and the acid acceptor other than octanediamine were not used in the remaining work.

References

[1] J. Cadotte, Evolution of composite reverse osmosis membranes, in: D.R. Lloyd (Ed.), Material Science of Synthetic Membranes, ACS Symp. Ser. No. 269, American Chemical Society, Washington, DC, 1985, p. 275.

[2] R.J. Petersen and J.E. Cadotte, Thin film composite reverse osmosis membranes, M.C. Porter (Ed.), Handbook of Industrial Membrane Technology, Noyes Publication, 1990, p. 307.

[3] R.E. Whitfield, L.A. Miller and W.L. Wasley, Interfacial polycondensation I. The formation of surface graft polymer on wool, J. Appl. Polym. Sci., 8 (1964) 1607-1617.

[4] R.E. Whitfield, L.A. Miller and W.L. Wasley, Wool stabilization by interfacial polymerization, Part IV: Polyureas, polycarbonates, and further studies on polyamides. Textile Res. J., 33 (1963) 440.

[5] R.E. Whitfield, L.A. Miller and W.L. Wasley, Wool fabric stabilization by interfacial polymerization. Part V: Copolymer, Textile Res. J., 33 (1963) 752.

[6] I. Loh and R.A. Moody, Electrically conductive membranes: synthesis and applications, J. Membrane Sci., 50 (1990) 31-49.

[7] M.C. Porter, Thermal-Phase-Inversion-Process, M.C. Porter (Ed.), Handbook of Industrial Membrane Technology, Noyes Publication, 1990, p.65.

[8] K. Rilling, M. Eng. Thesis, Department of Chemical Engineering, McMaster University, 1992.

[9] J.M. Dickson, K. Rilling, R.F. Childs, B.E. McCarry and D.R. Gagnon, Development of a functionalized thin film composite coating for the internal structure of polypropylene microfiltration membrane, to be submitted, J. Membrane Sci. (1997).

[10] B.J. Trushinski, J.M. Dickson, R.F. Childs and B.E. McCarry, Photochemically modified thin-film composite membranes. Part I: Acid and

ester membranes, J. Appl. Polym. Sci., 48 (1993) 187-193.

[11] J. Ji , R.F. Childs, J.M. Dickson and B.E. McCarry, Fabrication of thin film composite membranes with pendent photoactive diazoketone functionality, accepted J. Appl. Polym. Sci., Dec. 1996.

[12] P.D. Caesar, Organic Synthesis, N. Rabjohn (Ed.), Coll. Vol. 4, (1963) 693-695.

[13] E.L. Wittbecker and P.W. Morgan, Interfacial polymerization. I., J. Polym. Sci., 40 (1959) 289-297.

[14] R.J. Petersen, Composite reverse osmosis and nanofiltration membranes, J. Membrane Sci., 83 (1993) 81-150.

[15] P.W. Morgan and S.L. Kwolek, Interfacial polycondensation. II. Fundamentals of polymer formation at liquid interfaces, J. Polym. Sci. XL (1959) 299-327.

[16] S.A. Sundet, W.A. Murphey and S.B. Speck, Interfacial polycondensation. IX. Polysulfonamides, J. Polym. Sci., 40 (1959) 389-397.

[17] J. Ji, Ph.D Thesis, Department of Chemistry, McMaster University, 1996.

[18] P.C. Varelidis, T.P. Skourlis, J.V. Bletsos, R.L. McCullough and C.D. Papaspyrides, Characterization of coating of poly(hexamethylene adipamide) deposited on carbon fibers by interfacial polymerization techniques, J. Appl. Polym. Sci., 55 (1995) 1101-1110.

[19] A. Okamoto, T. Aoki and I. Mita, Kinetic study on reaction between polymer chains-ends-II, Eur. Polym. J., 19(4) (1983) 341-346.

[20] A. Okamoto, T. Aoki and I. Mita, Preparation and reactivity of a primary amino group attached to the centre of a polyethylene chain, Eur. Polym. J., 19(8) (1983) 661-665.

[21] Organic Chemistry, J.D. Morrison (Ed.), Wadsworth Publishing Company, 1979, p. 286.

[22] Condensation Polymer: Interfacial and Solution Polymerization, P.W. Morgan (Ed.), Interscience, New York, 1965.

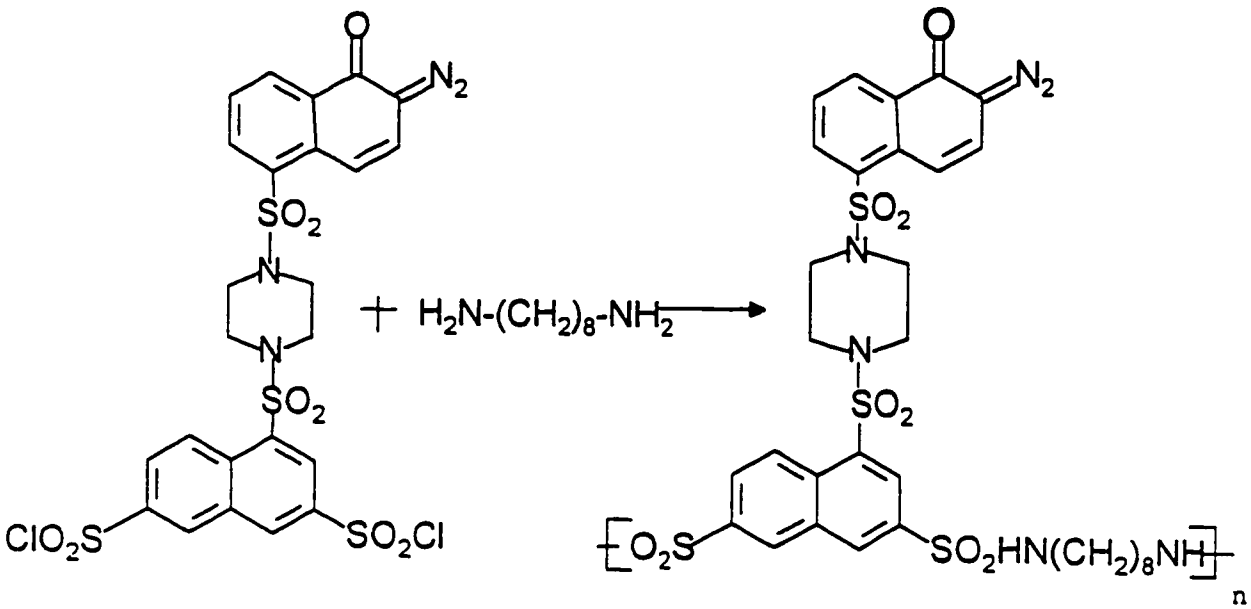

Monomer I

Polysulfonamide

Scheme 1. Polycondensation to produce the polysulfonamide. (One of three possible isomers of Monomer I is presented in this scheme. Other isomers of Monomer I are presented in Appendix A)

Table 1. Durability measurement of coating layer by Soxhlet extraction

Sample No.	Crosslinking agent (mol%)[1]	Mass gain (M_1) before Soxhlet (g)	Mass gain (M_2) after Soxhlet (g)	Mass loss[2] (%)
S-1	0	0.00765	0.00716	6.3
S-2	0	0.00888	0.00849	4.6
S-3	2	0.00758	0.00722	5.0
S-4	2	0.00754	0.00703	7.3
S-5	9	0.00720	0.00679	6.0
S-6	9	0.00945	0.00898	5.2

1 Mole ratio of crosslinking agent (NTSC)/monomer I.

2 Mass loss is defined as $[(M_1-M_2)/M_2 \times 100\%]$ - mass loss of coating layer during Soxhlet extraction. Mass loss of a nascent membrane was 2.0% during the Soxhlet extraction.

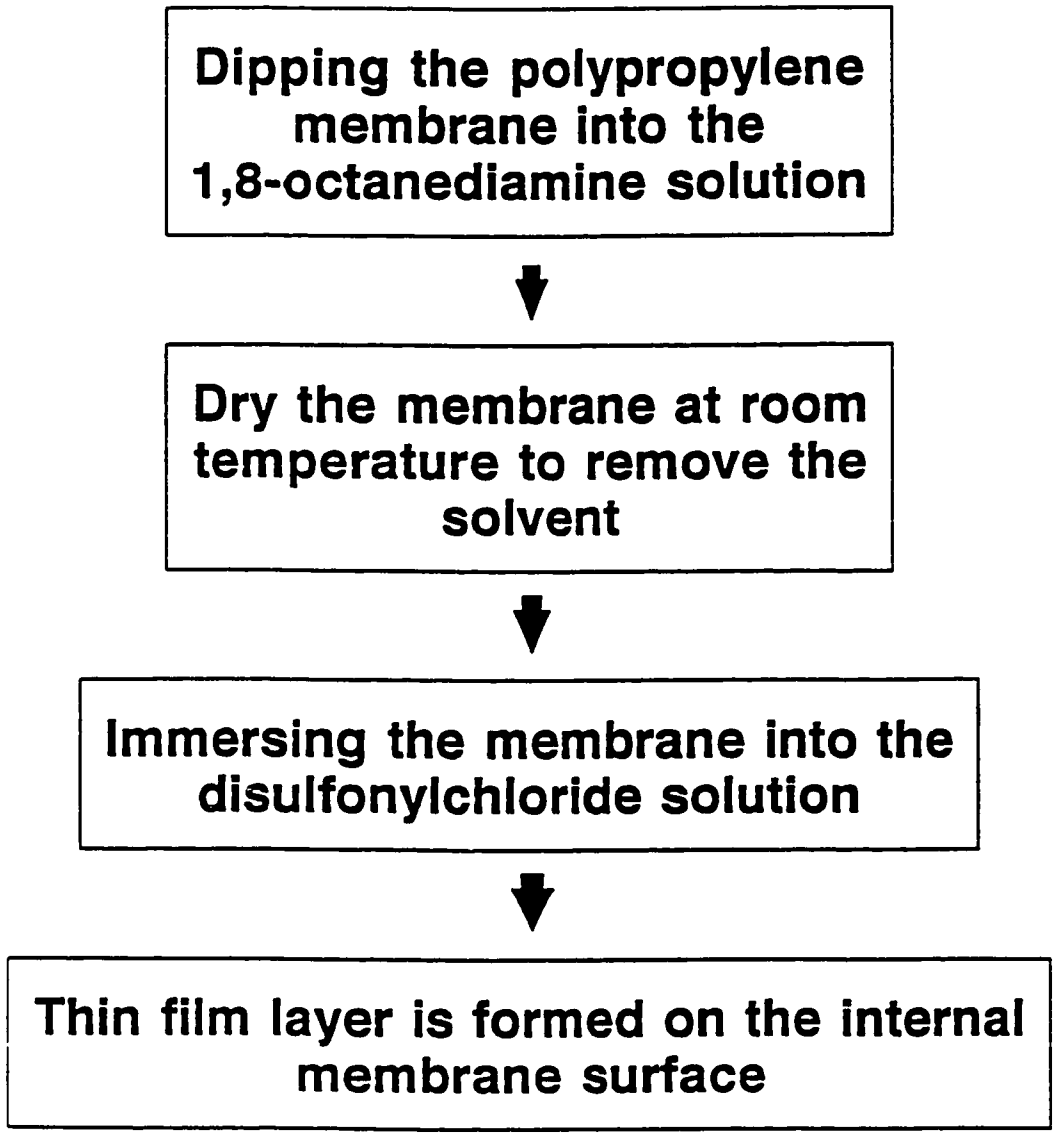

Figure 1. A flow chart of the modified interfacial polymerization process

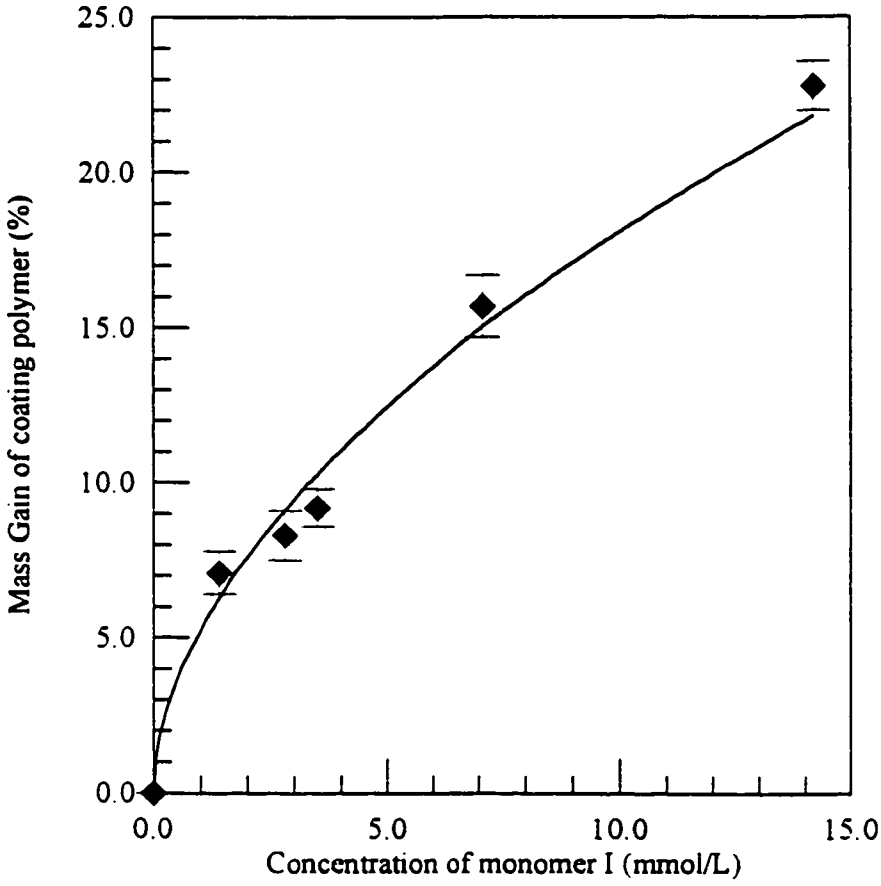

Figure 2. Effect of increasing concentration of monomer I on the mass gain of coating polymer in the coating process. Reaction time, 60 min; solvent, CH_2Cl_2; temperature, 30°C.

Figure 3. SEM morphology of the modified membrane made by interfacial polymerization with different monomer I concentrations. Reaction time, 60 min; solvent, CH_2Cl_2; temperature, 30°C. (a) Nascent membrane; (b) Mass gain: 8.3%, Concentration of monomer I: 2.8 mmol/L; (c) Mass gain: 15.7%, Concentration of monomer I: 7.1 mmol/L; (d) Mass gain: 22.2%, Concentration of monomer I: 14.2 mmol/L.

(a) Nascent membrane.

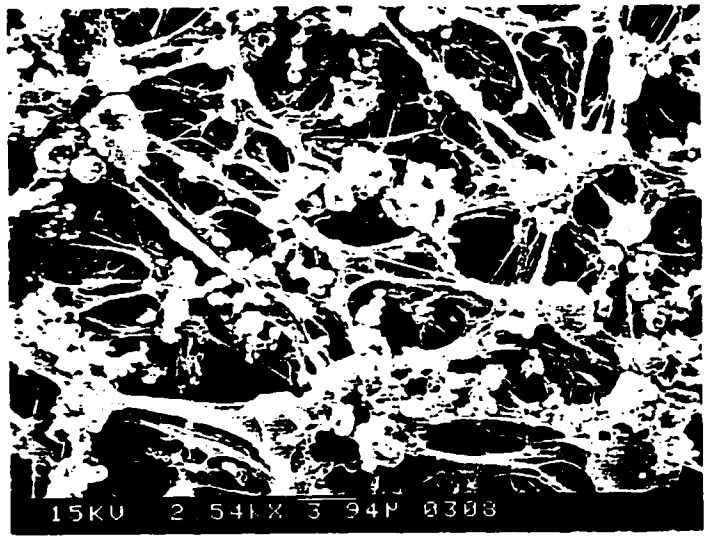

(b) Mass gain: 8.3%, Concentration of monomer I: 2.8 mmol/L.

(c) Mass gain: 15.7%, Concentration of monomer I: 7.1 mmol/L.

(d) Mass gain: 22.2%, Concentration of monomer I: 14.2 mmol/L.

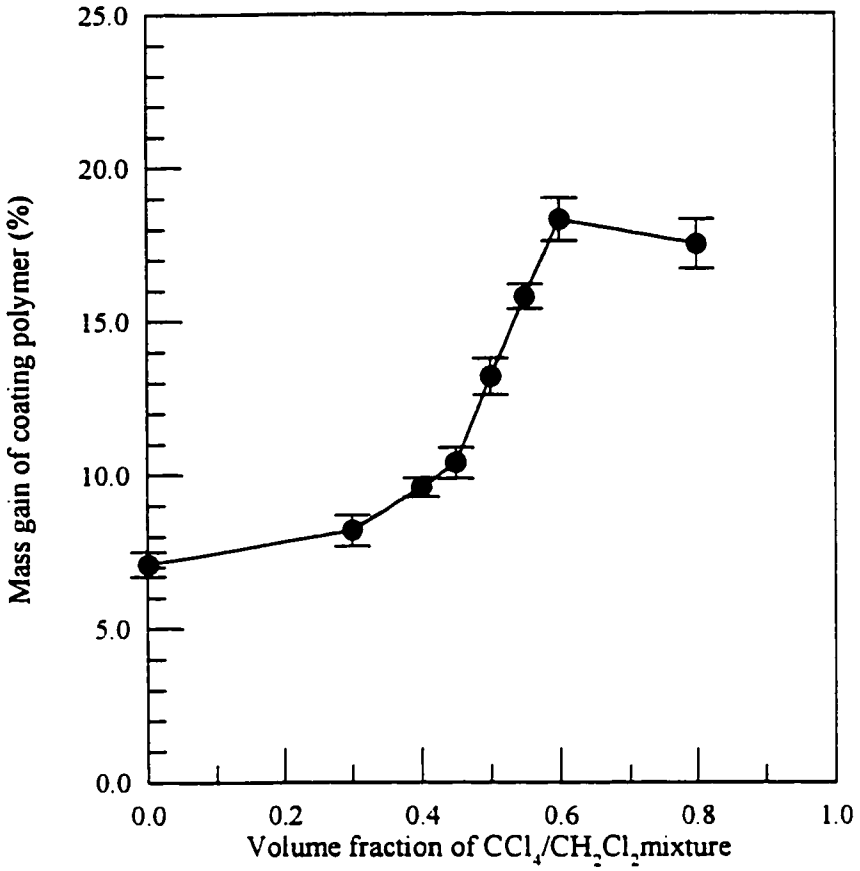

Figure 4. Effect of decreasing solvent strength on the mass gain due to coating polymerization. Reaction time, 60 min; temperature, 30°C; concentration of monomer I, 1.4 mmol/L.

(a)

Figure 5. SEM morphology of the modified membrane made by interfacial polymerization with different solvent strength. Reaction time, 60 min; temperature, 30°C; concentration of monomer I, 1.4 mmol/L. (a) Nascent membrane; (b) CCl_4/CH_2Cl_2: 0/100, Mass gain: 7.4%; (c) CCl_4/CH_2Cl_2: 30/70, Mass gain: 8.2%; (d) CCl_4/CH_2Cl_2: 40/60, Mass gain: 9.6%; (e) CCl_4/CH_2Cl_2: 45/55, Mass gain: 10.4%; (f) CCl_4/CH_2Cl_2: 50/50, Mass gain: 13.2%; (g) CCl_4/CH_2Cl_2: 55/45, Mass gain: 15.8%; (h) CCl_4/CH_2Cl_2: 60/40, Mass gain: 18.3%; (i) CCl_4/CH_2Cl_2: 80/20, Mass gain: 17.5%.

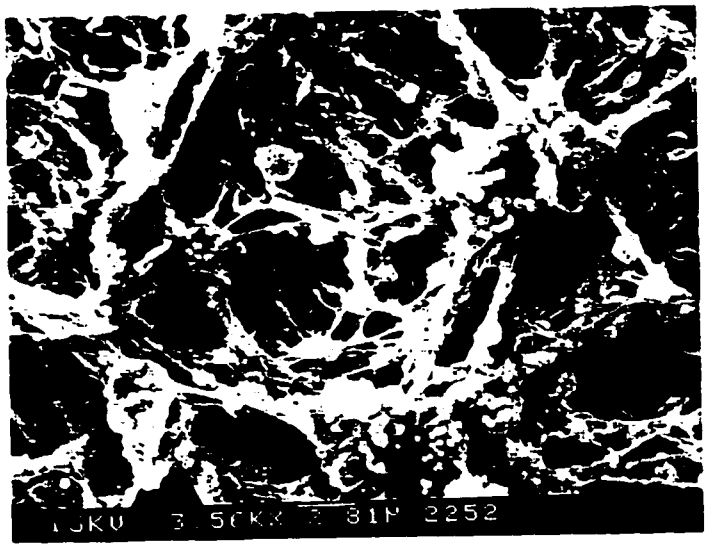

(b) CCl_4/CH_2Cl_2: 0/100, Mass gain: 7.4%.

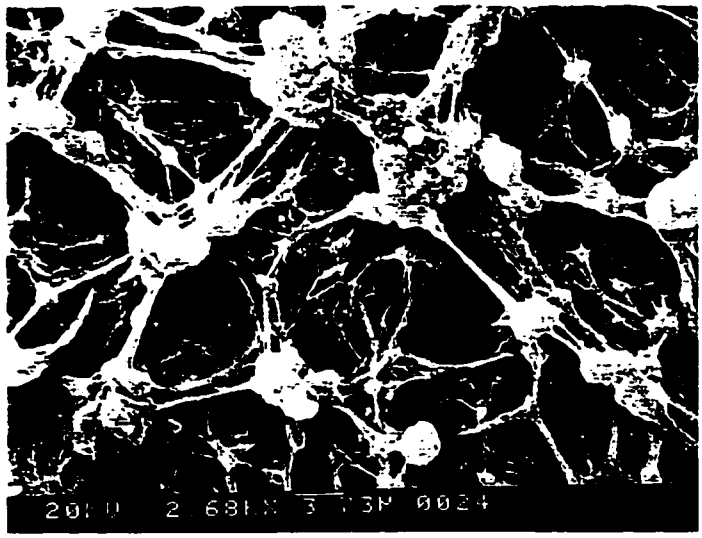

(c) CCl_4/CH_2Cl_2: 30/70, Mass gain: 8.2%.

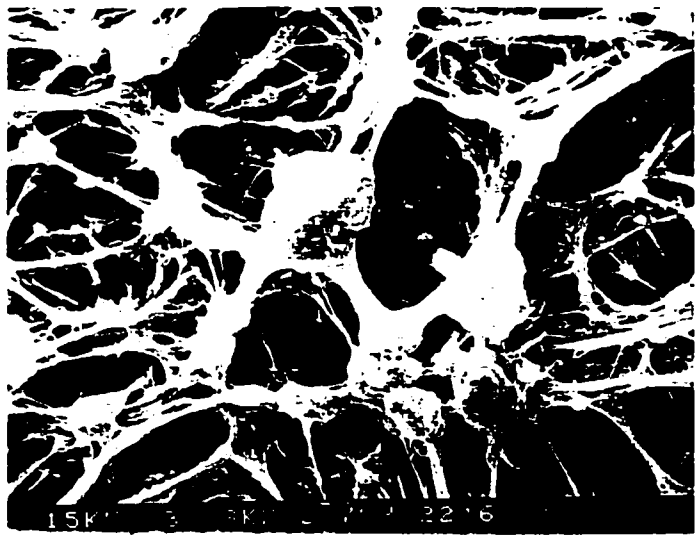

(d) CCl_4/CH_2Cl_2: 40/60, Mass gain: 9.6%.

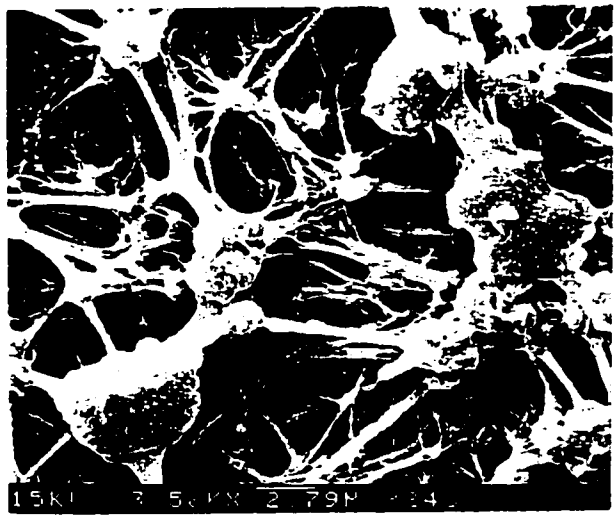

(e) CCl_4/CH_2Cl_2: 45/55, Mass gain: 10.4%.

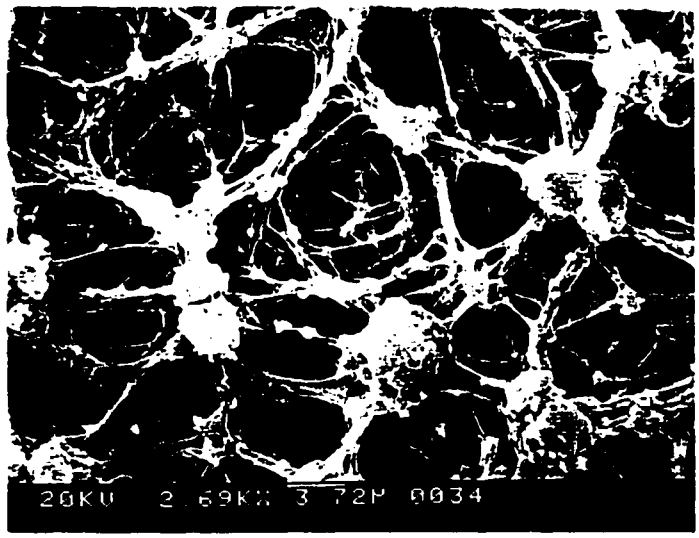

(f) CCl_4/CH_2Cl_2: 50/50, Mass gain: 13.2%.

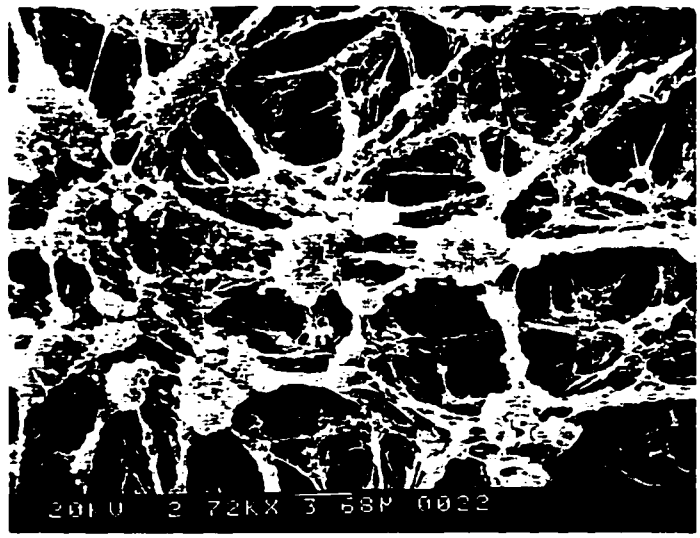

(g) CCl_4/CH_2Cl_2: 55/45, Mass gain: 15.8%.

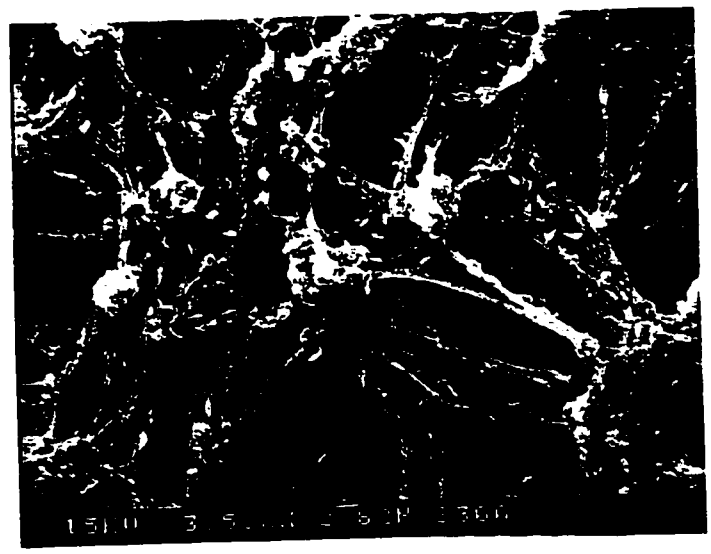

(h) CCl_4/CH_2Cl_2: 60/40, Mass gain: 18.3%.

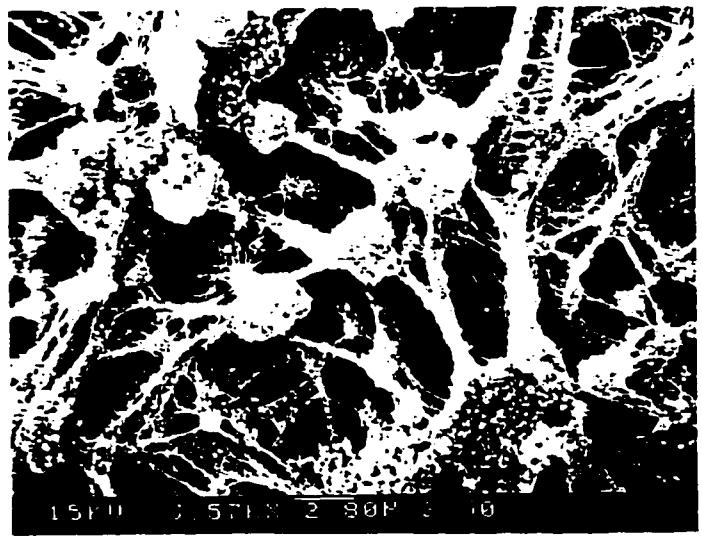

(i) CCl_4/CH_2Cl_2: 80/20, Mass gain: 17.5%.

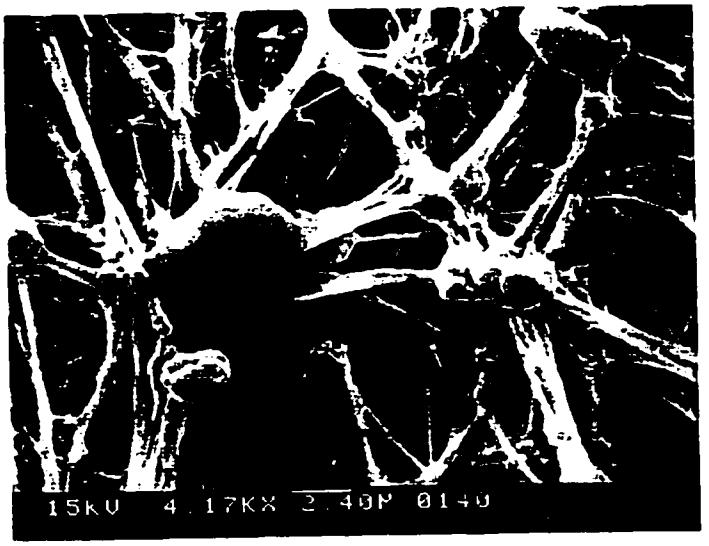

Figure 6. SEM of the membrane after deposition of octanediamine.

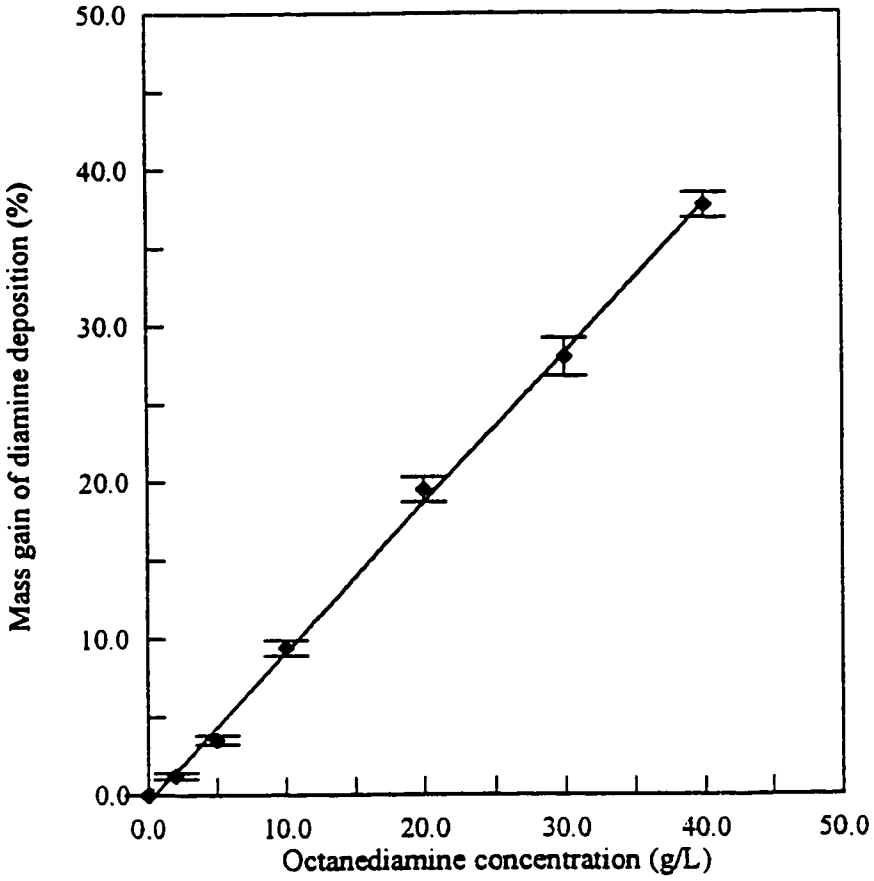

Figure 7. Effect of octanediamine concentration in methanol on the octanediamine loading in the membrane.

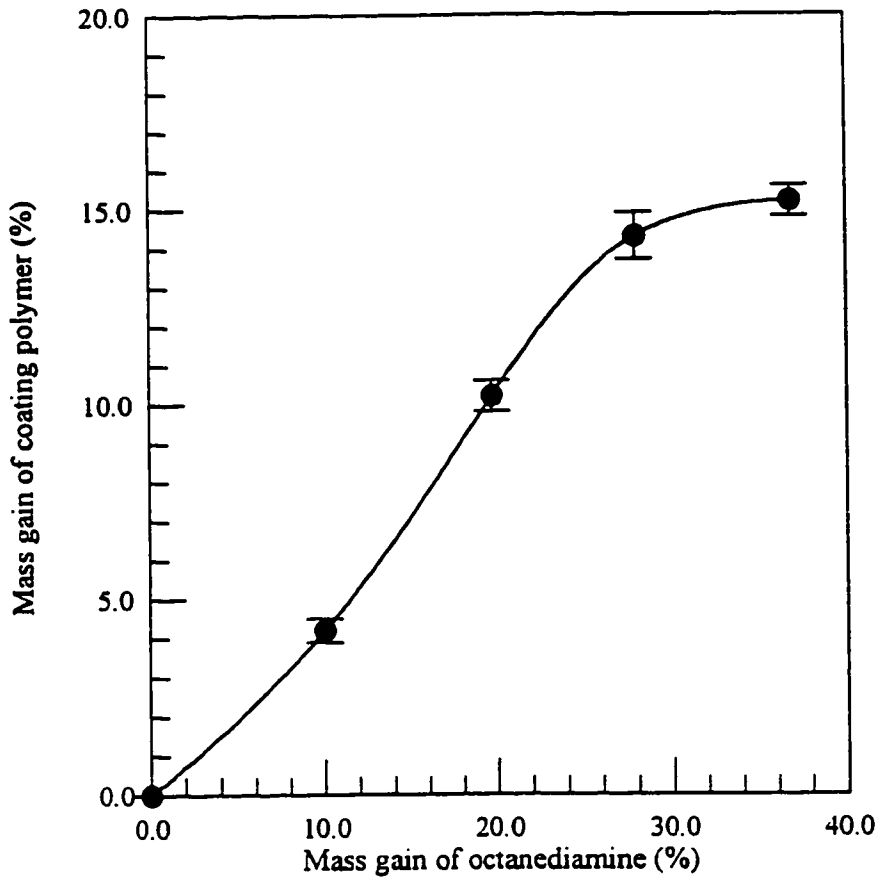

Figure 8. Effect of octanediamine mass gain on the coating polysulfonamide. Reaction time, 60 min; solvent (CCl_4/CH_2Cl_2), 45/55; temperature, 30°C; concentration of monomer I, 1.4 mmol/L.

(a) Mass of octanediamine deposition: 10%, Mass gain of coating polymer: 4.2%

Figure 9. SEM surface morphology of polysulfonamide coated membrane made at different octanediamine mass loading. Reaction time, 60 min; solvent (CCl_4/CH_2Cl_2), 45/55; temperature, 30°C; concentration of monomer I, 1.4 mmol/L. (a) Mass of octanediamine deposition: 10%, Mass gain of coating polymer: 4.2%; (b) Mass of octanediamine deposition: 20%, Mass gain of coating polymer: 10.4%; (c) Mass of octanediamine deposition: 37%, Mass gain: 15.2%.

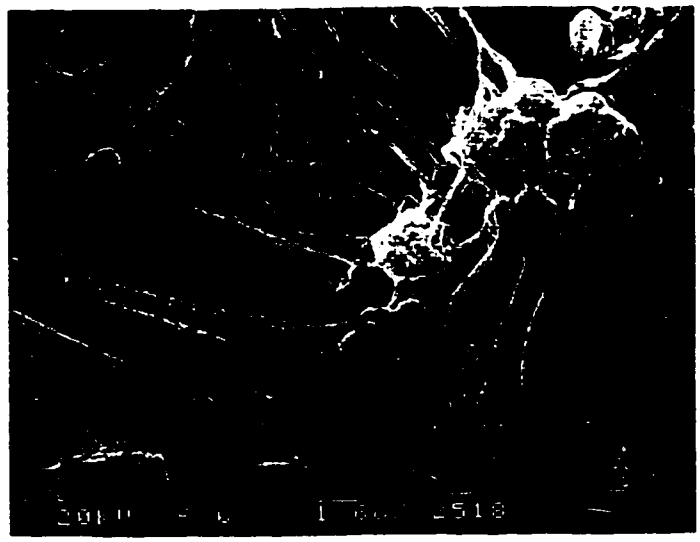

(b) Mass of octanediamine deposition: 20%, Mass gain of coating polymer: 10.4%

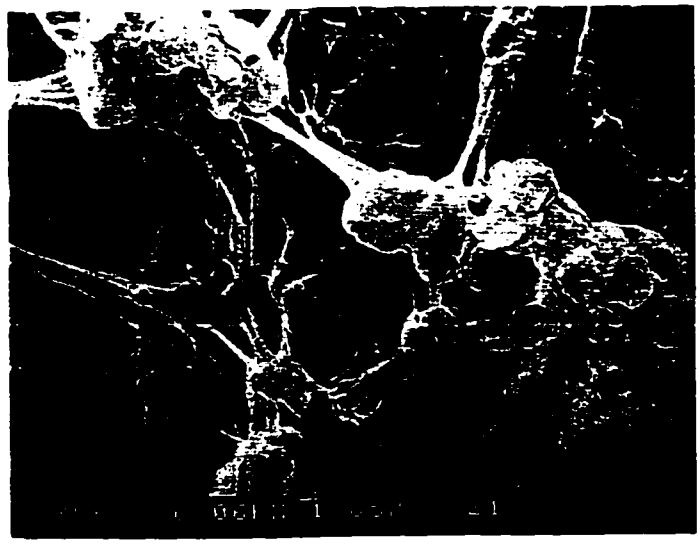

(c) Mass of octanediamine desoption: 37%, Mass gain of coating polymer: 15.2%

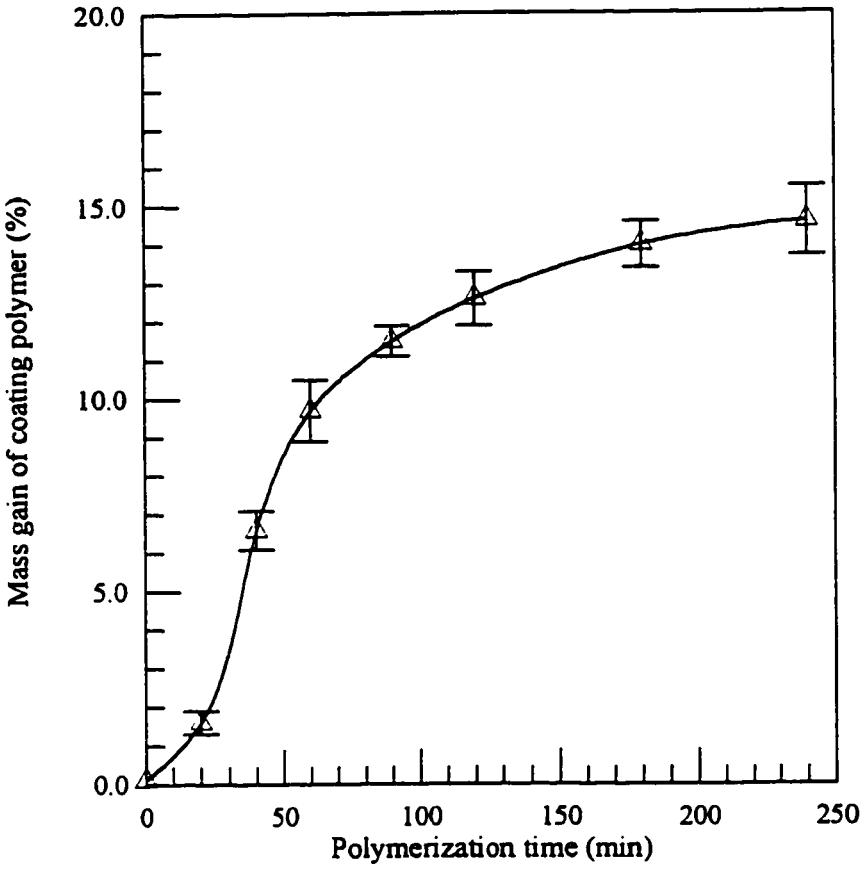

Figure 10. Effect of polymerization time on the coating polymer. Reaction time, 60 min; solvent (CCl_4/CH_2Cl_2), 45/55; temperature, 30°C; concentration of monomer I, 1.4 mmol/L.

(a)

(b)

Figure 11. SEMs surface morphology of coated membranes taken at different polymerization times. (a) 90 min, mass gain 11.7%. (b) 180 min, 14.3%.

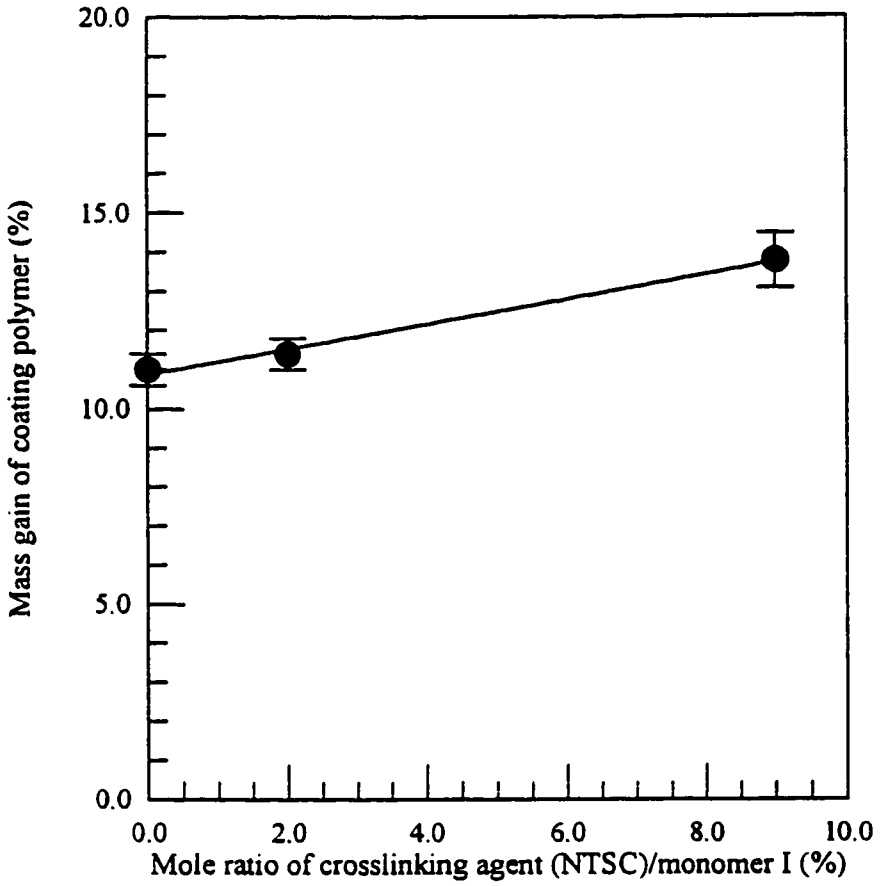

Figure 12. Effect of increasing crosslinking agent (NTSC) in the monomer I and NTSC mixture on the mass gain due to coating polymerization. Reaction time, 60 min; solvent (CCl_4/CH_2Cl_2), 45/55; temperature, 30°C; concentration of monomer I, 1.4 mmol/L.

Figure 13. SEM morphology of the modified membrane made by interfacial polymerization with 9% (mole) crosslinking agent. Reaction time, 60 min; solvent (CCl_4/CH_2Cl_2), 45/55; temperature, 30°C; concentration of monomer I, 1.4 mmol/L.

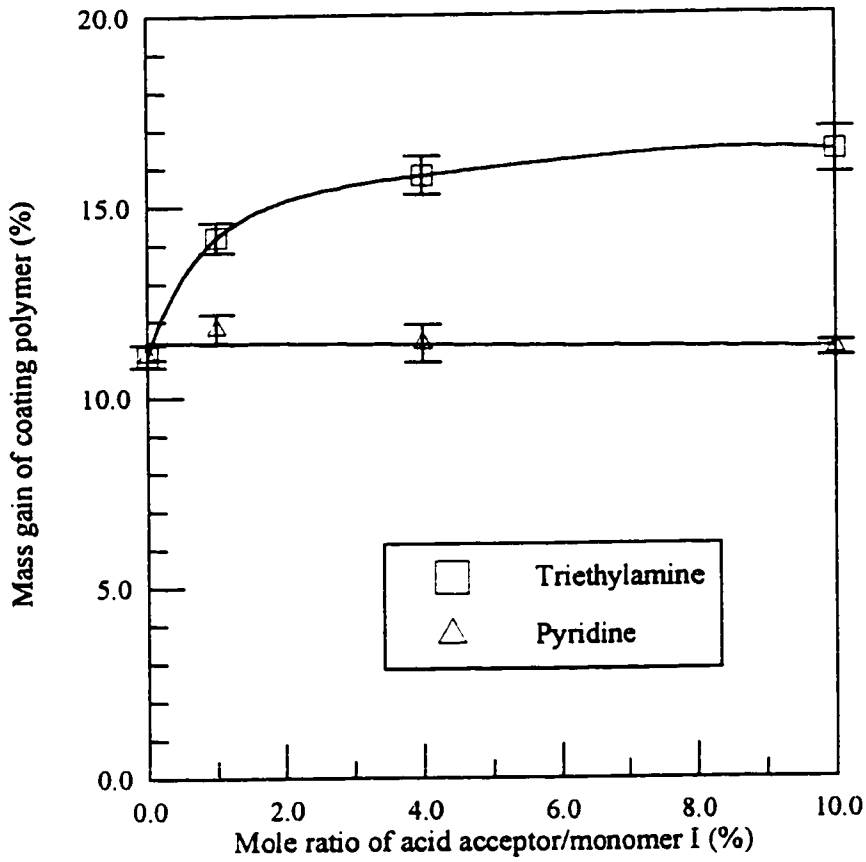

Figure 14. Effect of addition of acid acceptor (triethylamine or pyridine) on the mass gain due to coating polymerization. Reaction time, 60 min; solvent (CCl_4/CH_2Cl_2), 45/55; temperature, 30°C; concentration of monomer I, 1.4 mmol/L.

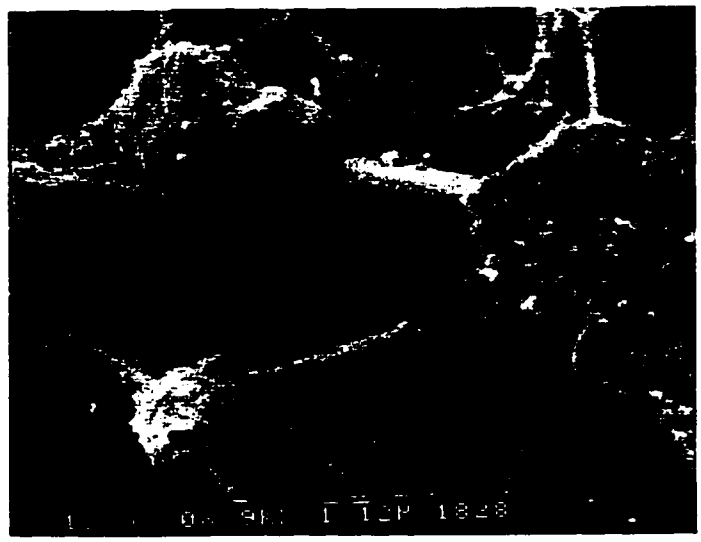

Figure 15. SEM morphology of the modified membrane made by interfacial polymerization with triethylamine concentration 10 times as high as the concentration of monomer I. Reaction time, 60 min; solvent (CCl_4/CH_2Cl_2), 45/55; temperature, 30°C; concentration of monomer I, 1.4 mmol/L.

(a)

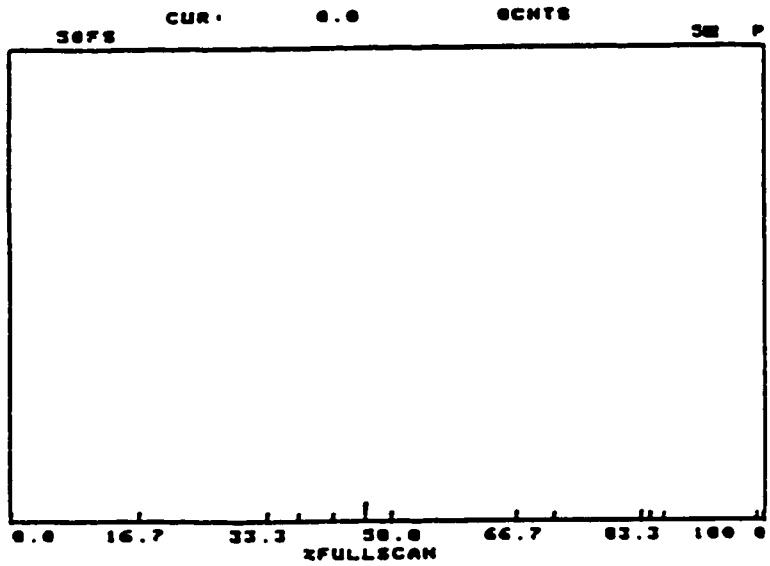

(b)

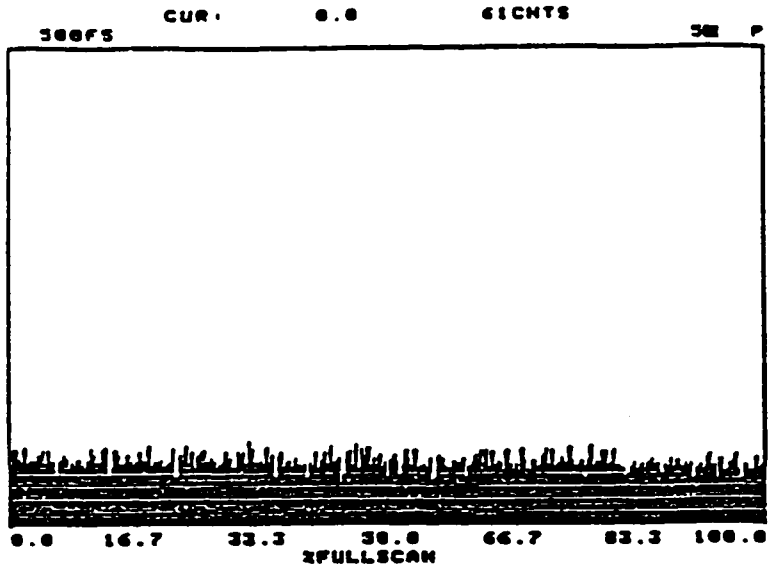

Figure 16. EDS spectrum of sulphur element analysis versus position in the membrane cross-section. (a) nascent membrane, fullscan: 50; (b) polysulfonamide coated membrane, fullscan: 500.

(a)

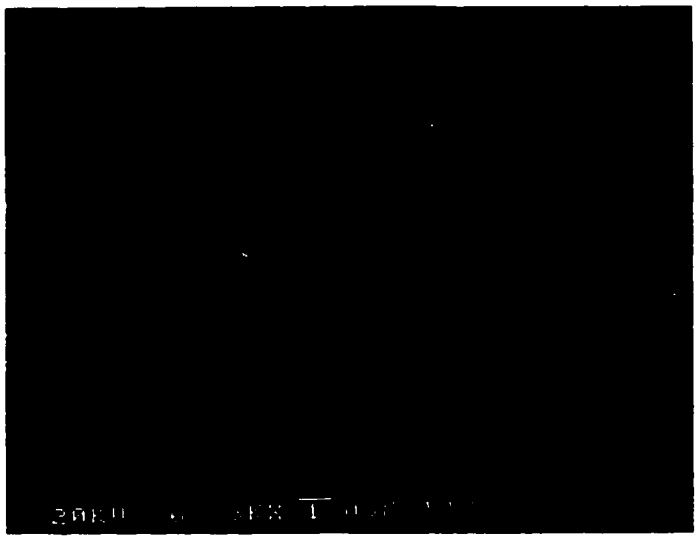

(b)

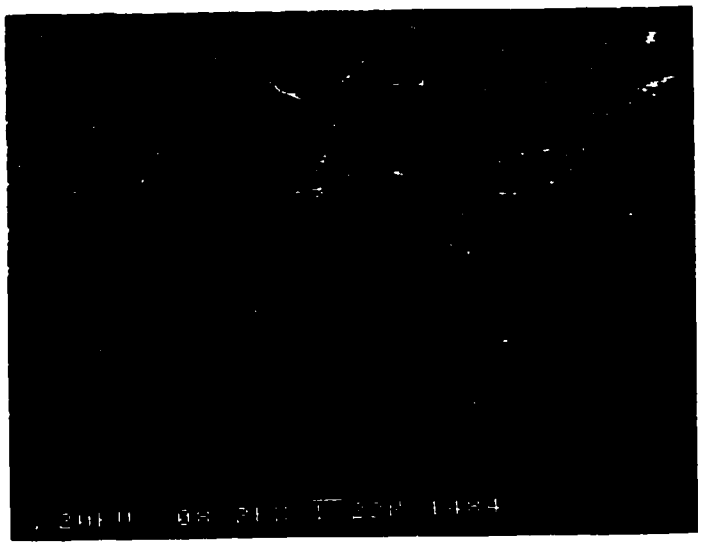

Figure 17. SEM cross-section morphology of the nascent membrane and modified membrane made without crosslinking agent. (a) Nascent membrane; (b) coated membrane.

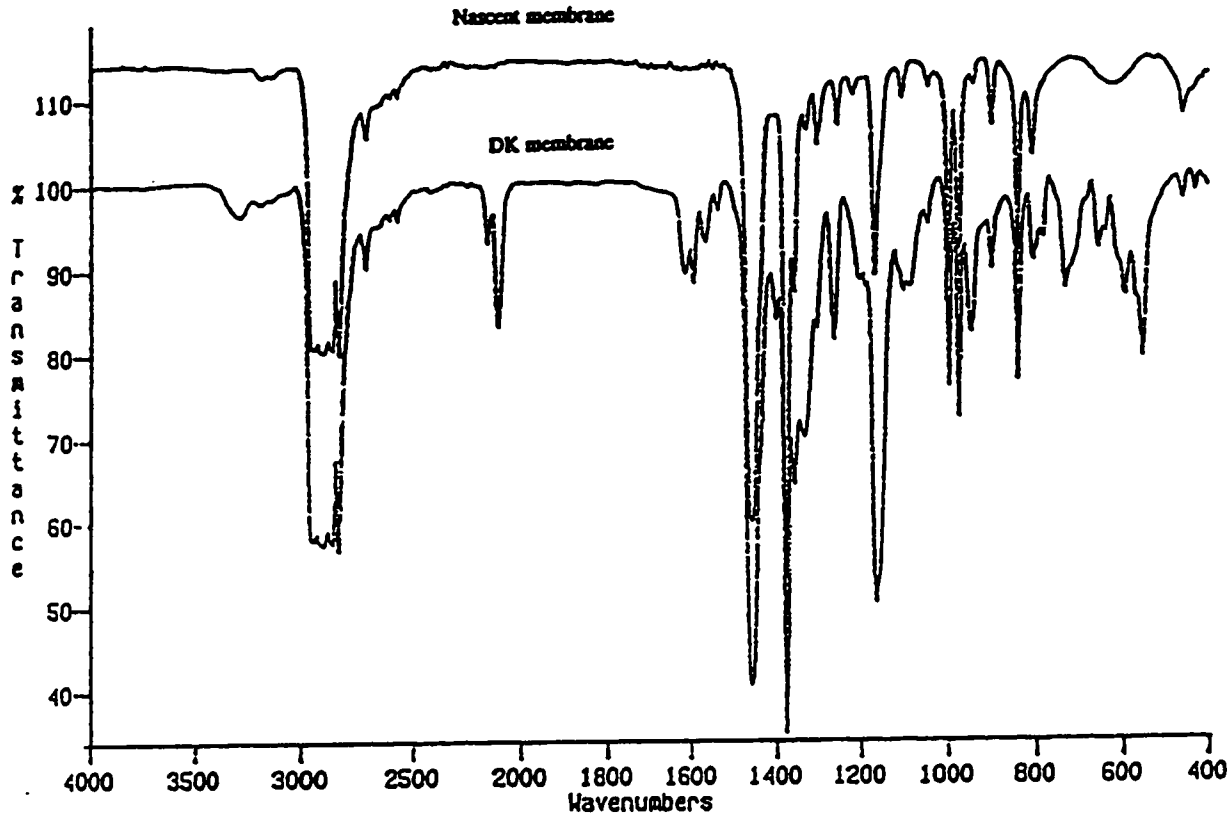

Figure 18. FT-IR spectra of nascent membrane and polysulfonamide coated membrane.

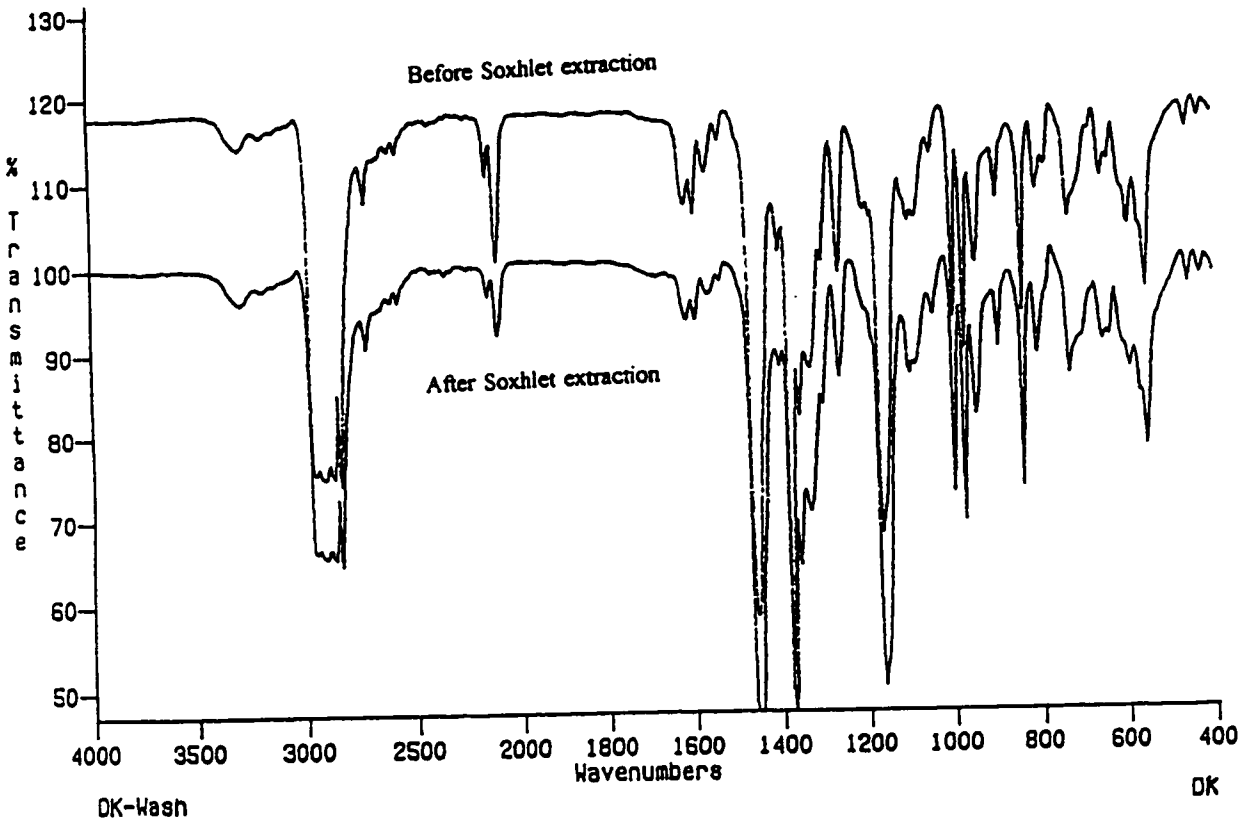

Figure 19. FT-IR spectra of the polysulfonamide coated membrane before and after Soxhlet extraction.

Chapter 3

Coating the Internal Surface of Polypropylene Microfiltration Membranes by Modified Interfacial Polymerization. Part II: Investigation of the Coating Mechanism.

ABSTRACT

This Chapter investigates the mechanism of this new type of interfacial polymerization for coating polysulfonamide on the membrane internal surface. The average molecular weight of coating polysulfonamide was determined via end-group analysis using neutron activation analysis to be 22,000 (standard deviation ca. 2200), which corresponds to a degree of polymerization of about 28. The end-group of coating polymer was dominated by the SO_2Cl group. A mechanism of the modified interfacial polymerization is hypothesised and evaluated by all of the evidence including those reported in Chapter 2. Most results obtained so far including the study of the monomer solubility in the chapter support the hypothesis. This mechanistic study defines the most important principles involved in modified interfacial polymerization and provides a better understanding of this new type of interfacial polymerization.

Keywords: Modified interfacial polymerization, Polysulfonamide, Coating, Internal surface.

Introduction

In the preceding papers [1,2], the technique of modified interfacial polymerization has been developed to coat polysulfonamide as a thin layer on the internal surfaces of polypropylene microfiltration membranes. A general methodology for this *in situ* coating of condensation polymers has been described [1,2]. This process consists of placing polypropylene microfiltration membranes into a diamine solution for a few minutes, drying off the solvent, immersing the membranes into an unstirred disulfonylchloride solution for an hour, then washing the membranes with solvent. An even, smooth thin film can be formed *in situ* upon the internal surfaces of the microfiltration membranes. Instead of an aqueous phase, diamine is in the solid phase when brought into contact with disulfonylchloride organic solution in this modified interfacial polymerization. Chapter 2 has outlined the effects of several variables on the modified interfacial polymerization process. The coating methodology was evaluated by various ways through FT-IR, SEM, EDS, and durability measurements, which confirmed that the internal surface of the polypropylene microfiltration membranes was evenly covered by a smooth layer of polysulfonamide. This technique demonstrates the possibility of coating the entire internal surface of tortuous microfiltration membranes with various desired polymers *via* the modified interfacial polymerization. The mechanism of the modified interfacial polymerization may be different from either conventional interfacial polymerization or solution polymerization at the molecular level. So, this new type of interfacial polymerization is studied further with emphasis on the mechanism of polymerization.

In order to understand the true mechanism of this new type of interfacial polymerization, a hypothesis for the modified interfacial polymerization and coating mechanism is proposed in this Chapter and tested by various evidence obtained so far. The effects of the most important variables on the modified interfacial polymerization, including selection of solvent, monomer concentration, polymerization time, and additives is further interpreted by the proposed mechanism. End-group analysis and average molecular weight measurement of the coated polysulfonamide using neutron activation analysis technique (NAA) without destroying the membrane has been developed and the data are presented.

3.1 Literature Review

The fundamental research on polyamide film formation by conventional interfacial polymerization was conducted by Morgan and coworkers [3,4]. They found that when a solution of a diacid chloride is brought into contact with an aqueous diamine solution, high molecular weight polymer forms in a fraction of a second near the interface. The reaction rate must be faster than the rate of mixing and considerably faster than any important side reactions at the polymerization site. There must be sufficient time to essentially complete the polymerization before the polymer precipitates or gels. The diamine nearly always can partition into the organic phase, whereas the acid chloride has little solubility in the aqueous phase. The reaction occurs in the organic phase next to the interface in the presence of an excess of diacid chloride. Mass transfer of the diamine is the rate-controlling step at all concentrations for these systems. The primary functions of the aqueous phase are to serve as a solvent medium for the

diamine and acid acceptor and to remove the byproduct, hydrochloride, from the polymerization zone. Thus, the interfacial polymerization system is sensitive to factors which change the transfer rate of diamine into the organic phase, the reaction rate, and the swelling of the polymer by the solvent.

The application of interfacial polycondensation of polyamide and various copolymers on wool fibers to make shrink-resistant wool fibers was described by Whitfield et al. [5-7]. The procedure is to firstly apply diamine solution to a wool fiber substrate to provide an extremely thin layer of the solution on the surface of the wool fiber, then dipping the wool fiber into the diacid chloride solution, forming an ultrathin film of the polymer on the surface of the wool fiber. Various routes for applying the diamine were investigated including a miscible solvent, an immiscible solvent and totally removing the solvent from the wool fiber. The best shrinkage resistance of wool fibers was obtained with an immiscible solvent. In the case of the dried wool fiber, it was suggested that polymerization occurred readily at the solid-liquid interface.

Cadotte et al. [8] developed polyamide thin film composite (TFC) membranes by interfacial polycondensation for reverse osmosis application. To prepare TFC membranes, polysulfone support films were saturated in a solution of various diamines, with possibly acid acceptor, and/or surfactant. After draining, the film was brought into contact with a hexane solution of various diacid chlorides plus a triacid chloride as a cross-linking agent. Thus, a thin coating layer was formed on the external surface of the polysulfone support membrane. These composite membranes demonstrated high flux and high salt rejection enhanced through optimization of interfacial polymerization parameters. The mechanism of this TFC technique was investigated by applying the principles of conventional interfacial polymerization. Data obtained indicated that polymer formation

occurred in the organic phase. The amine diffused across the water-solvent interface and reacted with the acyl halide in the organic phase. A smooth polymer film initially formed at the interface. Further polymer formation took place on the organic solvent side of the deposited film. This latter surface became increasingly rough as polymer formation proceeded. The polymer film was normally microporous, allowing for the transport of amine reactants and acid byproducts across the interfacial region.

Sundet [9] described to some degree the mechanism of interfacial polyamide formation, and concluded that an interfacially formed polyamide layer would be asymmetric and highly functional (i.e., many terminal groups). Chen and Chan [10] studied the mechanism of NS-100 membrane formation, in which a thin layer of polyamide was interfacially deposited on the top surface of a polysulfone support, including radio-labelled ethanolamine in the aqueous phase to measure residual levels of unreacted isocynate groups in the barrier layer. It was concluded that 110°C post-cure enhanced salt rejection by promoting additional formation of crosslinking *via* reaction of the residual isocynate groups. Overall, however, very little work has been published on the mechanism of the TFC technique.

3.2 Experimental

The coating process/modified interfacial polymerization was described previously in Chapter 2 of this thesis. A description of the coating process is presented as a flow chart in Figure 1 of Chapter 2.

The definition of mass gain and measurement of surface morphology were described in Chapter 2.

3.2.1 Materials

Monomer I was synthesised in our laboratory according to the method described elsewhere [11]. Octanediamine, methanol, dichloromethane, carbon tetrachloride, triethylamine, and trichloroacetic anhydride were purchased from Aldrich Chemical Co. Sodium hydroxide and standard HCl solution were from BDH. All reagents used in this Chapter were analytical grade. The physical and chemical properties of the polypropylene microfiltration membranes are presented in Chapter 2.

3.2.2 Turbidity measurement

Turbidity of polymer/oligomer in the organic solvent after the modified polymerization was measured by a HF Instruments Model DRT 1000 turbidity meter.

3.2.3 Solubility measurement

Octanediamine solubility

Octanediamine solubility in different mixtures of CCl_4/CH_2Cl_2 was determined by titration. Saturated octanediamine solutions were prepared by dissolving a large excess of octanediamine in different solvent mixtures with vigorous stirring, then filtering. 5 ml of filtrate was mixed with 50 ml deionized water in a flask with rigorous stirring. Octanediamine partitions into the aqueous phase. A 0.01 N HCl standard solution was used to titrate the octanediamine in the aqueous phase under rigorous stirring with a standard indicator of methyl red/bromocresol green mixture [12]. During the titration process, the octanediamine concentration in the aqueous phase is depleted. Thus,

octanediamine in the organic phase continuously partitions into the aqueous phase until the octanediamine is totally removed into the aqueous phase.

Monomer I solubility

The concentration of monomer I in different mixtures of CCl_4/CH_2Cl_2 was determined by ultraviolet (UV) spectrum because the diazoketone group in the pendent bond of monomer I has a characteristic peak near 330 nm [11]. Saturated monomer I solutions were prepared in the same way as the saturated diamine solution. The relationship between the concentration and peak intensity was calibrated using a series of known concentrations of monomer I solution.

3.2.4 Polysulfonamide end-group and average molecular weight measurement by neutron activation analysis (NAA)

After polymerization in the absence of crosslinking agent, the coated membranes were washed three times each in dichloromethane, methanol and carbon tetrachloride, successively. End-group analysis of coated polysulfonamide includes the measurement of SO_2Cl and NH_2 end-groups, independently.

(1) Coated membranes were immersed in 0.005 N NaOH solution for an hour to neutralize protonated amine end-groups of the polymer chain, then washed with deionized water very gently overnight. The amount of chlorine (N_1) on the coated membrane was detected nondestructively by neutron activation analysis (NAA). The amount (N_{10}) of chlorine on the nascent membrane, which was treated by the same approach, was measured as background. The substraction of N_{10} from N_1 represents the amount of SO_2Cl end-group.

(2) After the first chlorine measurement, the membranes were washed in a 20 vol% trichloroacetic anhydride solution containing triethylamine as an acid acceptor

for half an hour at room temperature, followed by washing with CH_2Cl_2, CCl_4 and deionized water. The level of chlorine remaining on the membranes (N_2) was again determined by NAA. The amount of chlorine (N_{20}) on nascent membranes which were treated by the same approach was also measured. The term, $[(N_2-N_{20})-(N_1-N_{10})]/3$, indicates the amount of NH_2 end-group on the coated polymer.

The total amount of end-groups was estimated by the sum of the SO_2Cl and NH_2 groups, as follows:

$$\text{TOTAL END-GROUP (Moles)} = (N_1-N_{10})+[(N_2-N_{20})-(N_1-N_{10})]/3$$

The above analysis allows an estimation of the average molecular weight of the coating polysulfonamide based on the total mass of coating polysulfonamide, as determined by a gravimetric method, divided by half of the molar amount of end-groups.

3.3 A hypothesis for the modified interfacial polymerization

The first step in modified interfacial polymerization (Figure 1a) is the deposition of octanediamine on the internal and external surfaces of the polypropylene support membranes. When the octanediamine loaded membranes are brought into contact with the disulfonylchloride solution, octanediamine (A) in the solid state dissolves in the organic solvent and diffuses into the organic phase to meet disulfonylchloride (B). At the outset, adjacent to the solid-liquid interface, the local concentration of diamine is much higher than that of disulfonylchloride. Presumably, disulfonylchloride is acylated to a large extent at one end or both ends to form dimer (AB) or trimer (ABA) (see Figure 1b). But, in the case of sulfonamide reaction, the mass transfer of the diamine is not the only rate-controlling step, because the reaction rate to form polysulfonamide (ca. 10^{-2} L mol^{-1}

s^{-1}) [13-15] is much lower than that to form polyamide (ca.10^2-10^6 L mol^{-1} s^{-1}) [16,17]. The BAB trimer may also be formed at the beginning of the reaction although the concentration of diamine is higher than the disulfonylchloride in the reaction zone. At this point, the interfacial polymerization is presumably controlled by the solubility of octanediamine into the organic phase, the mass transfer rate of the diamine and the reaction rate of sulfonamide.

As time progresses, the diamine not only reacts with the oligomer, but also diffuses deeper into the organic phase and reacts with new disulfonylchloride. Thus, the polymerization is controlled more by dissolving and diffusion of octanediamine in the organic phase. The depleted disulfonylchloride inside the membrane pore is replenished by the diffusion of free disulfonylchloride in the bulk phase into the pore. The initial replenishing process of disulfonylchloride can be done in a few seconds because the membrane is thin (ca. 90 μm) and the pores are large (ca. 1 μm). A simple diffusion model has been used to estimate the diffusion rate of the monomer I into the membrane pore. The diffusivity and molar volume of the monomer I was estimated based on the Wilke and Chang's correlation [18,19], using the Le Bas method to estimate the molar volume. The well-known, dimensionless number $D\theta/L$ represents the ratio of diffusion rate (D is diffusivity and θ is the time) versus the length of the diffusion path (L) which is the half of the membrane thickness in this case [20]. The result of this calculation indicates that the initial diffusion of the monomer I into the membrane pore can be done in less than 10 seconds, assuming the monomer I is consumed instantaneously inside of the pores. As polymerization processes, monomer I needs longer time to diffuse into the membrane pore because the monomer I outside of the membrane pores was not well mixed in an unstirred solution. At the later stage of the coating polymerization, the effective coating polymerization inside of the

membrane pores (adjacent to the membrane surface) is also controlled by the diffusion of monomer I into the membrane pores.

Polymerization leads to a series of incremental layers of polymer/oligomer from the solid-liquid interface extending to the organic solvent. The concentration and size of polymer/oligomer gradually decreases from the interface toward the organic phase. When the molecular weight of the oligomer exceeds the solubility limits, precipitation of polymer takes place. The precipitation initially occurs in the reaction zone located adjacent to the solid-liquid interface, where diamine concentrations are highest, then gradually extends into the organic solvent. The first polymer precipitates absorb on the membrane internal surfaces, which forms a physical barrier to restrict the diffusion of the diamine into the organic solvent, referred to Figure 1c. The diffusion rate of diamine into the organic solvent significantly slows down.

As precipitates are formed, polymerization does not stop entirely but greatly decreases in rate because of the lower mobility of the polymer chains and the decreased diffusion rate of the intermediates. These precipitates continuously react with free diamine, free disulfonylchloride or oligomer to form a thin polysulfonamide layer across the whole internal surface because the precipitates can still react. As time progresses, the precipitation takes place more deeply in the organic phase, and the reaction medium becomes turbid. The precipitates in the bulk phase either stick on the initial polymer coat, or disperse in the bulk phase as effectively lost oligomer/polymer. This qualitative hypothesis is shown diagrammatically in Figure 1.

In terms of the above hypothesis, only precipitates in the vicinity of the interface can be evenly coated on the membrane internal surface. The precipitates in the organic bulk phase, which consume reactants, are not beneficial for the

coating process. To improve the coating effectiveness, reaction and polymerization must take place in the vicinity of the solid-liquid interface. Thus, the selection of organic solvent becomes the key factor to obtaining a good coating of polysulfonamide. The principle requirements for modified interfacial polymerization are that the organic solvent (reaction medium) should have very low solubility for octanediamine, to limit the diamine dissolving and diffusing into the organic phase, and have high solubility for disulfonylchloride, and the reaction medium should be also a good solvent for polymerization. The following results were obtained, some of them was described in the Chapter 2, to elucidate and test the above hypothesised polymerization mechanism.

3.4 Results and Discussion

3.4.1 Monomer solubility

The solubility of monomer I measured in different volume ratios of CCl_4/CH_2Cl_2 is illustrated in Figure 2. The solubility of monomer I dramatically decreased when the amount of CCl_4 in the mixed solvent was increased. The solubilities of monomer I, at 45/55 (CCl_4/CH_2Cl_2) and 60/40 (CCl_4/CH_2Cl_2), were 3.5 mmol/L (2.6 g/L) and 1.4 mmol/L (1 g/L), respectively. The concentration of monomer I usually used in the modified interfacial polymerization was 1.4 mmol/L in the mixed solvent with 45/55 (CCl_4/CH_2Cl_2). The monomer I can be totally dissolved in such a reaction medium. When the percentage of CCl_4 in the mixed solvent exceeds to 60/40, the concentration of monomer I (1.4 mmol/L used as a standard monomer I concentration for the remainder of this study) exceeds the solubility of monomer I and monomer I can not be completely dissolved in such

poor solvents.

The solubility of octanediamine in the different mixed solvents, as shown in Figure 3, followed the same trend as for monomer I. The detailed results are in Appendix C. The addition of the non-polar CCl_4 into CH_2Cl_2 caused a decrease in octanediamine solubility. As a measure of the relative rate at which octanediamine was dissolved into the mixed solvent, the following experiments were performed. Membranes, preloaded with octanediamine, were exposed to different solvent mixtures, for different times, and then each membrane was dried and weighed to determine the remaining mass gain of octanediamine, as illustrated in Figure 4 This experiment approximately simulates the first step in the modified interfacial polymerization, that is the dissolution of the diamine. The results indicated that the octanediamine is completely exhausted inside the membrane pores after a one hour immersion of the diamine loaded membrane in the strong solvent CH_2Cl_2. For a mixed solvent with 50/50 (CCl_4/CH_2Cl_2), octanediamine is reduced to ca. 25% of the original value after a one hour immersion in this weaker solvent.

3.4.2 Average molecular weight of coating polysulfonamide

After polymerization, three kinds of end-groups are assumed to exist on the polysulfonamide coating layer, primary amine (NH_2), sulfonylchloride (SO_2Cl), and protonated amine (NH_2HCl). Since the coating polymer is very hard to be extracted completely by solvent, a new end-group analysis method for the coated polysulfonamide was developed using neutron activation analysis (NAA) without destroying the coated membrane. The characteristic element to detect was chlorine and the sensitivity of chlorine atom measurement by neutron activation analysis was less than 1 μg [21]. Linear polysulfonamide coating, without any trisulfonyl

chloride present, was used here to simplify the analysis.

The two-step NAA procedure for end-group measurement is described in Experimental. The first step was to convert the protonated amine end-group to amine end-groups by pH neutralization. The amount of Cl (N_1-N_{10}) measured in step one, shown in Table 1, represents the amount of sulfonylchloride end-groups. The second step was to convert primary amine end-groups into trichloride terminated groups. The reaction between primary amine end-group with trichloroacetic anhydride, using triethylamine as an acid acceptor, is presented in Scheme 1. The secondary amine in the sulfonamide bond is not be affected under such reaction conditions because of the reactivity difference between primary and secondary amines [22]. Hydrolysis of sulfonylchloride end-group seems to be a factor affecting the end-group calculation. However, the extent of hydrolysis of disulfonylchloride in the presence of the dilute base solution was determined to be very low and was neglected [11]. An other assumption made in the equation of end-groups calculation was that the amount of sulfonylchloride end-groups (N_1-N_{10}) was not affected during the second step treatment. The total chlorine amount measured after the second step was (N_2-N_{20}) which includes the amount of chlorine measured before (N_1-N_{10}). The amount of NH_2 end-group should be [(N_2-N_{20})-(N_1-N_{10})]/3 because trichloride attached to each primary amine end-group.

The average molecular weight of the linear polysulfonamide coated on the internal surface of microfiltration membranes was calculated by dividing the coating mass by half the molar amount of the end-groups. The average molecular weight of six samples made under identical conditions, shown in Table 2, was around 22,000 (standard deviation: ca. 2200) and average repeat units in one coating polysulfonamide chain was 28. The end-group ratio of SO_2Cl/NH_2 ranged from 1.9 to 3.1, except in sample M-8, which indicated that the coating polymer

chain was primarily dominated by SO_2Cl end-groups. Also, with increasing the octanediamine deposition on the membrane surface, the average molecular weight of coating polysulfonamide was decreased (Figure 6). The data plotted in Figure 6 was the average of three samples, and the error bar presented the standard deviation (see Appendix C). These results are interpreted below.

3.4.3 Polymerization process

The chemistry of modified interfacial polymerization is very simple. A typical chemical reaction employs a diamine (A) and a disulfonylchloride (B). The intermediate of this type of reaction is believed to react by an S_N2 mechanism (nucleophilic) [23,24], to form a protonated sulfonamide which is rapidly eliminated in the presence of more base. In this study, the proton acceptor is presumed to be either an amine on a diamine molecule or the end of an oligomer chain. Under the reaction conditions with no addition of the acid acceptor, the total amount of octanediamine deposited on one piece of support membrane was approximately 0.1 mmol, and no more than one half of the diamine could participate in polymerization. The total amount of monomer I was 0.07 mmol in the 50 ml solution which corresponds to the concentration of monomer I as 1 g/L. According to the hypothesis, the octanediamine first partitioned from the solid-liquid interface into the organic phase and then meets the disulfonylchloride. Since only a small portion of the organic solution is actually in the membrane pores, the diamine is locally in large excess. Also, the kinetics of sulfonamide reaction was such that the reaction rate of a second sulfonylchloride in disulfonylchloride was ten times lower than the first one [25,26]. Thus, the disulfonylchloride could be acylated to a large extent to form dimer (AB) or trimer ABA. Further dissolving

octanediamine could either react with the dimer (AB) or move forward into the organic phase to react with new disulfonylchloride. So, the reaction and polymerization should take place at relatively large distance into the organic phase.

The turbidity of the reaction medium increased as polymerization proceeded, as presented in Figure 5. Only 10% of the total octanediamine was used for the coating polysulfonamide. The large molecular structure of monomer I (Mw=705) caused the very low solubility in the weak solvent, CCl_4/CH_2Cl_2 (45/55), which was 3.5 mmol/L (2.6 g/L), as shown in Figure 2. The solubility of oligomer or polymer should be much less than this value. When the molecular weight of the first formed polysulfonamide exceeded the solubility limits, precipitation resulted. Evidence presented in Table 1 confirmed that the average molecular weight of coating polysulfonamide was relatively low; approximately 22000 corresponding to a degree of polymerization of 28 for a linear chain.

The polymer first formed precipitated adjacent to solid-liquid interface and these precipitated polymer formed a barrier to restrict the further diffusion of octanediamine into the organic phase. The depleted monomer I inside the membrane pore was compensated by the diffusion of monomer I from the bulk phase into the membrane pores. The diffusion process only needs a few seconds as estimated above. As polymerization progresses, free monomer I needs more time to diffuse into the membrane pores. The precipitated polymer continuously reacts with the free monomer I coming from the bulk solution. So, the final polymer chain was found to be primarily dominated by SO_2Cl end-group. The exception, found in Table 2, sample M-8, was probably caused by sample variation.

The pore size of the nascent membranes used in this work was 1 μm (measured by bubble point method at 3M). Most polymerization could take place

inside the membrane pore or in the vicinity of the external membrane surface. The theoretically calculated coating thickness was 8 nm in terms of mass gain (12%), density of coating polymer (0.95 g/cm^3) and specific surface area of the nascent membrane (15 m^2/g), which is measured *via* BET method by 3M. Actually, the coating layer may be less dense than bulk polymer so that the real thickness could be more than 8 nm. As yet, an appropriate method to measure the real thickness of coating polysulfonamide has not been found.

3.4.4 Evaluation of the hypothesis

According to the stated hypothesis, the modified interfacial polymerization was controlled by the solubility of octanediamine in the organic solvent, sulfonamide reaction rate, and diffusion rate of octanediamine and monomer I. As more polymerization took place in the vicinity of the solid-liquid interface, more coating polysulfonamide was obtained. Therefore, increasing reaction rate and decreasing the solubility of the diamine in the organic solvent could be beneficial to the coating process. The octanediamine solubility study suggested using a weaker organic solvent could reduce solubility of diamine and restrict the diamine diffusion extensively, thus reducing the size of the polymerization zone. The selection of solvent strength should play a key role in the coating process. This speculation was confirmed by evidence described in Chapter 2. When CCl_4 was added into the organic phase to reduce the solvent strength, the surface morphology became more even and smooth. Unfortunately, reducing the strength of the organic solvent led to a significantly lower solubility of monomer I, as illustrated in Figure 2, which was unfavourable for the coating process. Also, the less the strength of

the organic solvent, the lower the molecular weight of the coating polysulfonamide. A compromise had to be made between the strong solvent and poor solvent. The optimum reaction medium found to obtain an even and smooth coating layer was at volume ratio 45/55 of CCl_4/CH_2Cl_2, which is a relatively weak solvent for the coating polymer. Further increasing the percentage of CCl_4 in the solvent mixture, both monomer I and the oligomer solubility significantly decreased, which caused a precipitation of low molecular weight oligomer. Scattered beads and tiny chunks of polymer on the membrane internal coating surface were found by SEM (Chapter 2) with such a poor solvent.

Increasing the monomer concentration, to enhance the reaction rate, is hypothesized to be favourable for the coating process. This idea has been supported experimentally by either increasing the amount of loading diamine, or by increasing concentration of monomer I, as described in Chapter 2. Increasing the amount of octanediamine deposition would provide more diamine for polymerization to increase the mass gain of coating polysulfonamide. As the polymerization proceeded, more diamine participated in the reaction causing the formation of more polymer chains, thus, decreasing the average molecular weight of the coating polymer, as shown in Figure 6. In the final polymer coating, the layer adjacent to the membrane surface presumably contains the initially formed high molecular weight fraction, whereas a lower weight fraction formed within the organic phase away from the interface, lowering the average molecular weight of coating polysulfonamide. This result is consistent with the decrease of the average molecular weight of coating polysulfonamide, and increase in mass gain with increase in the amount of loading diamine. Matching the equivalent concentration of reactants in the polymerization zone is known to be important to obtaining high molecular weight coating polymer. However, the limited solubility of the

polysulfonamide and the solubility of loaded octanediamine in the weak solvent make this issue less feasible.

Addition of an acid acceptor, such as triethylamine, in the polymerization system is another route to increase the amount of octanediamine for polymerization, as the diamine does not have to act as an acid acceptor. In principle, the result of adding twice the moles of triethylamine as that of monomer I, shown in Chapter 2, was equivalent to doubling the amount of diamine available for polymerization. In contrast to polyamide formation by conventional interfacial polymerization [3,4], polymerization time is an important variable for the polysulfonamide coating process because the solid state octanediamine deposited on the nascent membrane internal surface needs time to dissolve and diffuse into the organic phase. Due to a relatively slow reaction rate, low molecular weight oligomer also needs time to grow to form long chain polymer and to precipitate. Thus, for the first 15-20 min of polymerization, the increase of mass gain of the coating polymer is very slow. As polymerization proceeded, the precipitation of polymer appeared to form a barrier covering the whole interface, which would retarded the diamine diffusion into the organic phase. Finally, when all of the source diamine had dissolved and diffused into the organic phase, additional coating was presumably much slower Polymerization apparently still occurred in the organic bulk phase and precipitated randomly on the membrane surface, but th polysulfonamide so made could not form an even coating layer. The agglomerated segments randomly stuck on the membrane internal surface to form "fish scales" as shown in Chapter 2. This physical evidence also strongly supports the proposed hypothesis.

The effect of addition of the crosslinking agent, reported in Chapter 2, appeared to be in conflict with the expected result. Addition of a trifunctional

crosslinking agent should have helped to form a polymer network which could easily cover the internal surface of the nascent membrane, significantly improving mass gain. This was not found when 1,3,6-naphthalene trisulfonylchloride (NTSC) was added to the polymerization system, although there was an increase of mass gain, as presented in Chapter 2. As mentioned previously, the kinetics of disulfonamide reaction shows that the reactivity of the second sulfonyl chloride in the naphthalene ring is ten times lower than the first one. The reactivity of the third sulfonyl chloride in NTSC may be speculated to be even lower than the second one. In this case, a part of NTSC in the polymerization system may not act as a trifunctional agent, only as a difunctional agent.

Overall, a hypothesis for the mechanism of the modified interfacial polymerization/coating process has been extensively investigated by studying the influence of most of the important variables on the coating process, including selection of solvent, monomer concentration, polymerization time, and addition of acid acceptor and crosslinking agent. Data obtained so far support the hypothesis or can be reasonably interpreted by the hypothesis. Since this modified interfacial polymerization is controlled by the reaction rate, the solubility of monomers, and the diffusion rate of diamine and monomer I in the organic phase, the process is more complex than the case of conventional polyamide interfacial polymerization. Our hypothesis gives us a qualitative picture for what is happening during the coating process, although the full details of the mechanism of modified interfacial polymerization are not completely understood. The mechanistic study defines the most important principles of modified interfacial polymerization which can be varied to control the coating process and obtain a better coating layer on the internal surface of the membrane. More detailed and quantitative study on this

mechanism need to be completed in order to provide a guide for this coating process.

3.5 Conclusions

An hypothesis for the modified interfacial polymerization/coating process, proposed diagrammatically in this chapter, was investigated experimentally along with data reported in Chapter 2. Most results either strongly supported the proposed hypothesis or can be reasonably interpreted by the hypothesis. Although the evidence is qualitative, the important principles discussed in this study about the coating mechanism give researchers a better understanding of this new type of interfacial polymerization.

This chapter also reported the development of a new method, using neutron activation analysis, to analyze the end-groups of linear polysulfonamide in the solid state, and to assess the average molecular weight of this polymer without destroying the membrane. The average molecular weight of thin film coating polysulfonamide was found to be 22,000 (standard deviation: ca. 2,200). End-group analysis of linear coating polysulfonamide indicates that the polymer chain was primarily dominated by SO_2Cl. Higher octanediamine concentrations slightly lowered the average molecular weight of the coated polysulfonamide.

References:

(1) J.M. Dickson, K. Rilling, R.F. Childs, B.E. McCarry and D.R. Gagnon, Development of a functionalized thin film composite coating for the internal structure of polypropylene microfiltration membrane, to be sumitted, J. Membrane Sci., (1997).

(2) Li Wang, J.M. Dickson, R.F. Childs, B.E. McCarry and D.R. Gagnon, Coating internal surface of microfiltration polypropylene membranes by modified interfacial polymerization. Part I: Coating technology, to be submitted, J. Membrane Sci., (1997).

(3) E.L. Wittbecker and P.W. Morgan, Interfacial polycondensation I, J. Polym. Sci., XL, (1959) 289-297

(4) P.W. Morgen and S.l Kwolek, Interfacial polycondensation II. Fundamentals of polymer formation at liquid interface, J. Polym. Sci., XL (1959) 299-327.

(5) R.E. Whitfield, L.A. Miller and W.L. Wasley, Interfacial polycondensation. I. The formation of surface graft polymers on wool, J. Appl. Polym. Sci., 8 (1964) 1607-1617.

(6) R.E. Whitfield, L.A. Miller and W.L. Wasley, Wool fabric stabilization by interfacial polymerization. Part III: Polyurethanes, Textile Research J., 32 (1962) 743-750.

(7) R.E. Whitfield, L.A. Miller and W.L. Wasley, Wool fabric stabilization by interfacial polymerization. Part IV: Polyureas, polyesters, polycarbonates, and further studies on polyamide, Textile Research J., 33 (1963) 440-444.

(8) J.E. Cadotte, R.S. King, R.J. Majerle and R.J. Petersen, Interfacial synthesis in the preparation of reverse osmosis membranes, J. Macromol. Sci.-Chem., A-15 (1981) 47-75.

(9) S.A. Sundet, Ion-rejecting surface layers based on the polyamide from

1,3,5-cyclo-hexanetricarbonyl chloride and m-phenylenediamine, Abstr. Int. Congr. Membr. Membr. Processes, Tokyo, 1987, p. 60A0906.

(10) S.P. Chen and K. Chan, Thin film composite membrane by interfacial reaction: mechanism of membrane formation, Proc. Int. Membr. Conf. on the 25th Anniversary of Membrane Research in Canada, 1986, p. 279.

(11) J. Ji, Ph.D Thesis, Department of Chemistry, McMaster University, 1996.

(12) Quantitative Organic Analysis via Functional Groups, S. Siggia and J.G. Hanna (Ed.), Fourth edition, John Wiley and Sons, New York, 1979 p. 356.

(13) Condensation Polymers: By Interfacial and Solution Methods, P.W. Morgan (Ed.), Interscience, New York, 1965.

(14) V.V. Korshak and T.M. Frunze, Synthetic Heterochain Polyamide, Israel Program for Scientific Translations Ltd, Jerusalem, 1964.

(15) L.V. Sokolov and L. Borisovich, Synthesis of Polymers by Polycondensation, Isreal Program for Scientific Translataion Ltd, Jerusalem, 1968.

(16) L.M. Litvinenko and A.F. Popov, Effects of the structure of alkylamines on their reactivities with aryl sulfonamides, Zh. Obshch. Khim., 38(9) (1968) 1969-1978.

(17) I. Mita, K. Toyoshima and A. Okamoto, Intramolecular catalysis and cyclization in the reaction of α, ω-diaminooligomethylenes with bifunctional sulfonyl chloride; Effects of chain length of polycondensation reaction, Eur. Polym. J., 19(8) (1983) 657-660.

(18) C.R. Wilke, Correction of diffusion coefficients in dilute solution, Chem. Eng. Progr., 45 (1949) 218.

(19) C.R. Wilke and P. Chang, Estimation of liquid diffusion coefficients, AIChE J., 1 (1955) 264.

(20) Mass-Transfer Operations, R.E. Treybal (Ed.), Third edition, McGraw-

Hill, New York, 1980, p. 90.

(21) Facilities for Chemical Analysis by Neutron Activition Techniques, McMaster Nuclear Reactor, McMaster University, 1993.

(22) B. Trushinski, J.M. Dickson, T. Smyth, R.F. Childs and B.E. McCarry, Studies on thin-film composite polysulfonamide reverse osmosis membranes: Fabrication, crosslinking, and chlorine resistance, Presented at annual AIChE meeting, Chicago, 1996.

(23) L.M. Litvinenko, N.T. Maleeva, V.A. Savelova and T.D. Kovach, Deuerium kinetic isotopic effect in sulfonamide-formation reactions, Zh. Obshch. Khim., 41(12) (1971) 2615-2618.

(24) L.M. Litvinenko and A.F. Popov, Effect of the Structure of arensulfonyl chloride on the rate of their reactions with aliphatic amine, Zh. Obshch. Khim., 36(9) (1966) 1517-1524.

(25) A. Okamoto, T. Aoki and I. Mita, Preparation and reactivity of a primary amino group attached to the center of a polymethylene chain, Eur. Polym. J., 19(8) (1983) 661-665.

(26) A. Okamoto, K. Toyoshima and I. Mita, Kinetic study on reactions between polymer chain-ends-II; Reaction between chlorosulfonyl-ended and primary amino-ended polyxylethylene followed by fluorometry, Eur. Polym. J., 19 (4) (1983) 341-346.

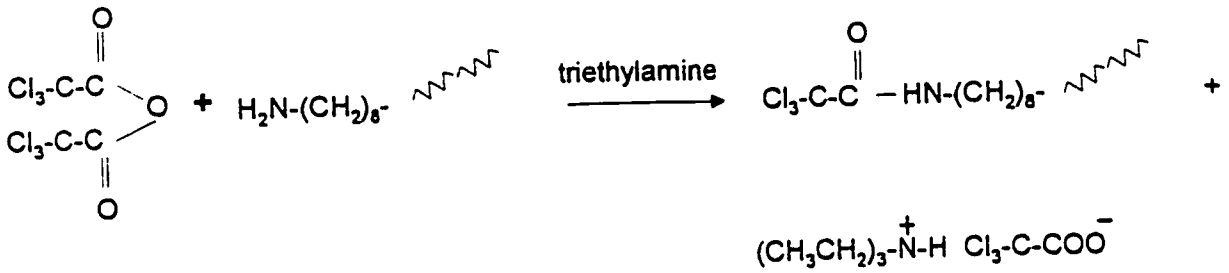

Scheme 1. Primary amine end-group reaction with trichloroacetic anhydride.

Table 1. End-group estimation by NAA and average molecular weight calculation

No.	Mass Gain (%)	DK[1] (g)	SO_2Cl[2] (μmol)	NH_2[3] (μmol)	Total End-group (μmol)	Mn	Repeat[4] Unit
M-3	12.3%	0.01049	0.68	0.22	0.90	23000	30.0
M-4	11.0%	0.01032	0.76	0.25	1.01	20000	26.3
M-5	11.3%	0.00920	0.62	0.33	0.95	19000	24.9
M-6	10.9%	0.00996	0.54	0.23	0.77	26000	33.3
M-7	11.5%	0.01062	0.67	0.36	1.03	21000	26.6
M-8	11.2%	0.00970	0.36	0.56	0.92	21000	27.2
					AVG	22000	28.1
					STD	2200	2.8

1 Mass of coating polysulfonamide containing photoactive diazoketone group.

2 SO_2Cl end-group is estimated by the term (N_1-N_{10}) as shown in the equation of total end-group estimation, in which $N_{10}=0$.

3 NH_2 end-group is estimated by the second term, $[(N_2-N_{20})-(N_1-N_{10})]/3$ as shown in the equation of total end-group estimation. N_{20} is measured to be 0.28 ±0.05 (μmol).

4 Repeat Units is calculated by the average molecular weight divided by the molecular weight of one repeat unit (Mw of one repeat unit is 776; from structure in Scheme 1, Chapter 2).

Table 2. Estimation of the ratio of the two types of end-group.

No.	SO_2Cl (μmol)	NH_2 (μmol)	SO_2Cl/NH_2
M-3	0.68	0.22	3.1
M-4	0.76	0.25	3.0
M-5	0.62	0.33	1.9
M-6	0.54	0.23	2.3
M-7	0.67	0.36	1.9
M-8	0.36	0.56	0.6

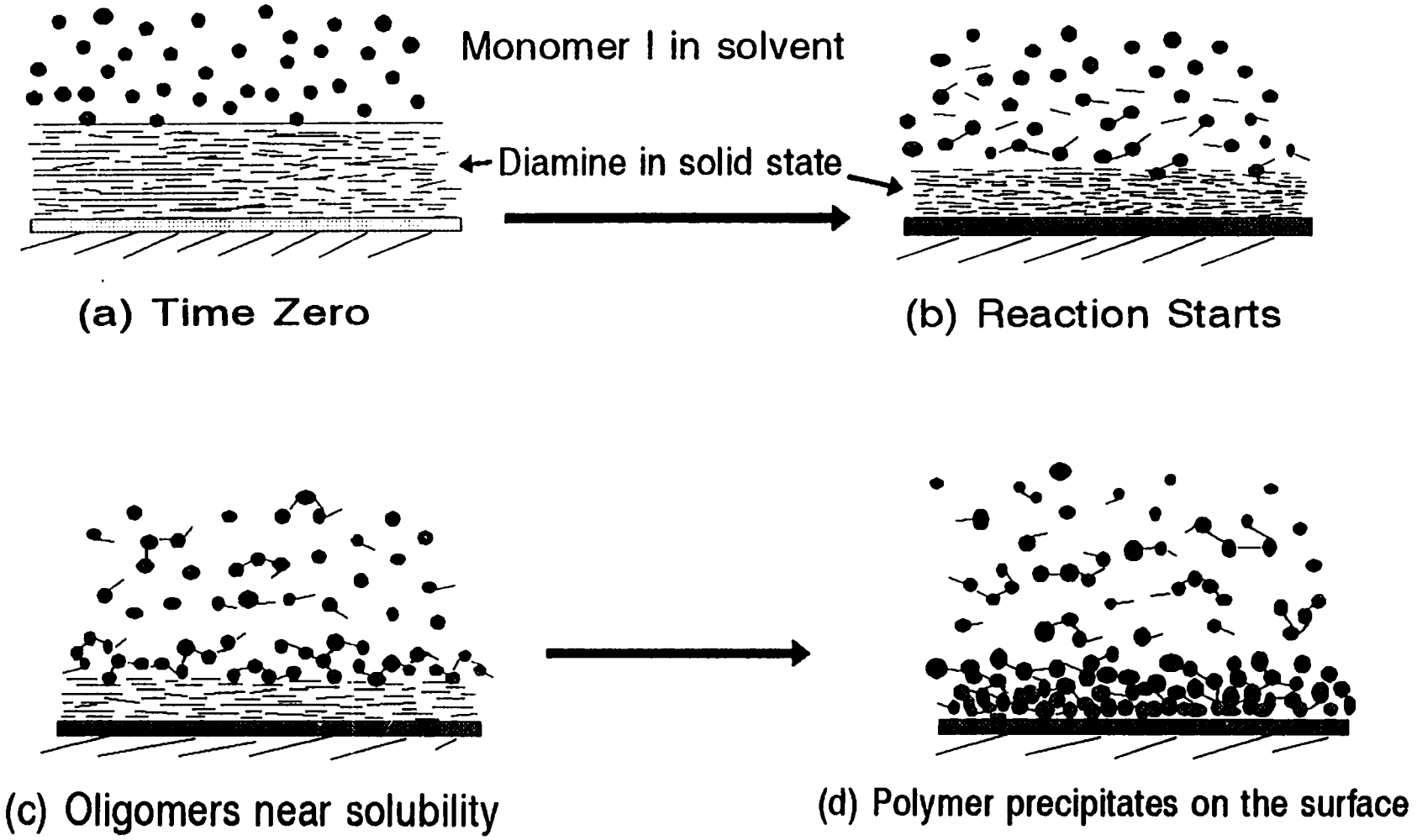

Figure 1. Schematic of modified interfacial polymerization process.

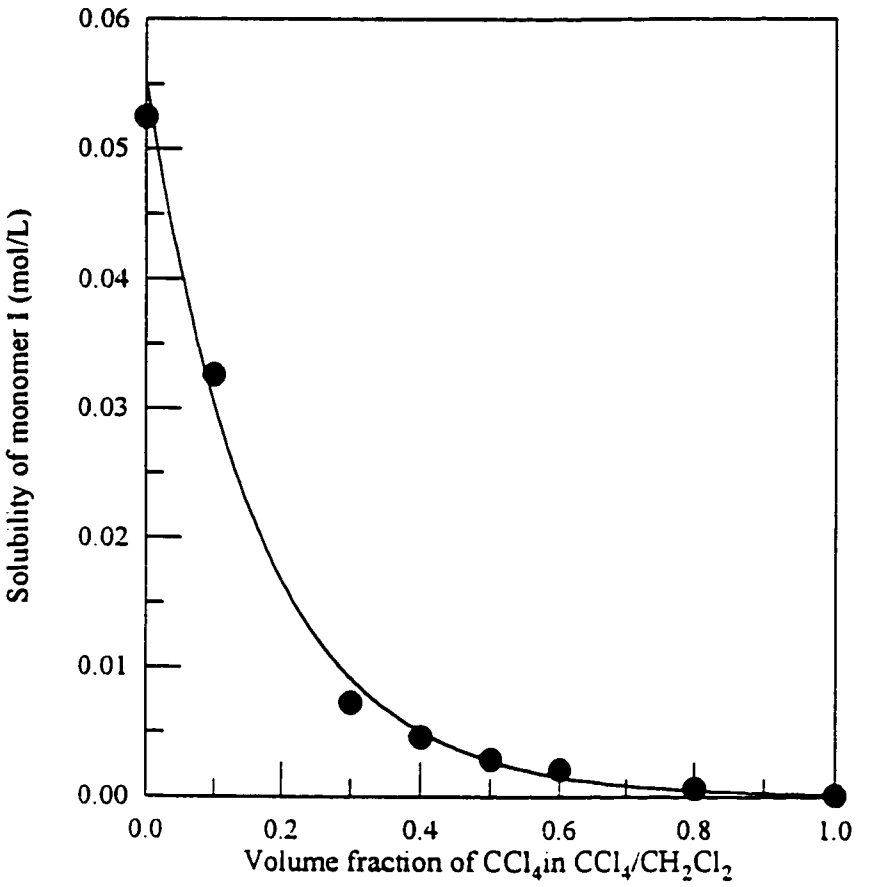

Figure 2. Solubility of monomer I in different CCl_4/CH_2Cl_2 mixtures.

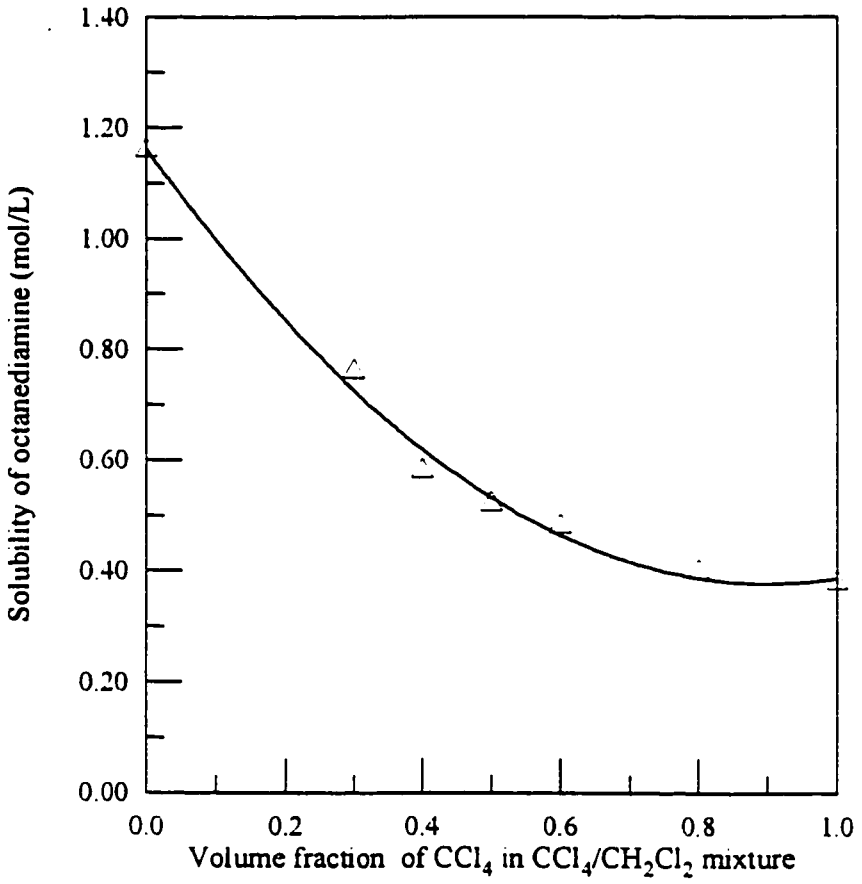

Figure 3. Solubility of octanediamine in different CCl_4/CH_2Cl_2 mixtures.

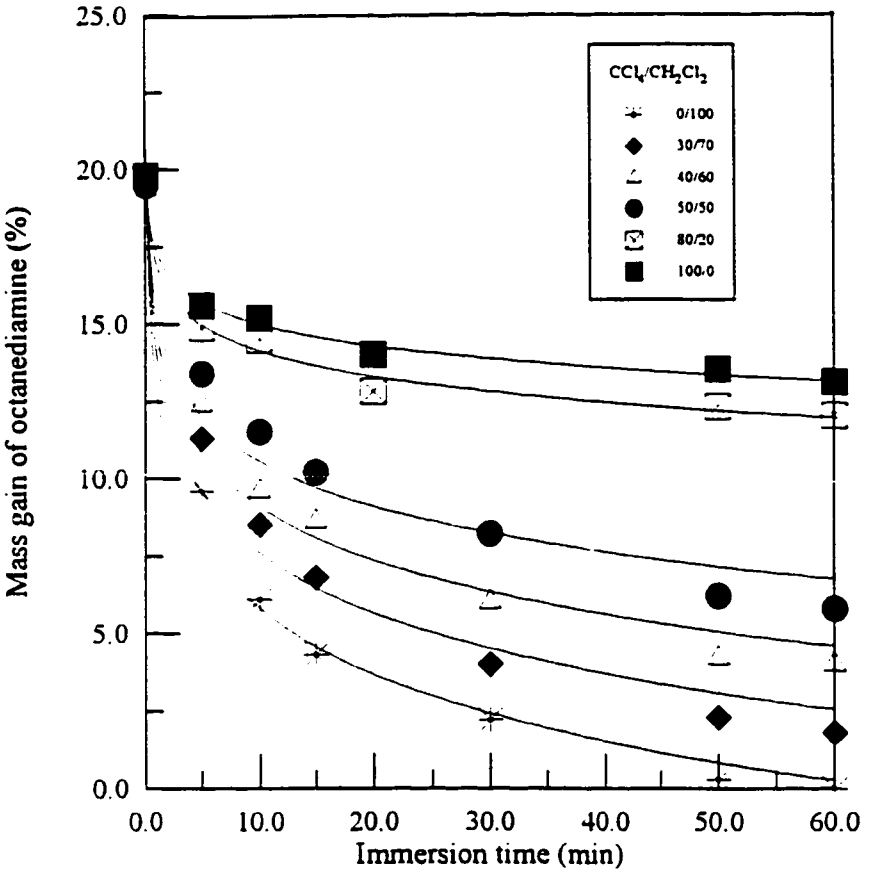

Figure 4. Dissolving of loaded octanediamine on the membrane surface into different solvent mixtures.

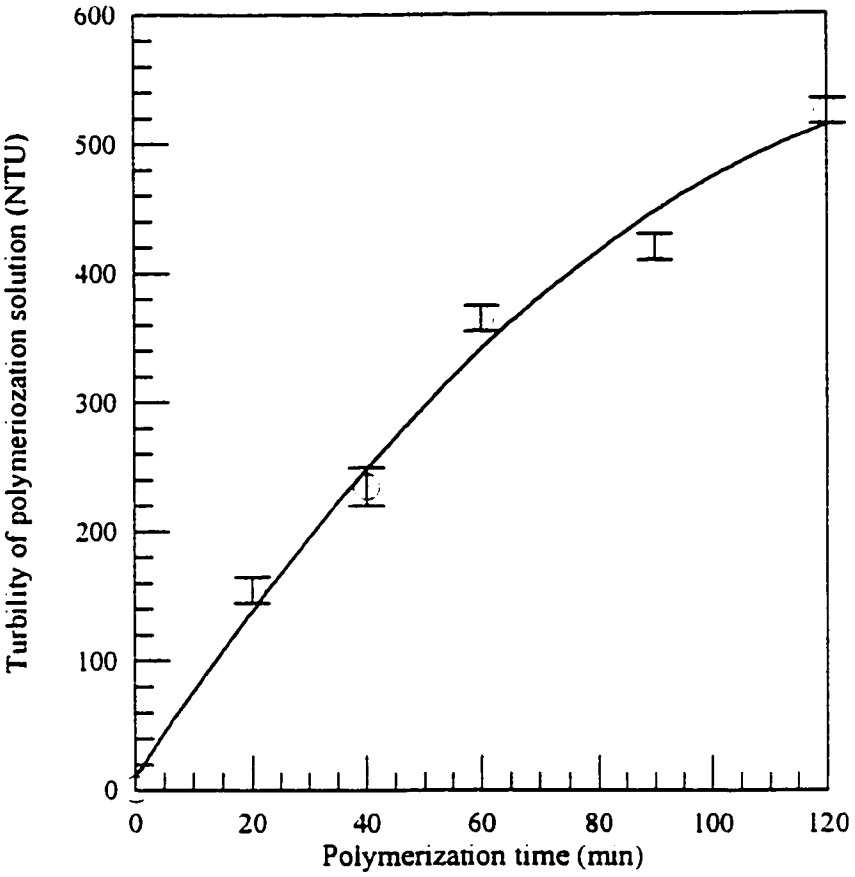

Figure 5. Effect of polymerization time on the turbidity of the reaction solution.

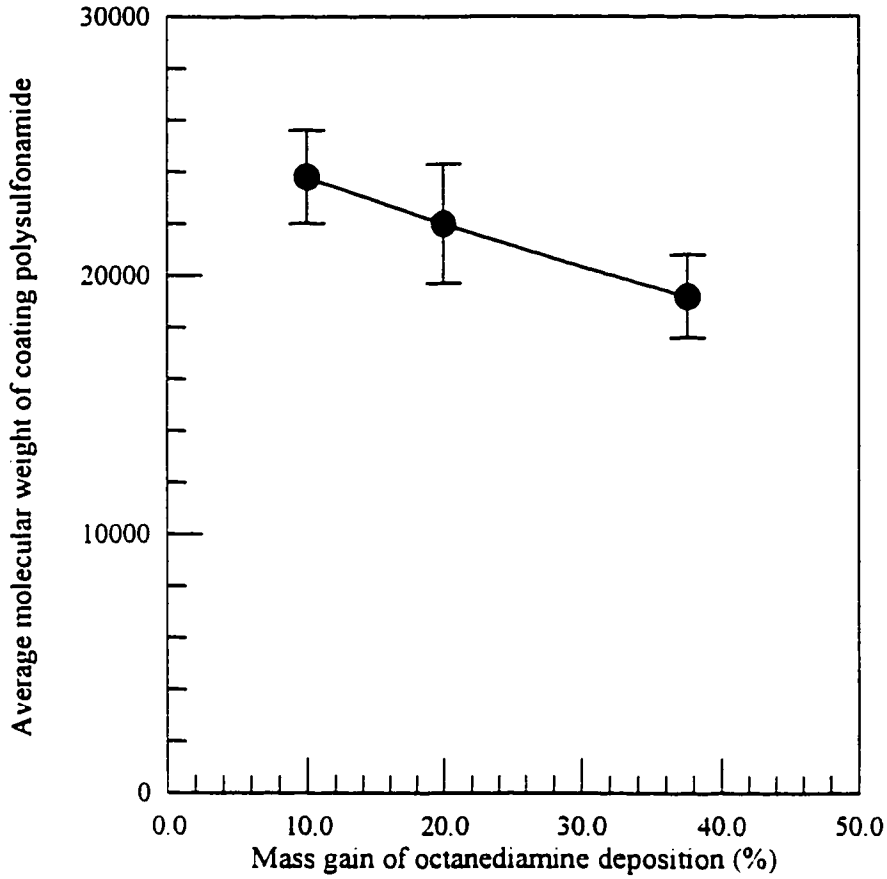

Figure 6. Effect of octanediamine mass gain on the average molecular weight of coating polysulfonamide.

Chapter 4

Coating the Internal Surface of Polypropylene Microfiltration Membrane by Modified Interfacial Polymerization. Part III: General Applicability of the Coating Technology.

ABSTRACT

This Chapter focuses on examining the other condensation polymers for this new coating technology. Polyester and polyamide were successfully coated on the internal polypropylene membrane surface by this new coating technology. By adjusting the parameters discussed in Chapter 2, the average mass gain of polyester and polyamide were 106% and 10.5%, respectively. The surface morphology of coating polyester and polyamide was analyzed by SEM. The chemical composition of the coating polyester was characterized by FT-IR.

Keywords: Polyester, Polyamide, Internal surface, Microfiltration membrane, Coating.

Introduction

The previous study of the coating technology is restricted to polysulfonamide containing the photoactive group, diazoketone, as described in Chapters 2 and 3. The advantage of this coating polysulfonamide is to allow further functionalize the membrane surface by a photochemical transformation. However, is it possible to apply this new technology to coat other condensation polymers on the internal surface of polyolefin microfiltration membrane? In Chapter 2, it has been found that the selection of solvent is a critical issue for obtaining a smooth and even coating layer. All variables of the coating process, studied in Chapter 2, were for the octanediamine and disulfonyl chloride system. In order to prove the general applicability of this coating technology, other monomer systems should be examined for this coating polymerization. Thus, an attempt has been made to coat polyester made by polycondensation of diacid chloride with polyethylene glycol, and polyamide made by polycondensation of diacid chloride and octanediamine, onto the internal surface of polypropylene microfiltration membranes. The preliminary results of these experiments are examined in this Chapter.

4.1 Experimental

4.1.1 Materials

The physical and chemical properties of polypropylene microfiltration membranes have been reported in Chapter 2. Hexane, methylene chloride, carbon tetrachloride, octanediamine, isophthaloyl chloride and trimesoyl chloride were

purchased from Aldrich Co. All chemical reagents used in this study were analytical grade.

4.1.2 Polyester coated membrane

The polypropylene microfiltration membrane was first soaked in a polyethylene glycol (Mn=200) solution (10 wt% in methanol), dried, and then put into an isophthaloyl chloride/trimesoyl chloride solution (total 10 g/L in hexane). Trimesoyl chloride was added into the solution as a crosslinking agent with two different ratios of 5:1 and 2:1 (isophthaloyl chloride: trimesoyl chloride) by weight. The polymerization was carried out at 50°C for 30 to 60 min. After the formation of the polyester coating layer, the membrane was washed with methylene chloride and methanol three times each.

4.1.3 Polyamide coated membrane

The polypropylene membrane was first soaked in octanediamine solution (20 g/L in methanol) for approximately 5 minutes, dried, and then put into an isophthaloyl chloride/trimesoyl chloride (5:1 by weight) mixture solution (total 2 g/L in methylene chloride). Trimesoyl chloride was added into the solution as a crosslinking agent. The polymerization was carried out at 50°C for 30 minutes. After the formation of the polyamide coating layer, the membrane was washed with methylene chloride and methanol three times each.

4.1.4 Mass Gain, SEM and FT-IR

The polyester and polyamide membranes were characterized by mass gain, SEM and FT-IR. The mass gain of the coating layer has been defined in Chapter

2. The surface morphology of the coated membrane was examined by SEM. FT-IR was employed to determine the chemical composition of the coating polymer.

4.2 Results and Discussion

4.2.1 Evaluation of polyester coated membrane

The chemistry of polyester formation is simple, as shown in Scheme 1. The diol group at the end of polyethylene glycol (PEG) chain reacted with diacid chloride to form polyester which eliminates HCl. As discussed in Chapter 2, the critical parameter involved in this new coating technology is the selection of solvent. Several solvents for coating polyester onto the internal surface of the microflitration membrane have been tested, as shown in Table 1. The results indicated that no coating polymer was formed on the internal surface of polypropylene membranes when using CH_2Cl_2 or CCl_4 as a polymerization medium. The coating polymerization worked by using hexane as a reaction medium. The mass gain of polyester coating layer can be up to 120% of the mass of base membrane, depending on the polymerization time.

CH_2Cl_2 and CCl_4 both are very good solvents for the polyethylene glycol [1]. Thus, the polyethylene glycol can rapidly dissolve into the solvent, to form the polyester in the bulk solution. No coating layer can be formed on the interface of the membrane. Hexane is a poor solvent for the polyethylene glycol [1] and the polymerization zone can be restricted into the area adjacent to the membrane surface. High mass gain is achieved, up to 120%. These results are in agreement with the previous discussion of selection of solvent for this new interfacial polymerization in Chapter 2. Also, these results are supporting evidence

to the hypothesis of the mechanism proposed in Chapter 3.

Polymerization time has an impact on the mass gain. When polymerization time increased from 30 min to 60 min, mass gain of coating polyester is enhanced from 78% to 106%, as shown in Table 1. By contrast, in a stirred homogeneous solution, the reaction between polyethylene glycol and diacid chloride can be completed in a second. However, the formation of the polyester layer at the solid-liquid interface dramatically slows down the diffusion of the polyethylene glycol into the organic solvent (the reaction zone), as hypothesized in Section 3.3. Afterward, the increase of the mass gain of coating polyester is controlled by the slow diffusion process through the initially formed polyester.

Increasing the amount of trimesoyl chloride in the reaction system has no significant impact on the mass gain of coating polyester, as presented in Table 1. This result is also consistent with previous results of polysulfonamide as shown in Chapter 2 [2]. According to Cadotte and coworkers, for the NS-100 reverse osmosis membrane [3], the interfacial reaction of trimesoyl chloride with piperazine produced primarily the linear polyamide, with only moderate cross-linking and one of the triacid chloride groups may be unreacted forming a carboxylic acid group when contacted with water, as shown in Scheme 1. Similarly, for the triacid chloride used here, linear polymer may be produced leaving one acid site unreacted. Hence, the relatively samll impact of increasing the amount of triacid chloride is observed.

The chemical composition of the coating polyester was characterized by FT-IR, as shown in Figure 1. Compared to the spectrum of a nascent membrane, the high intensity peak around 1730 cm^{-1} is contributed to C=O bond of the ester group. The other two characteristic peaks, at 1110 cm^{-1} and 1260 cm^{-1}, are attributed to C-O ether bond contained in the polyethylene glycol [4]. The

interesting feature found in the spectrum of the polyester coated membrane is a strong peak with high intensity around 734 cm^{-1} [4], which can be attributed to the C-Cl bond contained in the diacid chloride or triacid chloride. This result indicates that there are some unreacted acid chloride groups still remaining in the coating polyester layer; consistent with the above discussion.

The surface morphology of the coated membrane was examined by SEM, as presented in Figure 2. An even, smooth polyester coating layer on the internal surface of the PP membranes with a 95% mass gain is observed, compared to the surface morphology of nascent membrane as shown in Section 2.2.1. The coating polyester layer seems to make the surface morphology more smooth than that of the nascent membrane.

4.2.2 Evaluation of polyamide coated membrane

The interfacial reaction of diacid chloride, and triacid chloride with octanediamine is straight forward as shown in Scheme 2. Using an analogous procedure, a PP membrane coated internally with a polyamide is produced. These polyamide coated membranes were evaluated in a similar manner to the polyester membranes. An average mass gain of 10% was achieved using pure CH_2Cl_2 as the organic solvent, as shown in Table 2, similar to that achieved in previous preliminary work [2]. With increasing the concentration of octanediamine from 0.14 mol/L (20 g/L) to 0.28 mol/L (40 g/L), the mass gain of coating polyamide was increased from 10% to 15%, which is consistent with the result described in Section 2.2.3.

The surface morphology of the coated polyamide membrane was also examined by SEM. Figure 3 illustrated that there is little difference in the surface morphology of the coated polyamide, compared to the nascent membrane.

According to the previous discussion of the surface morphology of polysulfonamide coating in Chapter 2, this result can be interpreted as indicating that the coating polyamide layer is even and smooth, and distributed throughout the entire internal surface of the microfiltration membranes.

4.3 Conclusions

This Chapter demonstrated the coating of other condensation polymers onto the internal surface of microfiltration membrane using this new interfacial polymerization technique. The polyester and polyamide were evenly coated on the membrane internal surface, as determined by mass gain, SEM and FT-IR. By adjusting the reaction parameters, the coating polymerization process can be controlled. In particular, the organic solvent is a key factor to the success of the coating. The basic principles involved in the polyester and polyamide coating process are consistent with those discussed in Chapter 2, and also strongly support the hypothesis of the coating mechanism. However, the study for polyester coating and polyamide coating was just preliminary. Further study for these and other coating polymers is needed, including permeation characterization.

References

[1] J.M. Harris, Introduction of biotechnical and biomedical application of polyethylene glycol, in: J.M. Harris (Ed.), Polyethylene Glycol Chemistry, Plenum Press, New York, 1992.

[2] J.F. Wong, The experiemntal results of polyamide coating on the internal surface of PP microfiltration membranes by modified interfacial polymerization, Department of Chemistry, McMaster University, 1996. unpublished report.

[3] J.E. Cadotte, M.J. Steuck and R.J. Peterson, Research on in situ-formed condensation polymers for reverse osmosis membranes, NTIS Report No. PB 288287, 1978.

[4] D.L. Pavia, G.M.Lampman and G.S. Kriz, Introduction to Spectroscopy, Department of Chemistry, Western Washington University, Bellingham, Washington, 1979.

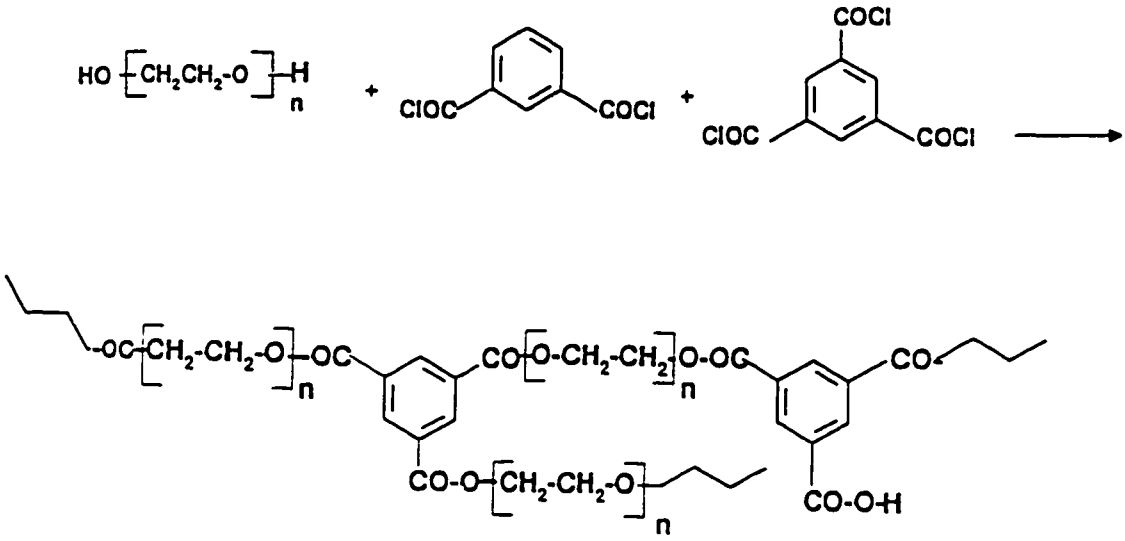

Scheme 1. Interfacial reaction of polyethylene glycol with isophthaloyl chloride and trimesoyl chloride to produce a polyester.

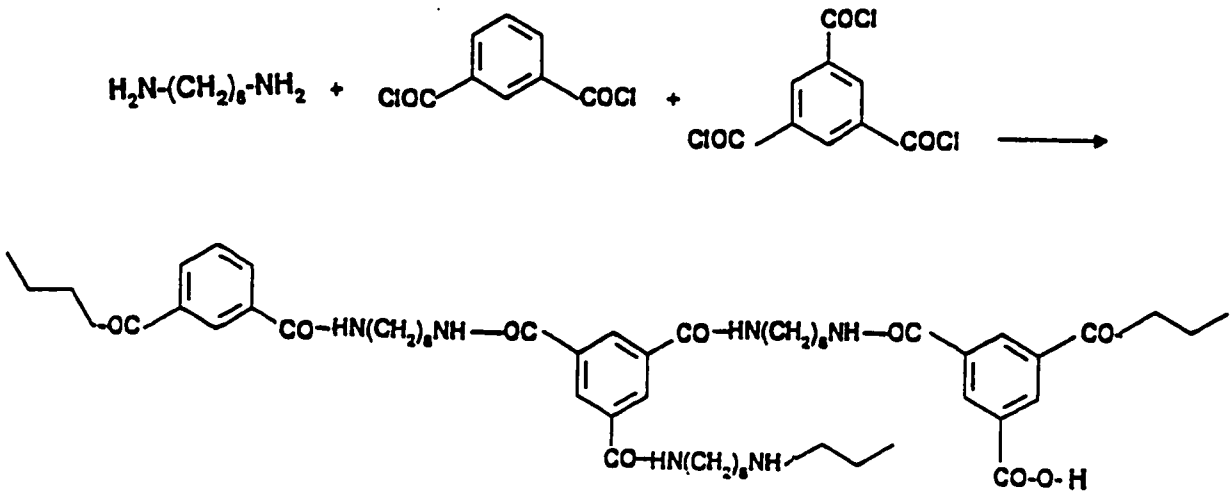

Scheme 2. Interfacial reaction of octanediamine with isophthaloyl chloride and trimesoyl chloride to produce a polyamide.

Table 1. Mass gain of polyester coated on the internal surface of polypropylene microfiltration membranes with different reaction conditions[a].

No.	Time (min)	Solvent	Di / Triacid Chloride (wt/wt%)	Mass Gain (%)[b]
PEG-1	30	Hexane	2:1	78.1±4.7
PEG-2	60	Hexane	2:1	101.5±6.5
PEG-3	30	Hexane	5:1	77.5±9.2
PEG-4	60	Hexane	5:1	106.7±11.6
PEG-5	30	CH_2Cl_2	5:1	0
PEG-6	30	CCl_4	5:1	0

[a] Temperature: 50°C; Concentration of isophthaloyl chloride/trimesoyl chloride (di/tri acid chloride): 10 g/L.

[b] All data shown in Table 1 are the average of two or more samples.

Table 2. Mass gain of polyamide coated on the internal surface of polypropylene microfiltration membranes with different reaction conditions[a].

No.	Concentration of diamine (mol/L)	Mass Gain[b] (%)
PA-1	0.14	10.1±0.6
PA-2	0.28	14.5±0.5

[a] Temperature: 30°C; Concentration of isophthaloyl chloride/trimesoyl chloride: 2 g/L (5:1); Solvent: CH_2Cl_2; Reaction time: 30 min.

[b] All data shown in Table 2 are the average of two or more samples.

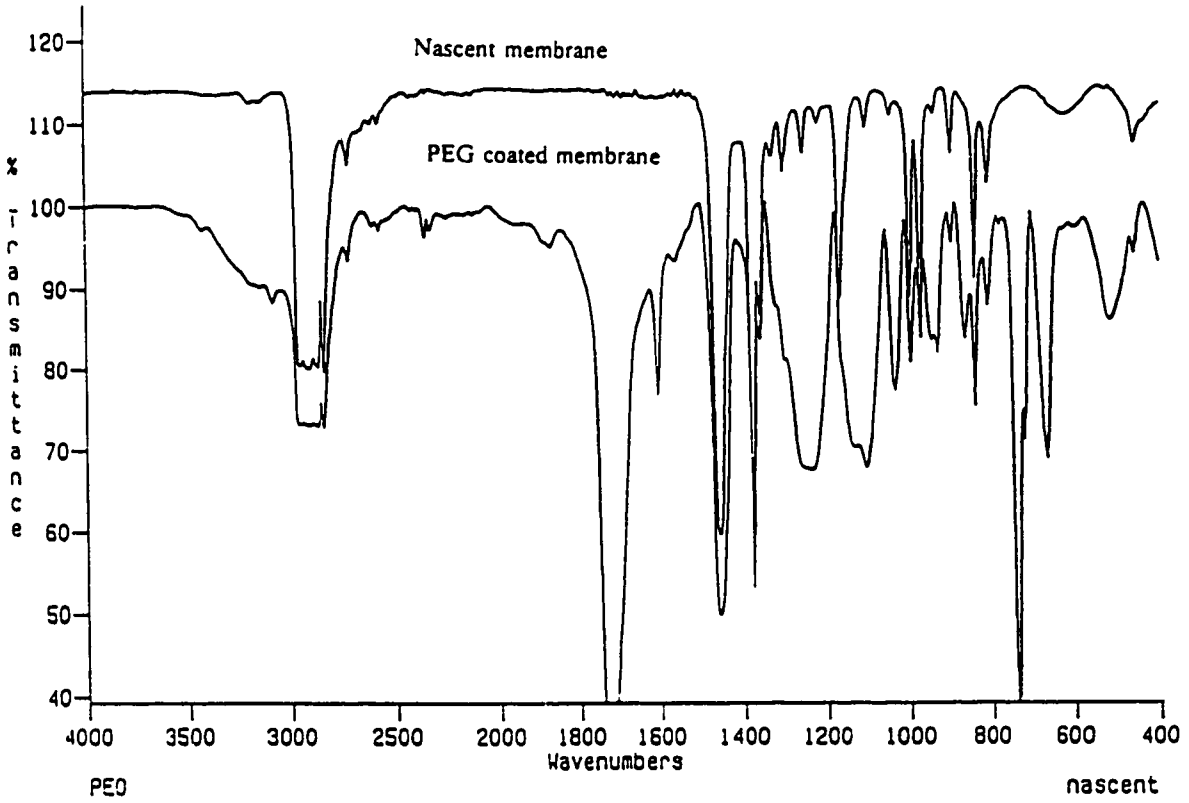

Figure 1. FT-IR spectra of the polyester coated membrane compared to the nascent membrane. Reaction conditions: temperature: 50°C; concentration of isophthaloyl chloride/trimesoyl chloride (2:1): 10 g/L; reaction time: 60 min; solvent: hexane.

Figure 2. SEM of surface morphology of polyester coated membrane with a mass gain of 95%. Reaction conditions: temperature: 50°C; concentration of isophthaloyl chloride/trimesoyl chloride (2.1). 10 g/L; reaction time: 60 min; solvent: hexane.

Figure 3. SEM of surface morphology of the polyamide coated membrane with a mass gain of 15%. Reaction conditions: temperature: 50°C; concentration of isophthaloyl chloride/trimesoyl chloride (5:1): 2 g/L; reaction time: 30 min; solvent: CH_2Cl_2.

Chapter 5

Functionalized Polypropylene Microfiltration Membranes by Photochemical Modification.

ABSTRACT

Modification of the surface chemical functionality of a polysulfonamide coated membrane containing a photoactive diazoketone group (DK) can be achieved *via* a photochemical reaction in the presence of an appropriate medium. Thus, membranes containing indene acid, glycolic acid ester, polyethylene glycol ester and bromoethyl ester functionalities were obtained from a standard precursor membrane. Surface analysis techniques including, FT-IR, neutron activation analysis, and surface wettability measurement, were employed to confirm the changes in the chemistry and surface properties of the coated membranes. The photochemical conversion of the starting diazoketone membranes to bromoethyl ester, indene acid and glycolic acid membranes was shown to proceed with 80%, 65% and 86% efficiency, respectively. The conversion of diazoketone group to polyethylene glycol ester is 40% due to a competing side reaction. The charge density of the diazoketone (DK) control membrane and corresponding functionalized membranes was also determined. The wetting surface tension, γ_w, was determined using a series of wetting solutions of different surface tensions. The photochemically modified membranes were found to be more hydrophillic than the starting DK membrane.

The microfiltration flux and separation performance of these membranes were examined using polystyrene latex (PSL) and carboxylate modified latex (CML) spheres as probes. A lower separation of PSL and CML spheres was found for the functionalized membranes compared to the starting DK membranes and the nascent membrane (uncoated). The pure buffer flux was found to increase after both coating and further photochemical modifications of the coating layer. These results suggest that the increase of hydrophilicity of the photochemically functionalized membranes was the dominant factor for changing the membrane performance. The degree of membrane fouling after the separation tests was studied by resistance-in-series analysis and SEM. The fouling degree of the functionalized membranes, indene acid and glycolic acid ester membranes, were found to be significantly reduced compared with to the nascent membrane, which led to an improvement in the effective life-time of the membranes .

Keywords: Photochemical modification, Indene acid, Glycolic acid, Polypropylene membrane, Microfiltration.

Introduction

Strong interest has been generated in recent years in the surface modification of polyolefin membranes by the introduction of chemical functionality. Indeed, functionalized polyolefin membranes are becoming commercially important with a variety of applications. Of all the various methods for the surface modification of polyolefin membranes, chemical modification is attractive in that the surface chemistry of polymeric membranes can be completely changed. Surface modification techniques include surface coating, surface degradation, surface hydrolysis, plasma discharge treatment, as well as radiation-induced, photochemically-induced, or catalytic-initiated graft co-polymerization. [1] The technique of graft copolymerization offers an effective approach to functionalizing polyolefin membranes, and expands the range of potential uses of the polyolefin. [2] The approach of surface coating with subsequent chemical modification is pursued in the current work.

Microporous polypropylene (PP) membranes, made by thermal induced phase separation (TIPS) method, are commonly used as microfiltration membranes. This polypropylene microfiltration membrane has many desirable properties as mentioned in Chapter 2 but is limited in its application in several technologically important fields due to the hydrophobic character and lack of chemical functionality. Many attempts have been reported on changing the surface properties of polypropylene membranes by surface modification. For instance, Fang and Shi [3] prepared dialysis membranes by grafting 2-hydroxyethyl methacrylate onto the surface of a PP thin film with γ-irradiation. The grafted

membranes showed improved permeability toward urea and uric acid. Hirotsu [4] reported water-ethanol permselective membranes through plasma graft polymerization of acrylic acid/methacrylic acid onto porous PP membranes. A high permselectivity of water was achieved with ionization of the acrylic acid and the methacrylic acid-grafted membranes.

One challenge encountered in these grafting technologies is the incompatibility of the base polyolefin membrane and the coating materials. In order to get a stable grafting layer and overcome the incompatibility between the monomer of modification and the base membrane (or film) surface, a two-step surface modification of polyolefins has been introduced. [5,6] Allmer et al. [5] studied a two-step grafting method to modify the polyethylene film surface for biomaterial applications. The first step was to graft the glycidyl methacrylate onto the polyethylene film surface by UV irradiation, then, polyethylene glycol (PEG) was attached to the grafted glycidyl methacrylate through reaction with the epoxy groups. The yield of PEG grafting reached 95%. The same grafting approach was also reported by Ogiara et al. [6] with different vinyl monomers. They found that it was easier to introduce the other hydrophillic monomer onto first acrylic acid grafted polyethylene film surface, compared to grafting those hydrophillic monomers directly on the polyethylene film surface, because the affinity between film substrate and monomers was an important factor for effective grafting.

Most grafting technologies mentioned above only graft the external surface of the polyolefin membrane because the grafting materials and initiators are difficult to get into the membrane pores and to graft inside the pores. For reverse osmosis and pervaporation applications, these grafting technologies are good enough to modify the top surface of the membrane which dominates the membrane selectivity. However, for microfiltration membranes, the desired functionality

should be evenly distributed on the entire internal surface of the membranes, which is a new challenge for grafting technologies. Only recently, Mika et al. [7] introduced a new class of polyelectrolyte grafted polypropylene or polyethylene microporous membranes with polyelectrolyte grafted at the top surface of the membrane as well as filling the membrane pores. The membranes showed an outstanding pH valve effect and the capability of rejecting small inorganic ions in reverse osmosis application.

In Chapter 2, a new surface coating technology has been reported to completely modify the entire internal surface of the polypropylene microporous membranes. The membrane surface properties have been changed after the coating with different polymers. This chapter demonstrates a unique method to functionalize polypropylene microporous membranes combining an initial internal surface coating and subsequent photochemical functionalization. The internal surface coating of polysulfonamide containing a photoactive diazoketone group, with microporous polypropylene membranes, was reported in Chapter 2. The coated membrane can be used as a precursor for further functionalization through converting the diazoketone group into various functionalities in the presence of an appropriate medium *via* UV irradiation. This route is expected to overcome the difficulties of conventional surface modification methods such as the preparation of a variety of different monomers and subsequent interfacial deposition as thin-films on the surface of a support membrane. Also, this technology is expected to give an even distribution of the functionality covering the whole internal membrane surface. Here, first attempts are reported to functionalize the polypropylene microporous membrane including conversion of the diazoketone group contained in the coating layer into indene acid, glycolic acid ester, bromoethyl ester, and polyethylene glycol ester functionalities on the membrane surface. The chemical

composition of functional groups on the membrane surface were qualitatively detected by FT-IR. The incorporation of the carboxylic acid functionality into the membrane coating layer by photochemical reactions have been examined by quantitatively determining the number of carboxylic acid groups on the membrane surface and by model compound reactions. A model compound chosen for the photochemical reaction in this study was bromoethanol which can form a bromoethyl ester membrane. Neutron activation analysis was employed to measure the amount of sodium and bromine associated with the carboxylic acid groups and bromoethyl ester groups on the membrane surface respectively. Both surface coating and photochemical functionalization change the surface properties of the membrane including charge density and surface wettability. The charge density of the corresponding functionalized membranes have been determined based on the amount of carboxylic acid groups present. The wetting surface tension, γ_w, was determined using a series of wetting solutions of different surface tensions. The microfiltration performance of these membranes were examined using polystyrene latex (PSL) and carboxylate modified latex (CML) spheres as probes. The fouling degree of the nascent, coated and corresponding functional membranes was studied by the resistance-in-series analysis and by SEM.

5.1 Experimental:

5.1.1 Materials

The physical and chemical properties of the polypropylene microfiltration membranes have been reported in Chapter 2. The preparation of a unique

photochemically active thin layer coated membrane in which the thin-layer contains a diazoketone group covalently bound to the polysulfonamide has also been previously described in Chapter 2. Methanol, glycolic acid, dichloromethane, carbon tetrachloride, polyethylene glycol (Mw=1000) and bromoethanol were purchased from Aldrich Chemical Co. Sodium hydroxide and standard HCl solution were from BDH. All reagents used in this chapter were analytical grade. Polystyrene latex (PSL) and carboxylate modified latex (CML) spheres with various particle size were purchased from Seradyn Inc.

The photoreactor used for photochemical surface modification of the DK membranes consists of four PRP 350 nm lamps fixed horizontally 3 cm apart and 14 cm from the membranes.

5.1.2 Photochemical reaction

The photochemical reaction is carried out in a photochemical reactor with four 350 nm lamps in the presence of an appropriate medium. The use of long wavelength (350 nm) light should allow the activation of the diazoketone group without any significant adsorption of light by molecules in the polymer back bone [8,9,10]. The base membrane should not be affected by the photoreactions and, as a result, the membranes should possess the same morphology as the starting DK membranes and differ only in the chemical composition of the coating layer.

Indene acid membrane

In the preparation of an indene acid membrane, the coated DK membrane was firstly wetted by methanol in a jar and then washed with deionized water three times in order to extract the residual methanol inside the membrane. After rinsing, the membranes were soaked in a petri dish containing 50 ml deionized water with

1 wt% acetic acid and then irradiated at 350 nm UV light for half an hour on each side. The presence of the acetic acid can eliminated the formation of a coloured (dye) by-product [11]. The polysulfonamide coated membrane (DK) containing the diazoketone group had a yellow colour. During the irradiation, the membranes lost the yellow coloration. The coated DK membranes, referred to as I-CON, were soaked in water for one hour without irradiation as a control compared to the indene acid membranes. Indene acid membranes are referred to as I-ACID.

Glycolic acid ester membrane

Glycolic acid solution was prepared by dissolving 2.0 g glycolic acid (26.2 mmol) in 100 ml distilled acetic acid in a 100 ml flask and 0.613 g (6.0 mmol) acetic anhydride was added to the solution in order to eliminate trace amounts of water present. The DK coated membrane was washed with dichloromethane in a dark jar, and dried under high vacuum for approximately four hours and then soaked in a petri dish containing 50 ml glycolic acid solution. The UV irradiation was performed with light at 350 nm for half an hour on each side of the coated membrane. The yellow coloration was lost during the irradiation. The resulting glycolic acid ester membranes referred to as G-ACID, were washed successively with acetic acid, diethyl ether and methanol three times each to remove any residual reactant and acetic acid. The coated DK membranes referred to as G-CON, were treated as above by soaking in glycolic acid solution for one hour in a dark jar, then washed with the above same procedure, and used as a control for a glycolic acid ester membrane (G-ACID),

Bromoethyl Ester Membrane

Bromoethanol was used as a model compound for the photochemical

reactions. The coated membrane was dried in the same way as the glycolic acid ester membranes and then soaked in a petri dish with 50 ml bromoethanol solution (20 vol%) using fresh diethyl ether as a solvent in order to avoid possible side reactions. The UV irradiation was performed as before. The resulting bromoethyl ester membrane referred to as B-ESTER, was washed with diethyl ether overnight to remove any residual reactants. A control membrane for bromoethyl ester functionality, referred to as B-CON, were made by the same approach without UV irradiation.

Polyethylene glycol ester membrane

Polyethylene glycol ester membranes, referred to as PEG-ESTER, were prepared by soaking the coated DK membrane into the 10 wt% polyethylene glycol (Mw=1000) solution in carbon tetrachloride. The UV irradiation was performed as before. The resulting membrane was washed by carbon tetrachloride and methanol.

5.1.3 FT-IR Spectroscopy

The chemical compositions of the corresponding functional groups on the membrane surface were evaluated using an FT-IR spectrometer (Biorad-Digilab FTS-40). Samples were prepared by compressing a piece of membrane in a metal die to form a thin, dense film.

5.1.4 Quantitative assessment of photochemical reactions

Conversion measurements of indene acid and glycolic acid ester membranes were directly carried out by determining the amount of sodium associated with the carboxylic acid group using neutron activation analysis (NAA). Both

photochemically modified membranes, indene acid and glycolic acid ester, were treated with 0.01 N sodium hydroxide for an hour to convert the carboxylic acid groups into their sodium salt. The membranes were then washed with methanol three times for approximately 30 hours total to remove any residual sodium hydroxide physically adsorbed on the internal membrane surface. The trace amount of sodium associated with carboxylic acid group was measured by neutron activation analysis. The amount of sodium in the initial DK membrane and the control membrane which is the DK membrane treated by the 0.01 N NaOH, were also measured as a background.

The conversion of the bromoethyl ester membrane was determined by directly measuring the amount of bromine by NAA on the internal surface of the bromoethyl ester membrane. The DK control membrane for bromoethyl ester, as mentioned above, was also measured as a background.

The photochemical reaction conversion for polyethylene glycol ester membrane was simply measured by a gravimetrical method because of the relative high molecular weight of the polyethylene glycol.

5.1.5 Membrane surface properties measurement

Membrane surface wettability

A series of test solutions with different surface tensions were prepared using various ratios of 2-ethoxy-ethanol and formamide (adapted from ASTM D-2578) [12,13]. The testing solutions were contained in individual syringes which allowed the administration of a droplet (ca. 0.05 ml) of each solution onto a strip of the membrane. Wetting was determined qualitatively by the membrane

becoming transparent, as viewed with a light box below the membranes. The solution with the highest surface tension that was able to wet the membrane was recorded as the wetting surface energy, γ_w.

Charge Density

The charge density of the functionalized membranes is defined as milli-equivalent of charged group per gram of membrane. The amount of charged group was determined using neutron activation technique, as discussed previously. In the case of the bromoethyl ester membrane, which was used as a model functionalized membrane, the bromine density on the membrane internal surface was defined as milli-equivalents of bromine per gram of membrane determined by NAA as discussed above.

5.1.6 Permeability and separation measurement

All membrane performance tests were performed in two stirred (450 rpm, 38.5 cm^2 effective area), 400 ml Nuclepore (Model S-76-400) cells. These cells are modified to include a thermocouple which can measure the cell temperature to ±1°C with a digital thermometer. Permeation fluxes were corrected to 25°C using the viscosity and density of water [14]. Each membrane sample was initially compacted at 20 kPa (at least 4L of buffer solution) until three successive flux measurements were constant. The buffer solution was made by ammonium chloride (1.6 g/L) and ammonium hydroxide (2.0 ml/L). The pH of the buffer solution is 9.

The cells were filled with 380 ml of feed. An initial feed sample (30 ml) was removed with a pipette for measuring of the initial feed concentration, C_i. After 100 ml of feed solution had passed under a pressure of 20 kPa, 40 ml of

filtrate was collected as a sample to determine mass and permeate concentration, C_e. Solution flux was determined by measuring the mass of permeate collected over a measured time. Solution concentrations were measured with an HF Instruments Model DRT 1000 turbidity meter [15], calibrated for each of the particular spheres. Calibrations were linear in nephelometric turbidity units (NTU) versus concentration. Polystyrene latex (PSL) and carboxylate modified latex (CML) spheres with a narrow particle size distribution (ca. 203 nm), 100 ppm buffered to pH 9, were used as feed solutions. After microfiltration, a 30 ml sample was taken of the remaining feed solution and the concentration was recorded as the final feed concentration, C_f. The separation factor was defined as follows:

$$Separation(\%) = \frac{(C_{af} - C_e)}{C_{af}} \times 100\% \qquad (1)$$

where C_{af} is an average of the initial and final feed concentrations, $(C_i+C_f)/2$.

The pure buffer permeation flux (PBP) measured before and after the solution filtration were used to determine the internal fouling resistance by the resistances in series analysis [16-18]. PBP-1 referred to the pure buffer flux measured before the solution test. The fouled membranes, after the separation test, were rinsed three times by pure buffer solution and then 800 ml of buffer solution was passed through the membrane. The pure buffer permeation flux was measured three time successively, the average of the three values was referred to as PBP-2. The qualitative extent of membrane fouling after the separation test was visibly detected by scanning electron microscopy (ISI-DS300).

5.2. Results and Discussion

5.2.1 Qualitative assessment of the photochemical transformation of the diazoketone group

The photochemical conversion of diazoketone group incorporated into the coating layer has been shown to yield initially a ketene as an intermediate. Capture of this ketene with water gives *1H*-indene-3-carboxylic acid as the ultimate reaction product [19,20]. The different functionalities, such as indene acid, glycolic acid ester, bromoethyl ester and polyethylene glycol ester, can be achieved by irradiating the initial DK membrane in an appropriate medium (Scheme 1).

The chemical composition of the different functionalities incorporated into the coating layer have been determined qualitatively by FT-IR. Previous research has shown that the chemical composition of the coating layer of the DK membrane was not affected by the dark exposure to the reaction medium including water, acetic acid, glycolic acid and polyethylene glycol [21]. The only cause for the formation of the functionality on the coated DK membrane surface was the UV irradiation. For the nascent, DK, indene acid and glycolic acid ester membranes, the FT-IR spectra are presented in Figure 1. After photochemical reaction, the characteristic diazoketone peaks at around 2117 cm^{-1} and 2665 cm^{-1} disappeared and were replaced by a peak at around 1720 cm^{-1}, characteristic of a C=O group, which strongly proves the indene acid formation on the membrane surface [8]. For the glycolic acid ester functionality, two characteristic peaks were found around 1716 cm^{-1} and 1756 cm^{-1} which overlapped to some extent. These peaks represents the two kinds of C=O bond in the ester linkage and carboxylic acid, respectively.

For the polyethylene glycol ester membrane, the same trend was found as presented in Figure 2. After the photochemical reaction with polyethylene glycol, FT-IR spectra showed a characteristic peak around 1723 cm^{-1} which was attributed to the C=O bond in the ester linkage, and another peak around 1145 cm^{-1} which was attributed to the stretch of C-O bond in the polyethylene glycol [22].

The above evidence in the FT-IR spectra qualitatively confirmed that the desired functionalities, indene acid, glycolic acid ester and polyethylene glycol ester, were successfully incorporated into the coating layer at the membrane internal surface.

5.2.2 Quantitative assessment of photochemical transformation of the diazoketone group.

Bromoethyl ester membrane

The photochemical transformation of bromoethanol, as a model compound, onto the membrane coating layer has been examined. The bromine attached on the coating layer can be directly detected by neutron activation analysis without any further post-treatment. The bromine amount physically adsorbed on the DK control membrane was also measured as a background and the amount of bromine after the photochemical reaction with bromoethanol presented in Table 1, was corrected for the background. The percent conversion of this reaction was found to be 81.5 ±2.0%. All data showed in this section and the following sections are the average of two or more samples. The detailed experimental results are in Appendix D.

Indene acid and glycolic acid ester membranes

In order to measure the efficiency of photochemical reaction with water and glycolic acid, the carboxylic acid group incorporated onto the membrane surface was convert to the sodium salt using very dilute base as mentioned in Experimental. The theoretical amount of diazoketone group, as presented in Table 2, was calculated based on the total mass of coating polymer divided by the molecular weight of one repeat unit of the coating polysulfonamide. The sodium ion associated with the acid group in the membrane coating layer was quantitatively detected by neutron activation analysis. In order to wash away the sodium ions adsorbed physically on the membrane surface without dissociating the sodium salt of the carboxylic acid, methanol was chosen as a washing solvent because sodium hydroxide was fairly soluble in methanol [23]. These data indicate the total amount (μmol) of carboxylic acid attached to the membrane surface after the entire procedure including the photoreaction and post-treatment. The amount of residual sodium on the DK control membranes was detected as a background for corresponding membranes. The sodium found on the DK control membrane may physically adsorb on the membrane surface or associated with sulfonic acid end-groups of the coating polysulfonamide caused by the hydrolysis of sulfonyl chloride groups during the polysulfonamide formation, photochemical reaction, or post-treatment.

The photochemical reaction conversion of diazoketone membrane in water was 67.1 ±6.7% which was corrected by the DK membrane background, as shown in Table 2. This conversion is surprisingly lower than the bromoethyl ester membranes. The photochemical reaction rate of *1*-diazo-*2(1H)*naphthalenone in the presence of water is much faster than with the hydroxyl reagent [24]. The lower conversion of the indene acid membrane is possibly due to the decarboxylation of

the indene acid group in the post-treatment. This decarboxylation of indene acid on the membrane coating layer in the presence of methanol will lead to the loss of the desired carboxylic acid group [25] as shown in Scheme 2.

The rate of decarboxylation of the model compound (*3H*-indenecarboxylic acid-4 diethylsulfonamide) in a variety of solvents had been studied previously [25]. They found that the rate of decarboxylation of indene acid, based on the model compound, in the presence of methanol was 9.1×10^{-7} s^{-1}. Based on this rate constant, approximately 15% of indene carboxylic acid on the membranes surface can be decarboxylated in the 30 hours washing with methanol. The real photochemical reaction conversion of indene acid would be higher than 80% if the effect of the decarboxylation of indene acid during the post-treatment is taken into account. This estimated conversion is consistent with the photochemical conversion of bromoethanol on the membrane surface as reported previously.

Glycolic acid was poorly soluble in either dichloromethane or carbon tetrachloride solvents. This solubility limitation led to the use of anhydrous acetic acid as a solvent for the photochemical reactions. The acetic acid not only dissolved the reagents but acted as a catalyst for the photochemical conversions [26,27]. The acetic acid must be dry, as described in the Experimental, to avoid the competing side reaction with water to form the indene carboxylic acid. In the case of the glycolic acid ester membranes, there is a methylene unit between the carboxylic acid and indene ring which is expected to stabilize the functional group from decarboxylation. The photochemical reaction conversion in the presence of glycolic acid was 85.9 ±2.0%. The reaction conversion of the glycolic acid ester membrane may include a small portion of indene acid functionalities because it was not possible to completely avoid trace amounts of water in the reaction system. However, the glycolic acid functional group is the major product on the membrane

surface as presented by the FT-IR spectra as shown previously. Also, the reaction conversion of glycolic acid membranes indicates that no substantial decarboxylation of the acid group occurred on the glycolic acid ester membrane during the washing process comparing to the indene acid membrane. Several side reactions such as photochemical formation of an azo-dye product, can be suppressed in the presence of acetic acid as a reaction media [26,27].

Polyethylene glycol ester membranes

The photochemical reaction conversion of polyethylene glycol (Mw=1000) was determined by gravimetrical method because of the relative high molecular weight of polyethylene glycol. The reaction conversion was found to be 40% as shown in Table 3. This low conversion compared to other functionalized membranes is probably due to the competing side reaction of diazoketone with water which existed in the reaction medium. This idea is supported by the sodium labelled analysis of polyethylene glycol ester membrane using the same method as for indene acid or glycolic acid ester membranes. Sodium was found after the post-treatment and this result is consistent with the hypothesis that some of the diazoketone groups react with water to form indene acid functionality on the membrane surface because water is much more reactive than the polyethylene glycol [24]. According to the sodium labelled analysis by NAA, the conversion of indene acid for polyethylene glycol membranes is approximate 38%. If the indene acid functionality is taken into account, total photochemical reaction conversion of the diazoketone group approaches 78%. This conversion is also in agreement with the other photochemical reaction as mentioned above.

5.2.3 Membrane surface properties

Charge density

The surface properties of the membranes were changed by both the coating and the photochemical modification. The polypropylene microfiltration membrane is inherently neutral and hydrophobic. After the photochemical modification, carboxylic acid groups were introduced onto the membrane surface and would be expected to make the membrane negatively charged at high pH. The charge density of indene acid and glycolic acid ester membrane can be defined as milli-equivalents of carboxylic acid group per gram of membrane. The DK membrane treated with the same NaOH solution was measured as a control for sodium labelled experiments.

Measurement of carboxylic acid groups on the membrane surface was based on the amount of sodium associated with the acid group as described previously. The charge densities of indene acid and glycolic acid ester membranes, after subtraction of the background, were found to be 0.071 ±0.008 and 0.091 ±0.007 meq/g, respectively, as revealed in Table 4. These charge densities are relatively low compared to other negatively charged membranes reported in the literature, where charge densities are typically around 0.9-1 meq/g or even higher [28-30]. The carboxylic acid groups of the photochemically modified membrane are mostly concentrated on the surface coating layer, not on the base materials. Thus, the effective charge density of the coating layer could be as high as 0.71 and 0.91 meq/g because the coating polymer mass is 10% of the base membrane. The effective charge density of the coating layer is very close to the reported charge density of negatively-charged membranes by other researchers.

Membrane surface wettability

Through-pore wetting of the membrane with a series of solvent mixtures of varying surface tensions was selected in this study, due to the inherent difficulty in interpreting contact angle data from a heterogeneous (i.e. porous) surface. Another reason for choosing this method was that the through-pore wetting of a membrane is a property of practical interest. The quantitative relationship between the surface tension measured by through-pore wetting, γ_w, and the more commonly used surface tension, γ_c, measured by contact angle, is not completely clear. However, we believe the trends reported in this study are indeed indicative of changes in the surface of the porous membrane. The wetting surface energy,γ_w, was defined as the value of the solution with the highest surface tension that was able to wet the membrane. The wetting surface energies of the nascent polypropylene membrane, DK membrane, and corresponding functional membranes, are presented in Table 4. The surface wettability was also modified by both coating and photochemical modification. Increases in surface wetting energy were found after both polysulfonamide coating and further photochemical functionalization; increasing in the order nascent polypropylene membrane, DK membrane, and corresponding functional membranes.

As can be seen in Table 4, a marginal increase in surface wetting energy on the membranes after photochemical funtionalization was observed instead of a significant increase of the surface wetting energy as expected. A possible explanation is that the functionalized polymer surface was reorganized by diffusion of organic functional groups away from the surface by a change in environment, such as drying the indene acid, glycolic acid ester, and polyethylene glycol ester membranes in air [31,32]. A surface with hydrophillic groups has a high surface energy which may generate a driving force to reshape the material into a

hydrophobic and thermodynamically more stable structure. If the surface molecules are mobile enough, the polar groups will turn away from the surface into the coating polymer matrix, with a subsequent decrease in surface energy and loss of wettability. This effect has been observed on polyolefins treated with a corona discharge where the oxidized surface layer dissipates during storage [31,32].

5.2.4 Permeability and separation tests

Permeability and separation tests were performed on the nascent membrane, DK membrane, indene acid membrane, glycolic acid membrane and control membranes. Polyethylene glycol ester membranes were not selected to test separation performance because of the low conversion of PEG functionality. All flux and separation data presented in this section or the following sections are the average of at least three samples. The detailed experimental results are in Appendix D.

Pure buffer permeation flux

Pure buffer permeation flux (PBP) measurements of nascent, polysulfonamide coated (DK), non-irradiated DK control, indene acid and glycolic ester membranes were carried out in a 450 ml stirred cell with pure buffer solution (pH=9.0) at 20 kPa. The results, shown in Figure 3, are the average of two or more membrane samples. An increase in pure buffer flux from the nascent, to DK and photochemically functionalized membranes was observed. The indene acid membrane demonstrated the highest pure buffer flux. This increase of pure buffer

permeation flux can be attributed to the increase of hydrophilicity of the membrane surface after both coating and further photochemical modification.

Separation test

In general, the major separation mechanism involved in microfiltration is sieving which depends on the pore size and separated particle size. However, the membrane surface properties, such as electrostatic interaction and hydrophobic interaction, also play a role in the microfiltration process. Electrostatic interactions exist between charged sites on the membrane surface and the charge groups on the separated latex particles. Hydrophobic interactions result in the adsorption of latex spheres on the hydrophobic surface. This is analogous to the tendency of hydrophobic molecules to separate into clusters in water. So, both coating and further photochemical modification of microfiltration membranes can have a significant impact to the membrane separation performance.

Separation tests of nascent, DK coated, DK control, indene acid, and glycolic acid ester membranes, were carried out in the same apparatus mentioned previously using polystyrene latex spheres (PSL) with a particle size of 204 nm and carboxylate modified latex spheres (CML) with the particle size of 203 nm as probes. The concentration of both PSL and CML test solution is 100 ppm. The test solutions were buffered to pH=9 to ensure that both the CML spheres and functionalized membranes were negatively charged. Both DK control membranes for the indene acid (I-CON) and glycolic acid ester membrane (G-CON) have been tested as revealed in Table 5. The pure buffer permeation flux of the DK control membrane is the same as the DK membranes within the range of experimental error. This result is consistent with the previous result that there was not any detectable changes on the chemical composition of the DK control membrane

compared to the DK membranes [21]. The highest rejection of both particles, PSL and CML, were found to be approximate 66% with the nascent membrane, as presented in Table 5 and Figure 4. After coating of polysulfonamide, the rejection of both particles became lower, ca. 45% for PSL and ca. 38.6% for CML, while solution fluxes became higher (0.9-0.93 kg $m^{-2}s^{-1}$), as shown in Figure 5. The further photochemical functionalization of coating layer resulted in a significant lower separations for both particles within the range of ca. 9-18% for either indene acid or glycolic acid ester membranes. The fluxes were further enhanced to 1.09-1.36 kg m^{-2} s^{-1}. The lowest separation of the CML 203 nm sphere was found to be ca. 9.6% with the indene acid membrane.

The expected, significant enhancement of the CML sphere separation by the negatively charged membrane, indene acid or glycolic acid membranes, due to electrostatic repulsion between particle and membrane surface has not been observed. In contrast, separation of the CML spheres with indene acid membranes was lower (ca. 9.6%) than the rejection of PSL spheres (ca. 18.8%). In the case of the glycolic acid ester membrane, the separation of CML particles (ca. 13.3%) was slightly lower than the rejection of the PSL spheres (ca. 15.6%), but still within the range of experimental error, as depicted in Table 5 and Figure 4. These results seem to be in conflict with other researchers [33-35]. One possible explanation is that the charge density of the indene acid or glycolic acid ester membranes (0.07-0.09 meq/g) is lower than that of sulfonated polysulfone ultrafiltration membranes reported by Nakao et al. (0.88 meq/g) [30]. Although the theoretical effective charge density of our membranes is very close to the reported value, the question remains that how effective these charge groups perform. Also, the electrostatic interaction may be weakened by adsorption of electrolyte from the surrounding buffer solution onto the membrane surface. These changes of

membrane separation performance, are directly related to the modification of membrane surface chemical properties because the physical structure of the membrane did not change significantly after the coating and further photochemical modification, as mentioned previously. The decrease of rejection of both particles (PSL and CML) and the increase of solution flux is mainly due to reducing hydrophobic adsorption of latex spheres on the modified membrane surface. The PSL and CML latex easily absorbed on the nascent membrane surface due to the hydrophobic interaction [36]. SEM pictures (Figure 6) taken on tested nascent membranes showed significant adsorption of the latex on the membrane top surface, which partially blocked the membrane pores. After polysulfonamide coating, SEM (Figure 7), a reduced adsorption of PSL and CML latex on the membrane top surface was observed. Further photochemical functionalization of the coating layer caused a further reduction of the latex particles on the membrane top surface (Figures 8 and 9). There are two factors causing the change of membrane separation performance after the photochemical functionalization: (1) the photochemical modification increases the hydrophilicity of the membrane surface and reduces the adsorption of PSL and CML latices on the membrane surface; and (2) for the rejection of negative charged CML latexes, electrostatic repulsion between the negative charged site of the latex and the carboxylic acid group on the photochemically functionalized membrane surface leads to even less adsorption of the CML latexes on the membrane surface. However, hydrophilicity of the membrane surface seems to be a dominate factor controlling the membrane separation performance. The higher flux of CML solution, compared to PSL solution, was observed in Figure 5. Since the CML latex has a more hydrophillic surface than the PSL, this additional hydrophilicity reduces the adsorption of CML latex to the membrane surface, which is consistent with the above discussion.

Moreover, the surfactant involved in the CML or PSL solution may have an influence on membrane performance by temporary adsorption of the surfactant on the membrane surface [36]. Although no extra surfactant was added during separation tests, the concentration of ionic-surfactant added by the manufacturer to stabilize the latex solution was not clearly identified. After dilution of the commercial latex solution, the surfactant concentration was believed to be quite low, perhaps less than 10 ppm. Also, the influence of the involved surfactant is systematic. This effect is reported separately in Chapter 6.

5.2.5 Membrane fouling analysis

In order to identify the fouling extent of the corresponding membranes in the separation of CML and PSL particles, a resistance-in-series analysis was carried out to better understand the parts played by internal pore plugging versus irreversible adsorption of the separated particles in membrane fouling. A practical model of microfiltration resistance is attained by Darcy's Law. [16-18]

$$J=\Delta P\ \mu R_t \tag{2}$$

where J is total flux, μ is the dynamic viscosity of the solution, assumed to be 1 kg $m^{-1}s^{-1}$, and R_t is the total resistance to solution flux.

The total resistance consists of the resistance of the membrane (R_m); resistance caused by external fouling (R_{ef}) due to the concentration polarization of latex spheres and reversible adsorption of spheres on the membrane surface and the resistance of internal fouling due to entrapped latex particles or irreversible adsorption of spheres at the membrane internal surface (R_{if}).

$$R_t=R_m+R_{if}+R_{ef} \tag{3}$$

Pure buffer flux measured before the separation test (PBP-1) can be used to determine the resistance of the membranes (R_m) from following equation:

$$J_{PBP\text{-}1} = \Delta P / \mu R_m \quad (4)$$

As mentioned previously, the fouled membrane after the separation test was washed with pure buffer solution to eliminate the external membrane fouling resistance (R_{ef}) caused by concentration polarization and reversible adsorption of the latexes at the membrane surface. Thus, pure buffer permeation flux after washing the tested membrane is a function of the resistance of membranes (R_m) and resistance of internal fouling (R_{if}) only, as revealed in the following equation:

$$J_{PBP\text{-}2} = \Delta P / \mu (R_m + R_{if}) \quad (5)$$

According to equations (2), (3), (4) and (5), total resistance (R_t), membrane resistance (R_m) and internal fouling resistance (R_{if}) can be determined by total latex solution flux (J), pure buffer flux before separation test ($J_{PBP\text{-}1}$) and the pure buffer flux after the separation test ($J_{PBP\text{-}2}$).

Total resistance, membrane resistance and internal fouling resistance with corresponding membranes are depicted in Table 6 and Figure 10. The membrane total resistance and internal fouling resistance decreased with the DK membrane and further decreased with photochemical functionalization. This trend is in agreement with SEM's taken on the corresponding fouled membranes, as depicted in Figure 6-9. It was found that the internal fouling of both negatively charged membranes, indene acid and glycolic acid ester, was lower with CML 203 spheres than with PSL 204 spheres. This result suggests that the electrostatic repulsion between the charged latexes and the charged membrane can reduce the irreversible adsorption of latex particles on the membrane surface, decrease the degree of the membrane fouling and therefore improve the membrane life-time.

5.3 Conclusions

A polysulfonamide layer, containing a diazoketone (DK) photoactive group, was evenly coated on a polypropylene microporous membrane internal surface as described in Chapter 2. Various functionalities, such as indene acid, glycolic acid, polyethylene glycol ester and bromoethyl ester have been further introduced into the coating layer by photochemical reaction in the presence of an appropriate medium. The change in the chemistry and surface properties were confirmed by FT-IR and neutron activation analysis. In the case of bromoethyl ester membrane, the photochemical reaction conversion was found to be 80%. The conversion to indene acid and glycolic acid ester membranes were 65% and 86%, respectively. For the polyethylene glycol ester membrane, only 40% diazoketone group is converted to the polyethylene glycol ester functionality and a part of diazoketone group is converted to indene acid functionality due to the existence of water in the reaction system.

The charge density of the DK control membrane and the corresponding functionalized membranes were determined using neutron activation analysis of sodium species associated with the carboxylic acid group on the membrane surface. Decarboxylation of indene carboxylate was assumed to reduce the desired charge density of the indene acid membrane. The highest charge density was achieved on a glycolic acid ester membrane (ca. 0.097 meq/g), which was lower than that reported by other researchers. Wettability of the membrane surfaces was also slightly changed by both the polysulfonamide coating and further photochemical modifications. The wetting surface energy increased in the order of nascent, polysulfonamide coated, glycolic acid ester and indene acid membranes. These results suggest that the membrane surface became more hydrophillic after both

coating and photochemical functionalization, compared to the nascent membrane.

After photochemical modification, the microfiltration characteristics of the membranes still remained, but the flux and separation of the functionalized membranes changed significantly which was directly related to the change in the membrane surface properties. The desired separation enhancement of negatively charged membranes with negatively charged particles (CML) due to electrostatic repulsion as compared with the neutral PSL spheres was not observed during our study. The presence of surfactant and electrolyte screening may affect the electrostatic repulsion of the functionalized membrane. The results of membrane performance tests suggest that the increase of hydrophilicity of the photochemically functionalized membranes was the dominant factor affecting the membrane separation performance. The extent of internal fouling of the negatively charged membranes in separation of PSL spheres or CML spheres was quite low compared with the DK control membranes. Also, with the indene acid membranes or glycolic acid ester membranes, the degree of internal fouling for CML latexes was lower than for PSL latexes. The results indicate that the surface modification is likely beneficial for cleaning and recovery of the microfiltration membranes performance, and hence could improve the membrane effective life-time.

References

(1) A.K. Mukherjee and B.D. Gupta, Graft copolymerization of vinyl monomers onto polypropylene, J. Macromol. Sci.-Chem., A19(7), (1983) 1069-1099.

(2) G. Xu and S. Lin, Functional modification of polypropylene, J. Marcomol. Sci., Rev. Macromol. Chem. Phys., C34(4), (1994) 555-606.

(3) Y. Fang and T. Shi, Polypropylene dialysis membrane prepared by cobalt-60 gamma-radiation-induced graft copolymerization, J. Membrane Sci., 39 (1988) 1-9.

(4) T. Hirotsu, Water-ethanol separation by pervaporation through plasma graft polymerized membranes, J. Appl. Polym. Sci., 34 (1987) 1159-1172.

(5) K. Allmer, J. Hilborn, P.H. Larsson, A. Hult and B. Banby, Surface modification of polymers. V. Biomaterial applications, J. Polym. Sci., Part A: Polym. Chem., 28 (1990) 173-183.

(6) Y. Ogiwara, M. Takumi and H. Kubota, Photoinduced grafting of acrylamide onto polyethylene film by means of two-step method, J. Appl. Polym. Sci., 27 (1982) 3743-3750.

(7) A.M. Mika, R.F. Childs, J.M. Dickson, B.E. McCarry and D.R. Gagnon, A new class of polyelectrolyte-filled microfiltration membranes with environmentally controlled porosity, J. Membrane Sci., 108 (1995) 37-56.

(8) S.K. Chadda, B.E. McCarry, R.F. Childs, C.V. Rogerson, I.O. Tse-Sheepy and J.M. Dickson, Novel thin-film composite membranes containing photoreactive groups, Part I: Choosing the photochemical group, J. Appl. Polym. Sci., 34 (1987) 2713-2732.

(9) B.J. Trushinski, J.M. Dickson, R.F. Childs and B.E. McCarry, Photo-chemically modified thin-film composite membranes. I. Acid and ester

membranes, J. Appl. Polym. Sci., 48 (1993) 187-198.

(10) B.J. Trushinski, J.M. Dickson, R.F. Childs, B.E. McCarry and D.R. Gagnon, Photochemically modified thin-film composite membranes. Part II: Bromoethyl ester, dioxolan, and hybroxyethyl ester membranes, J. Appl. Polym. Sci., 54 (1995) 168-174.

(11) W. Ando, Photochemistry of the diazonium and diazo groups, in: The Chemistry of Diazonium and Diazo Groups, S. Patai (Ed.), John Wiley & Sons, New York, 1978, Part 1, p. 341.

(12) ASTM D-2578

(13) G.H. Shipman, US Patent #4,539,256 (1985).

(14) Reverse Osmosis, S. Sourirajian (Ed.), Academic Press, New York, 1970.

(15) Standard methods for the examination of water and wastewater, M.A. Franson (Ed.), Fourth Edition, John Wiley & Sons, New York, 1975.

(16) K.M. Persson, G. Trägårdh and P. Dejmek, Fouling behaviour of silica on four different microfiltration membranes, J. Membrane Sci., 76 (1993) 51-60.

(17) C. Visvanathan and R. Ben Aim, Studies on colloidal membrane fouling mechanism in crossflow microfiltration, J. Membrane Sci., 45 (1989) 3-15.

(18) R.J. Wakeman and E.S. Tarleton, Colloidal fouling of microfiltration membranes during the treatment of aqueous feed streams, Desalination, 83 (1991) 35-52.

(19) J.K. Almestead, B. Urwyler and J. Wirz, Flash photolysis of α - diazonaphthoquinones in aqueous solution: determination of rates and equilibria for keto-enol tautomerization of 1-indene-3 carboxylic acid, J. Am. Chem. Soc., 116 (1994) 954-960.

(20) J. Andraos, A.J. Kresge and V.V. Popik, Kinetics and mechanism of

isomerization of 1H-indene-1-carboxylic acid to 1H-indene-3-carboxylic acid in aqueous solution and determination of their keto-enol equilibrium constants and acid dissociation constants of keto and enol forms. Implication on the photolysis of diazonaphthoquinones, J. Am. Chem. Soc., 116 (1994) 961-967.

(21) J. Ji, R.F. Childs, J.M. Dickson and B.E. McCarry, Fabrication of thin film composite membranes with pendent, photoreactive diazoketone functionality, J. Appl. Polym. Sci., in press (1997)

(22) Infrared spectroscopy, in: Introduction to Spectroscopy, D.L. Pavia, G.M. Lampman and G.S. Kriz (Ed.), Saunders College Publishing, Pennsylvania, 1979.

(23) Nonaqueous electrolytes handbook, volume 1, G.J. Janz and R.P.T. Tomkins (Ed.), Academic Press, New York, 1972.

(24) J. Ji, Ph.D Thesis, Department of Chemistry, McMaster University, 1996.

(25) B.J. Truhinski, Fabrication and characterization of photochemically modifiable thin-film composite and microfiltration membranes, Third annual report to 3M Canada Inc., 1992.

(26) The chemistry of ketenes, allenes and related compounds. Part 1., S. Patai (Ed.), Wiley Interscience, Chichester, 1980

(27) P.J. Lillford and D.P.N. Satchell, Acylation. Part XXXII. A comparison of the charge distributions in keten and in dimethylketen and a determination of the relative reactivity of these compounds towards *m*-chloroaniline. J. Chem. Soc. (B), 1970, 1016-1023

(28) D. Bhattachayya, D.P. Schaaf and R.B. Grieves, Negatively-charge ultrafiltration membrane, Can. Chem. Eng., 54 (1976) 185-189.

(29) D. Bhattachayya, M.G. Balco, C. Cheng and S.E. Gentry, Use of

negatively-charged ultrafiltration membranes, in: Ultrafiltration Membranes and Applications, A.R. Cooper (Ed.), Plenum Press, New York, (1980) pp. 605-608.

(30) S. Nakao, H. Osada, H. Kurata, T. Tsuru and S. Kimura, Separation of proteins by charged ultrafiltration membranes, Desalination, 70 (1988) 191-205.

(31) D.R. Gagnon and T.J. McCarthy, Polymer surface reconstruction by diffusion of organic functional group form and to the surface, J. Appl. Polym. Sci., 29 (1984) 4335-4340.

(32) K. Allmer, A. Hult and B. Ranby, Surface modification of polymers. I. Vapour phase photografting with acrylic acid, J. Polym. Sci., Part A: Polym. Chem., 26 (1988) 2099-2111.

(33) R.M. McDonogh, A.G. Fane and C.J.D. Fell, Charge effects in the cross-flow filtration of colloids and particulates, J. Membrane Sci., 43 (1989) 69-85.

(34) R.M. McDonogh, K. Welsch, A.G. Fane and C.J.D. Fell, Flux and rejection in the ultrafiltration of colloids, Desalination, 70 (1988) 251-264.

(35) R.M. McDonogh, C.J.D. Fell and A.G. Fane, Surface charge and permeability in the ultrafiltration of non-flocculating colloids, J. Membrane Sci., 21 (1984) 285-294.

(36) K. Rilling, Master Thesis, Department of Chemical Engineering, McMaster University, 1992.

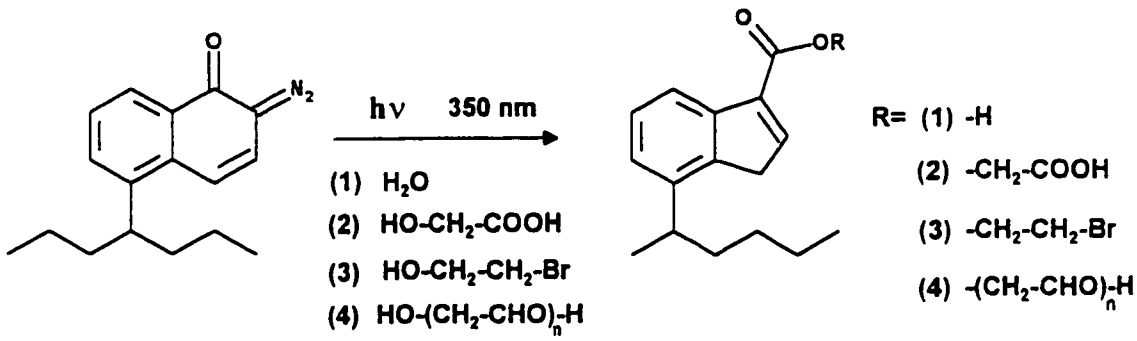

Scheme 1. Photochemical reaction of diazoketone with different reagents

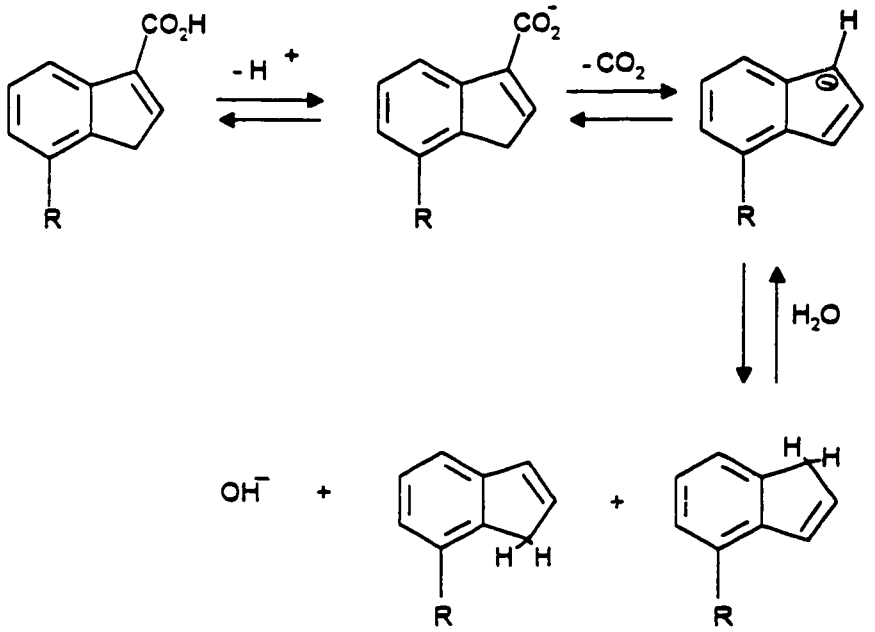

Scheme 2. Mechanism of decarboxylation of indene acid functionality.

Table 1. Photochemical reaction conversion of bromoethyl ester membranes

Membrane	Mass Gain (%)	DK[a] (μmol)	Br[b] (μmol)	Conversion (%)
B-ESTER	11.0 ±0.2	8.42 ±0.17	6.86 ±0.31	81.5 ±2.0

[a] DK is the amount of diazoketone group available on the membrane coating layer in the NAA sample.

[b] The bromine amount shown was corrected for the background. The bromine background was 1.83 ±0.15 μmol.

Table 2. Photochemical reaction conversion of indene acid and glycolic acid ester membranes.

Membrane	Mass Gain (%)	DK[a] (μmol)	Na[b] (μmol)	Conversion (%)
I-ACID	11.2 ±0.3	4.95 ±0.31	3.34 ±0.54	67.5 ±6.7
G-ACID	11.0 ±0.2	5.53 ±0.05	4.75 ±0.07	85.9 ±2.0

[a] DK is the amount of diazoketone group available on the membrane coating layer in NAA sample.

[b] The amount of Na was corrected for background. The background of Na on the DK control was 0.29 ±0.06 μmol.

Table 3. Photochemical reaction conversion of polyethylene glycol ester membranes.

Membrane	Mass Gain (%)	DK (μmol)	Conversion to PEG-ester[a]	Total Conversion
PEG-ESTER	12.4 ±0.6	8.55 ±0.46	40.3 ±2.4%	78.2 ±5.6%
			Conversion to I-ACID[b]	
			37.9 ±3.2%	

[a] Conversion of PEG-ester functionality was measured by a gravimetrical method.

[b] Conversion of indene acid functionality of PEG-ester membrane was determined the same way as for indene acid membranes.

Table 4. Surface properties of nascent, DK, indene acid, glycolic acid ester and polyethylene glycol ester membranes.

Membrane	Charge density (meq/g)	Wetting surface energy, γ_w (dyne/cm)
Nascent	-------	35.0 ±0.025
DK	-------	36.0 ±0.025
I-ACID	0.071 ±0.008	37.5 ±0.025
G-ACID	0.091 ±0.007	37.0 ±0.025
PEG-ester	0.043 ±0.003	37.5 ±0.025

Table 5. Flux and separation of nascent, DK, control, indene acid and glycolic acid ester membranes with 204 nm PSL and 203 nm CML spheres[a]

	PSL 204			CML 203		
Memb.	PBP[b] (kg/m^2 s)	Flux (kg/m^2 s)	Separation (%)	PBP[b] (kg/m^2 s)	Flux (kg/m^2 s)	Separation (%)
Nascent	1.45 ±0.07	0.78 ±0.07	66.0 ±5.5	1.48 ±0.01	0.82 ±0.05	65.4 ±3.7
DK	1.54 ±0.06	0.93 ±0.03	38.6 ±4.1	1.56 ±0.06	0.91 ±0.03	45.3 ±2.6
I-CON	1.54 ±0.04	0.96 ±0.04	36.9 ±3.8	1.55 ±0.02	0.95 ±0.04	41.9 ±3.8
G-CON	1.53 ±0.05	0.94 ±0.03	41.1 ±4.3	1.54 ±0.05	0.94 ±0.04	44.6 ±3.3
I-ACID	1.66 ±0.01	1.09 ±0.01	18.8 ±2.7	1.67 ±0.03	1.36 ±0.02	9.6 ±0.3
G-ACID	1.62 ±0.02	1.11 ±0.04	15.6 ±2.8	1.65 ±0.04	1.18 ±0.04	13.3 ±2.8

[a] 204 nm PSL and 203 CML spheres at 100 ppm buffered to pH=9. Tests were carried out at 20 kPa, 25° C±2°C, and 450 rpm.

[b] PBP is flux with pure buffer permeation.

Table 6. Internal (R_{if}) and external (R_{ef}) fouling resistance[a] of nascent, DK and functionalized membranes.

Membrane	PSL 204		CML 203	
	R_{if} ($x10^{-6}$ m^{-1})	R_{ef} ($x10^{-6}$ m^{-1})	R_{if} ($x10^{-6}$ m^{-1})	R_{ef} ($x10^{-6}$ m^{-1})
Nascent	11.2 ±1.2	1.1 ±0.5	10.9 ±1.3	1.1 ±0.3
DK	7.6 ±0.9	0.9 ±0.4	9.2 ±1.1	0.9 ±0.6
I-ACID	4.9 ±0.6	0.6 ±0.3	2.3 ±0.3	0.4 ±0.1
G-ACID	4.1 ±0.5	1.1 ±0.2	3.5 ±0.5	1.0 ±0.2

[a] Internal fouling is caused by entrapped latex particles and/or irreversible adsorption of spheres on the membrane surface. External fouling resistance is caused by the concentration polarization of latex spheres and/or reversible adsorption of spheres on the membrane surface.

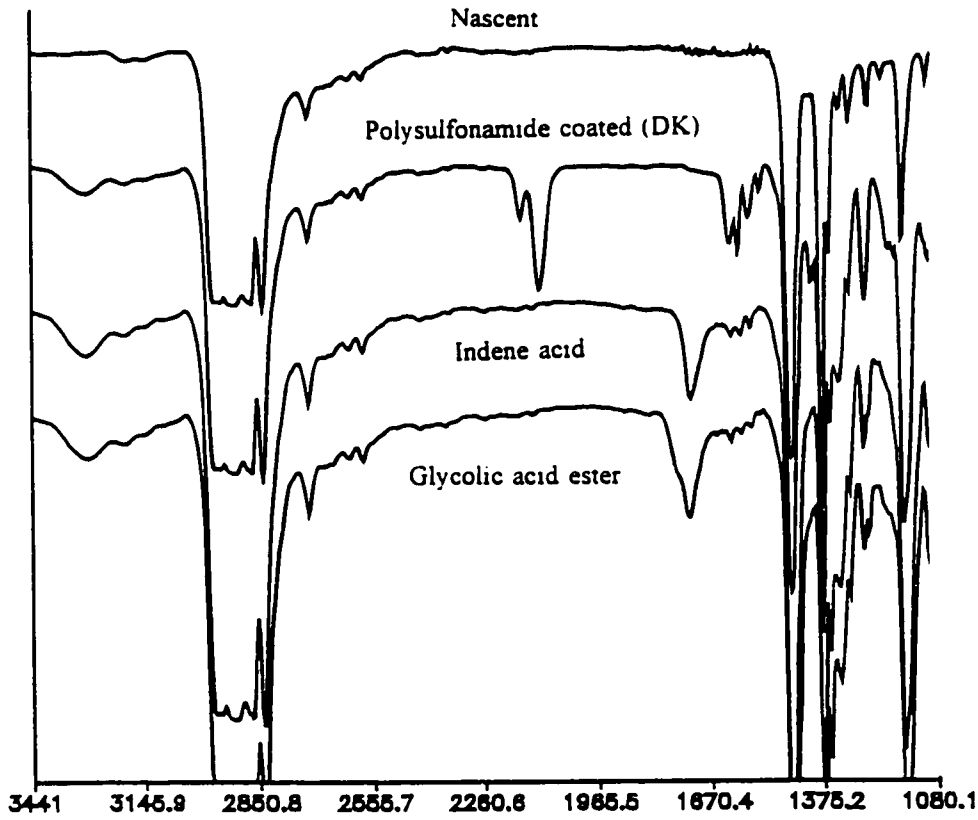

Figure 1. FT-IR spectra of nascent, DK, indene acid and glycolic acid ester membranes.

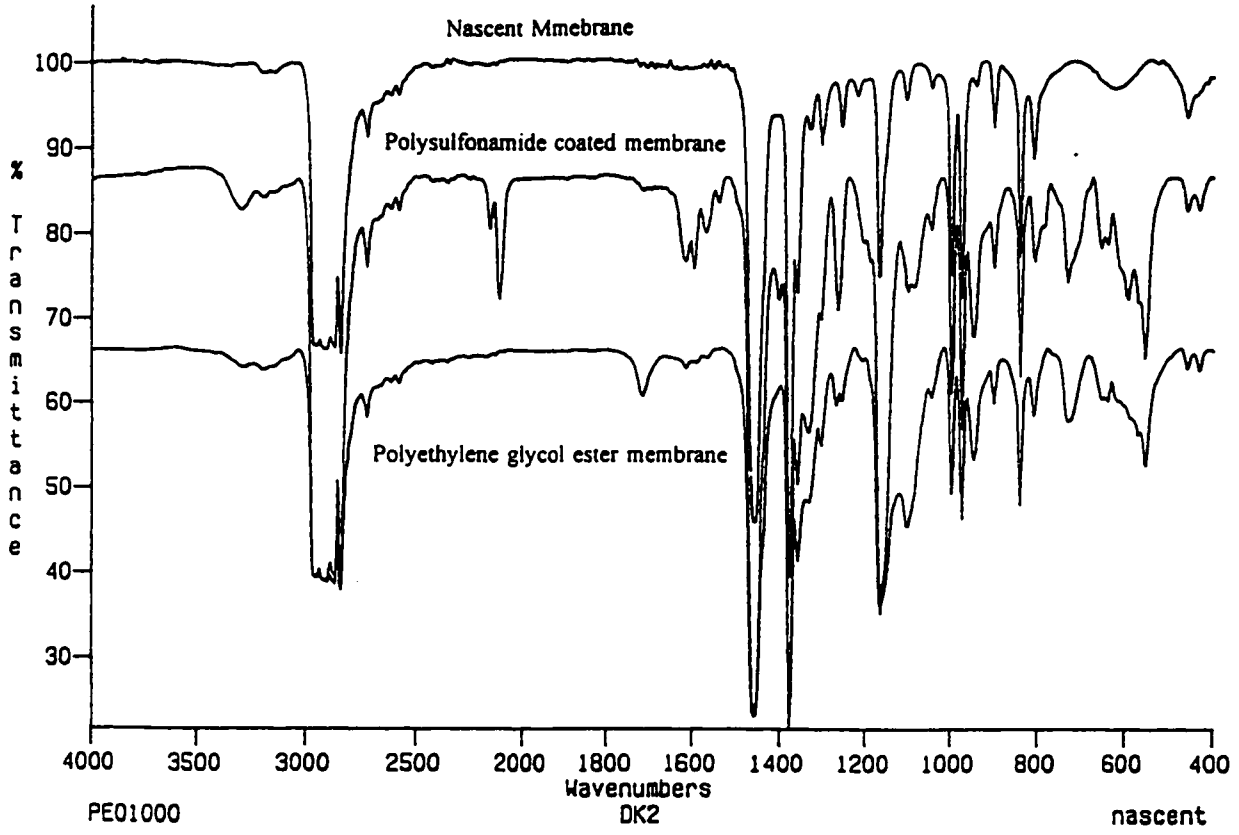

Figure 2. FT-IR spectra of nascent, DK and polyethylene glycol ester membranes.

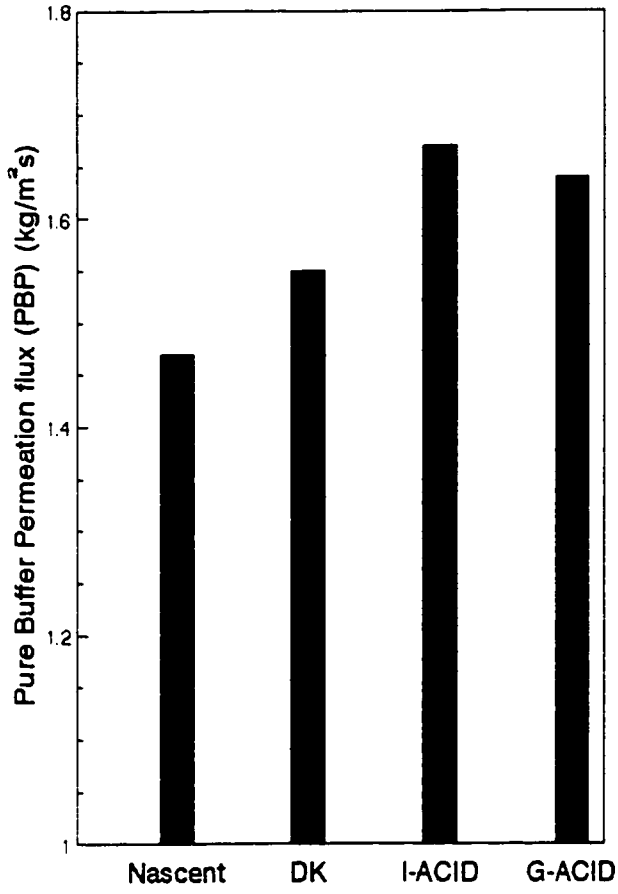

Figure 3. Pure buffer permeation flux of nascent and modified membranes. Buffer pH: 9.0; pressure: 20 kPa; temperature: 25°C±1°C @ 450 rpm.

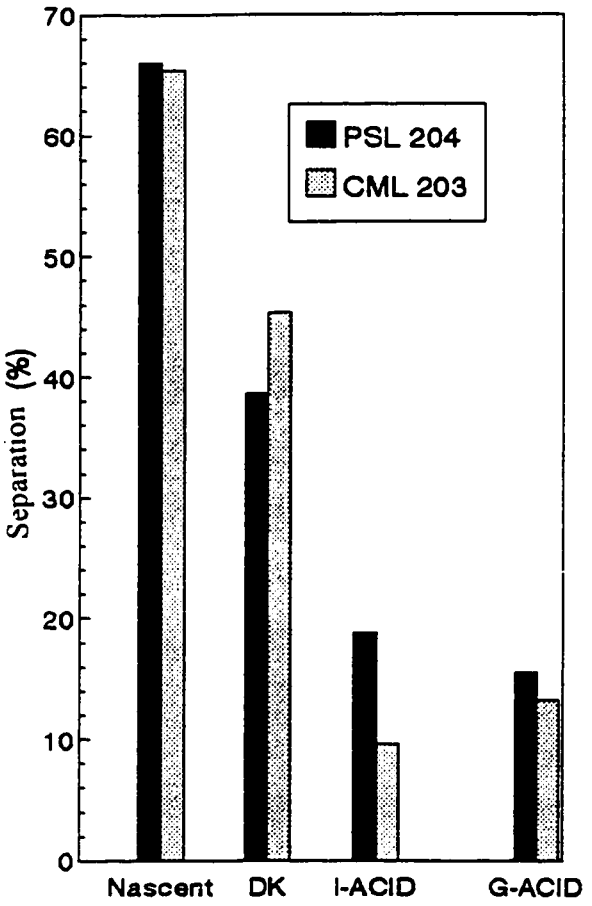

Figure 4. Separation performance of nascent and modified membranes with PSL 204 and CML 203 spheres. Buffer pH: 9.0; pressure: 20 kPa; temperature: 25°C±1°C @ 450 rpm.

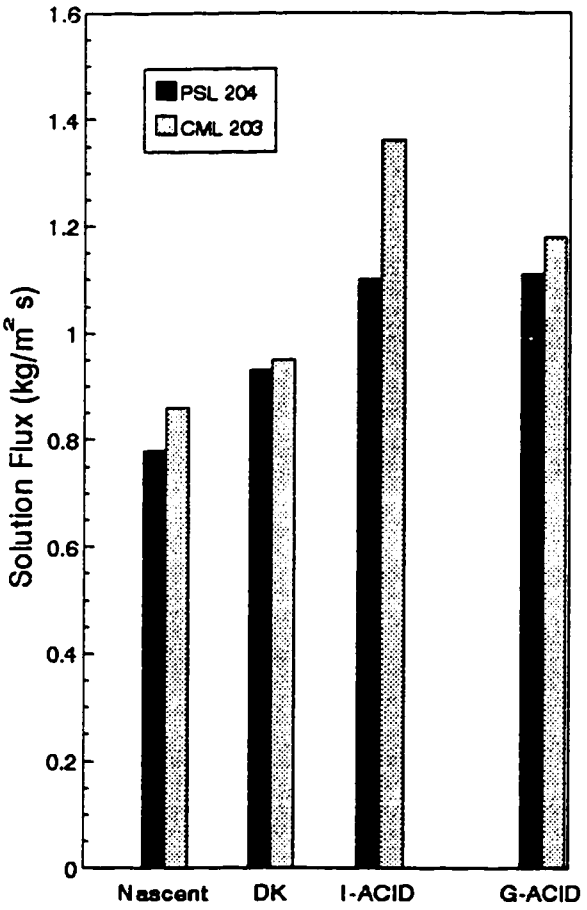

Figure 5. PSL 204 and CML 203 Solution flux of nascent and modified membranes. Buffer pH: 9.0; pressure: 20 kPa; temperature: 25°C±1°C @ 450 rpm.

(a) (Top)

(a) (Bottom)

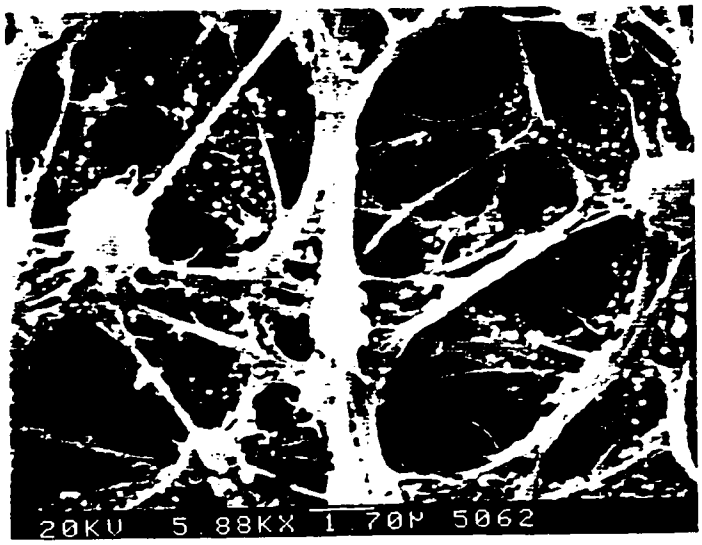

Figure 6. SEMs of nascent membranes after separation of PSL 204 and CML 203 latex spheres. Buffer pH: 9.0; pressure: 20 kPa; temperature: 25°C±1°C @ 450 rpm. (a) Nascent membrane surface fouled with PSL 204; (b) Nascent membrane surface fouled with CML 203.

(b) (Top)

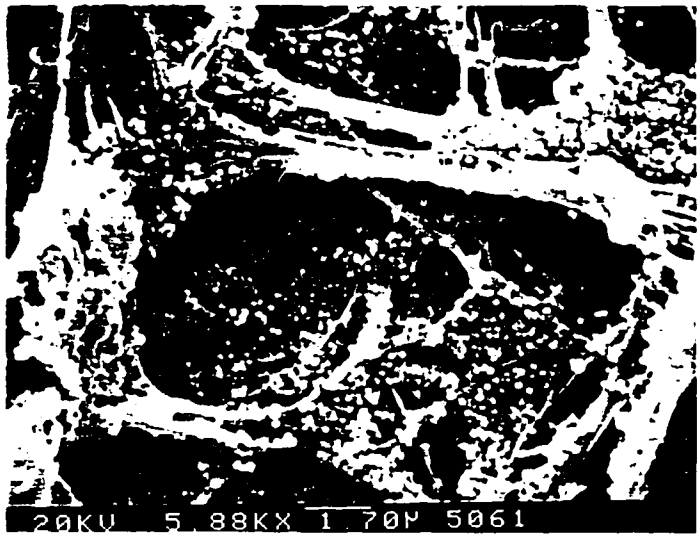

(b) (Bottom)

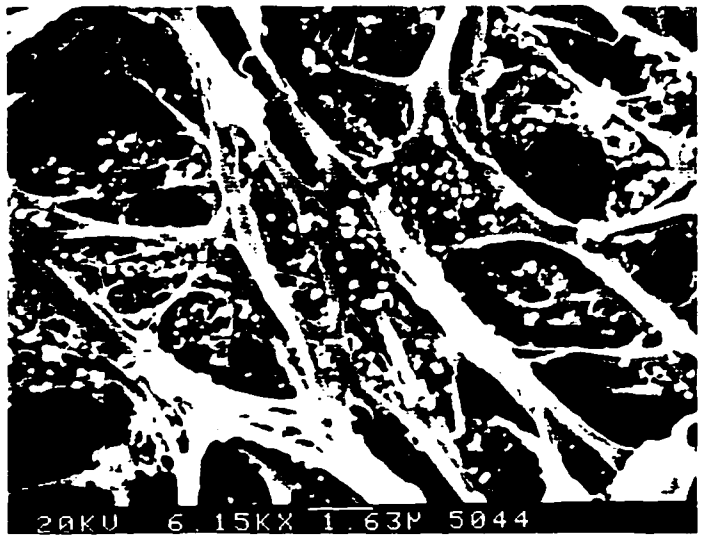

(a) (Top)

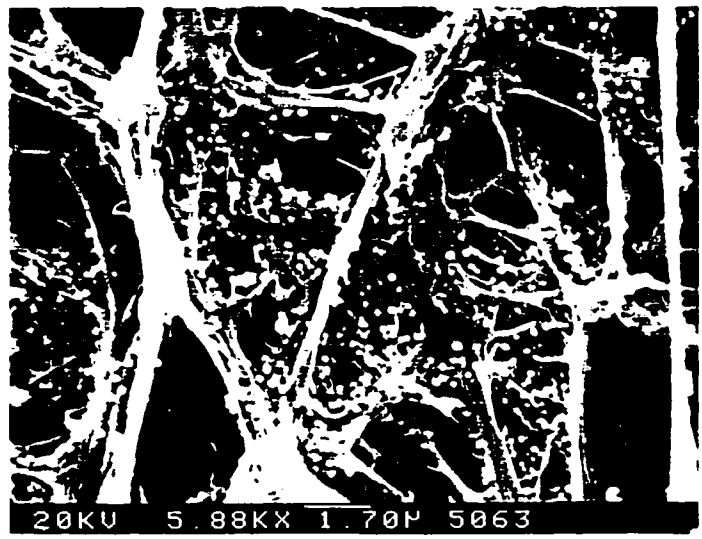

(a) (Bottom)

Figure 7. SEMs of DK membranes after separation of PSL 204 and CML 203 latex spheres. Buffer pH: 9.0; pressure: 20 kPa; temperature: 25°C±1°C @ 450 rpm. (a) DK membrane surface fouled with PSL 204; (b) DK membrane surface fouled with CML 203.

(b) (Top)

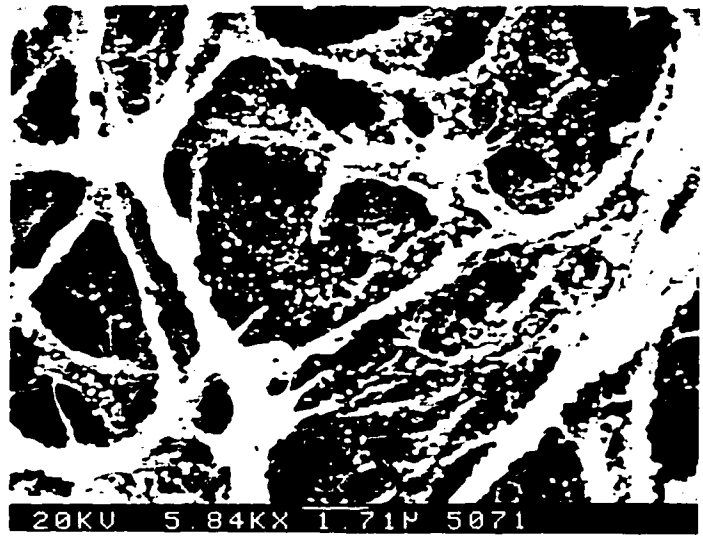

(b) (Bottom)

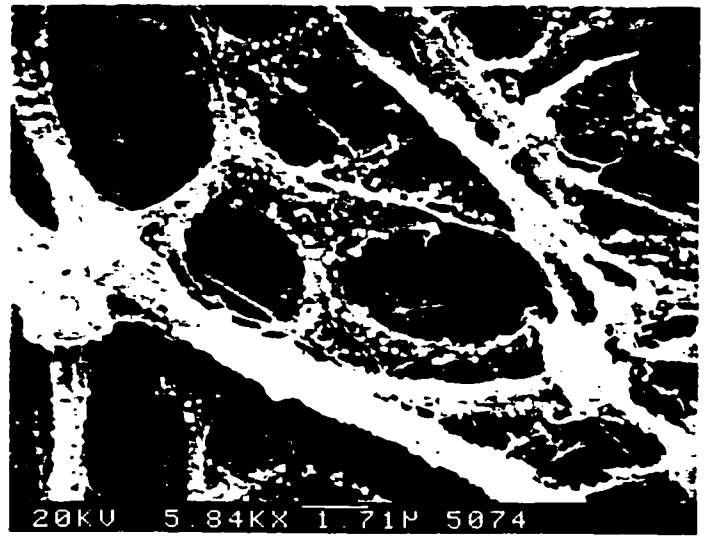

(a) (Top)

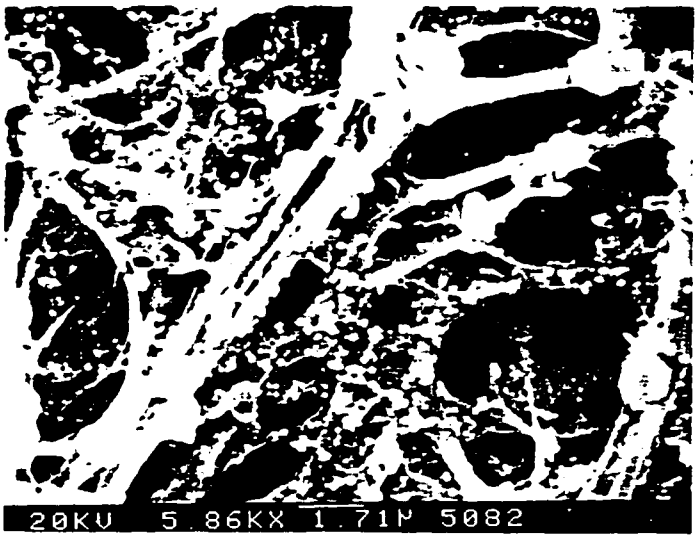

(a) (Bottom)

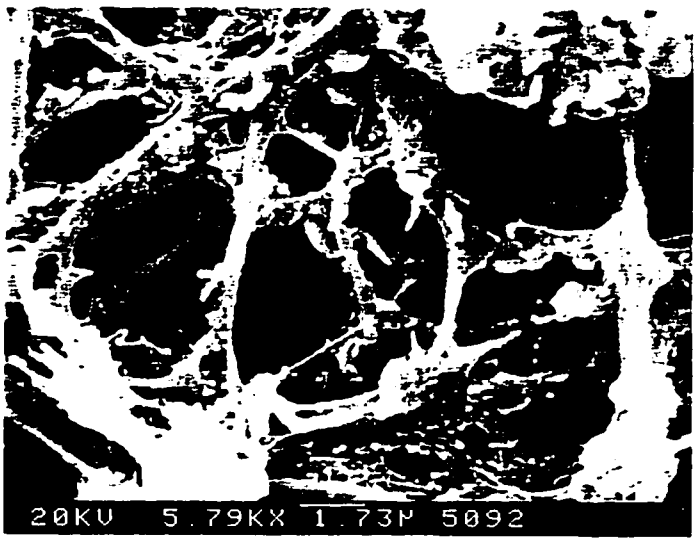

Figure 8. SEMs of indene acid membranes after separation of PSL 204 and CML 203 latex spheres. Buffer pH: 9.0; pressure: 20 kPa; temperature: 25°C±1°C @ 450 rpm. (a) Indene acid membrane surface fouled with PSL 204; (b) Indene acid membrane surface fouled with CML 203.

(b) (Top)

(b) (Bottom)

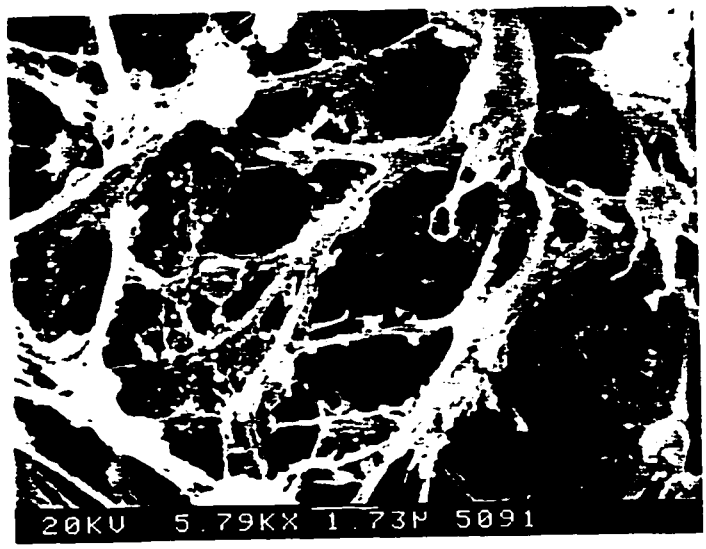

(a) (Top)

(a) (Bottom

Figure 9. SEMs of glycolic acid ester membranes after separation of PSL 204 and CML 203 latex spheres. Buffer pH: 9.0; pressure: 20 kPa; temperature: 25°C±1°C @ 450 rpm. (a) Glycolic acid ester membrane surface fouled with PSL 204; (b) Glycolic acid ester surface fouled with CML 203.

(b) (Top)

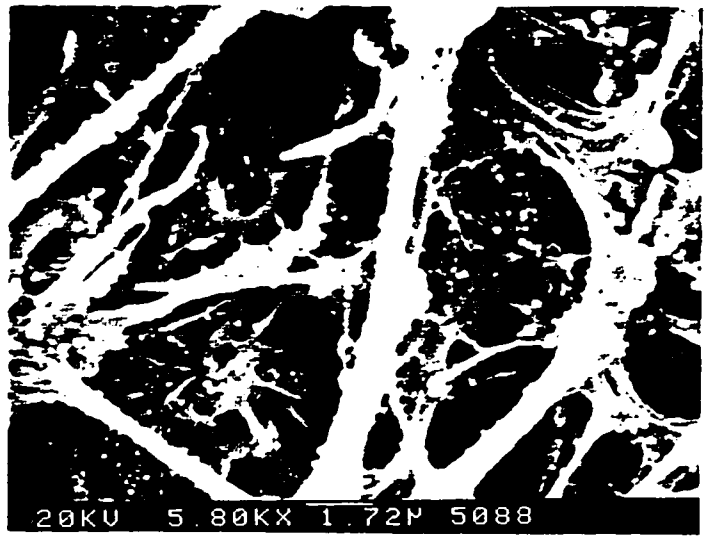

(b) (Bottom)

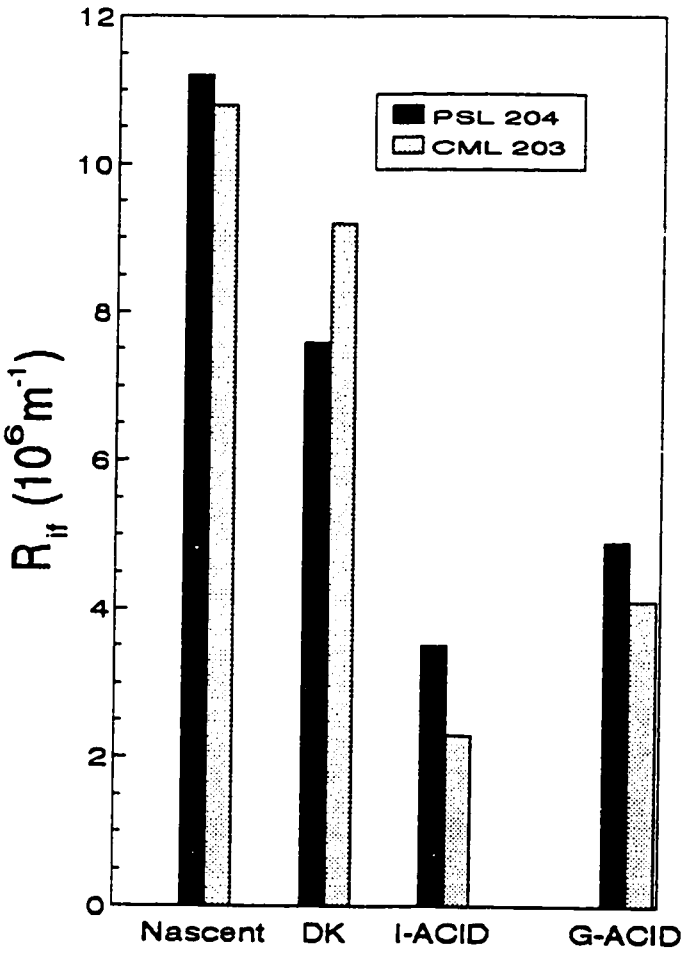

Figure 10. Internal fouling resistance of nascent membranes and modified membranes caused by separation of PSL 204 and CML 203 latex spheres.

Chapter 6

Effect of Triton X-100 on Polypropylene Microfiltration Membrane Performance

ABSTRACT

The influence of a non-ionic surfactant, Triton X-100, on polypropylene microfiltration membrane performance has been investigated using a 100 ppm polystyrene latex (PSL) spheres testing solution in a dead-end cell. A remarkable change of membrane performance was found after the addition of Triton X-100 to the feed solution. Such a phenomenon was explained in terms of membrane surface properties. The fouling degree of each tested membrane was examined by SEM and also analyzed by a resistance-in-series model. In order to clarify the function of Triton X-100 in the membrane separation performance, polyethylene glycol ester membrane was introduced to mimic the membrane with the adsorption of Triton X-100. The results suggested that the Triton X-100 in the testing solution not only temporarily modified the membrane surface properties but also prevented the PSL particles from aggregating, particularly in the membrane matrix.

Keywords: Microfiltration, Polypropylene membrane, Triton X-100, Polyethylene glycol ester membrane, Hydrophobic interaction.

Introduction

In principle, both microfiltration (MF) and ultrafiltration (UF) membranes work by a sieving mechanism, with pressure as the driving force. The most serious limitation to the application of MF or UF operations is a continuous decrease of permeation flux. This flux decline is generally due to fouling. The fouling of microfiltration membranes is a result of the accumulation of the separated material at the membrane surface, which is due to (1) material adsorption by the filling of pores and covering of the surface, (2) inertial impaction of material to the membrane matrix because of the high initial flux, and (3) slow back-diffusion of material to the bulk solution. The adsorption of foulants (separated solute) on the membrane surface can be attributed to different types of interactions between the membrane surface and the separated solutes: hydrophobic interactions, hydrogen bonding, van der Waals interactions and electrostatic effects [1]. These interactions modify the sieving effect and often dominate the performance of a UF membrane [2-4]. Among those interactions, hydrophobic interactions often play an important role when UF membranes are fouled by organic compounds. There are numerous observations showing a marked difference in fouling tendency of hydrophobic and hydrophillic membranes [5-7]. The importance of the interactions between solute and membrane has been recognized for a long time.

The effect of protein or colloid fouling in microfiltration or ultrafiltration processes on permeate flux has been reviewed by Marshall et al. [8]. The deposition of protein or colloids has been identified not only on the membrane top surface, but also within the MF membrane structure. Attia et al. [9] showed that casein both formed a layer on the surface of the 0.8 μm MF membrane and

penetrated the membrane structure to deposit within the pores. Pusch and Walch [10] showed electron micrographs of the top surface of a 3 μm Nuclepore membrane after filtration of latex/styrene particles. Even though the styrene particles were only one-tenth of the pore diameter, they interacted with the pore walls of the membrane, thus forming agglomerates that finally blocked the pores.

A number of workers studied the effect of the feed properties on the MF membrane performance. All of them focused on the effects of concentration, pH, ionic strength of the feed solution.and pretreatment of the membrane. The effect of surfactant in the feed solution on the membrane performance was neglected in the microfiltration process, and only reported in the ultrafiltration, presumably because the size of most surfactant is two orders of magnitude smaller than the pore size of MF membranes.

Improvement of UF membrane performance has been investigated by the addition of the surfactant into the separated solution or pre-treating the UF membrane with surfactant before the test [11-13]. For example, it has been found that the efficiency of removing nitrate ions from water, using ultrafiltration, is an increasing function of the cationic surfactant concentration [11], and a good nitrate rejection can be achieved even when the surfactant concentration is well below the critical micellar concentration of surfactant. These results indicate that the adsorption of surfactant molecules plays an important part in the transport mechanism. Detergent treatment of the UF membranes can also enhance the solution flux, which is considered as a temporary surface modification operation for UF membranes [13].

Current research has demonstrated the surfactant effect on the ultrafiltration membrane performance. This chapter presents the evidence supporting the surfactant effect on the polypropylene microfiltration membrane with pore size of

approximately 1 μm and high porosity (ca. 80%). The choice of a surfactant-free polystyrene latex sphere as a probe, minimizes the possible interference of other surfactant. The adsorption behaviour of Triton X-100 on the polypropylene membrane surface is studied in terms of dynamic adsorption process. The wettability of the membrane surface is determined through a pore-penetration method. To further explicate the influence of the surfactant on the membrane performance, polysulfonamide coated membrane and polyethylene glycol ester membrane are introduced for comparison. The role of membrane surface chemistry in the membrane separation performance is explored qualitatively.

6.1 Experimental

6.1.1 Materials

The physical and chemical properties of polypropylene (PP) microfiltration membrane have been described in Chapter 2. Triton X-100 (Aldrich Chemical Co.) was chosen as a surfactant in this study for several reasons. Firstly, our interest is to observe effects associated with hydrophobic/hydrophillic interactions only, any electrical effects with ionic surfactant should be avoided. Secondly, Triton X-100 is available in high purity and is non-toxic, and relatively insensitive to pH and electrolytes. The detailed properties of Triton X-100 are listed in Table 1. Surfactant-free polystyrene latex (PSL) spheres with uniform particle size (ca. 304 nm) obtained from International Dynamic Inc., were used as a probe. The PSL used in this study is different from used in Chapter 5. PSL spheres from Seradyn Inc. include approximately 0.1% anionic surfactant. PSL spheres from International Dynamic Inc. is completely surfactant-free. The PSL spheres are

stabilized in aqueous solution by charged-groups on the sphere surface. PSL (304 nm) solution concentrations were calibrated and measured with an HF Instruments Model DRT 1000 turbidity meter [14]. The calibrations are linear in nephelometric turbidity units (NTU) versus PSL concentrations. Triton X-100 concentrations studied in this Chapter are 0.015, 0.045 and 0.1 mmol/L, respectively, which are far below the critical micellar concentration (CMC) of Triton X-100 (0.25 mmol/L) [15].

6.1.2 Permeability and separation measurement

All membranes were tested in two stirred (450 rpm, 38.5 cm^2 effective area), 400 ml Nuclepore cells (Model S-76-400), modified to include a thermocouple, which, with a digital thermometer, measured the cell temperature to ±1°C Each membrane sample was initially compacted at 13.8 kPa (at least 4L of buffer solution) until three successive flux measurements were constant. The results presented are the average of 3 membranes.

Polystyrene latex (PSL) spheres with a narrow particle size distribution (ca. 304 nm), 100 ppm buffered to the required pH, were used as feed solution. The dead-end cells were filled with 380 ml of feed. The concentration of initial feed, C_i, was measured before each test. After 100 ml of solution had passed through the membrane under a pressure of 13.8 kPa, 40 ml of permeate was collected to determine permeate mass and concentration, C_e. Solution flux was determined by mass collected over a fixed time. Another 30 ml sample was collected from the feed side and the concentration was recorded as the final feed concentration, C_f. The separation factor was defined as follows:

$$Separation(\%) = \frac{(C_{af} - C_e)}{C_{af}} X100\% \quad (1)$$

where C_{af} is an average of the initial and final feed concentrations.

The pure buffer permeation flux (PBP) measured before and after microfiltration were used to determine the degree of fouling by the resistance-in-series analysis. The pure buffer flux measured before the solution test is referred to as PBP-1. The fouled membranes, after the separation test, were rinsed three times by pure buffer solution. The pure buffer permeation flux was measured again, and referred to as PBP-2. The extent of membrane fouling after the separation test was visibly examined by scanning electron microscopy (ISI-DS300).

6.1.3 Dynamic adsorption of Triton X-100

The dynamic adsorption of Triton X-100 was measured by placing the membrane in a clean dry cell, followed by adding of 400 ml of pure surfactant solution at the required concentration. The mass gain of Triton X-100 adsorption on the membrane surface was determined gravimetrically, using an accurate five decimal balance, after 400 ml, 800 ml and 1200 ml of Triton X-100 solution, had passed through the polypropylene microfiltration membrane, respectively. The desorption process of Triton X-100 was monitored after washing the membrane with 300 ml deionized water. Control experiments, in the absence of the surfactant with the PP membranes were carried out as a background.

6.1.4 Polysulfonamide coated membrane and polyethylene glycol ester membrane

In order to further explore the efficacy and the role of physically adsorbed Triton X-100 in membrane separation performance, polysulfonamide coated membranes (DK) and polyethylene glycol (PEG) ester membranes are introduced for comparison because polyethylene glycol has a similar chemical structure as the hydrophillic tail of Triton X-100. The preparation of the DK membranes and the polyethylene glycol ester membranes was reported in Chapter 5.

6.1.5 Membrane surface properties

The measurement of the membrane surface wettability, using through-pore penetration method with a series of solutions has been reported in Chapter 5.

6.2 Results and Discussion

6.2.1 Dynamic adsorption of Triton X-100

The adsorption of Triton X-100 on the hydrophobic ultrafiltration membrane surface have been reported by a number of researchers [16-18]. It has been found that the flux decline was remarkable during the ultrafiltration of the Triton X-100 solution because of the adsorption of Triton X-100 at the UF membrane surface. The pore size of the nascent membrane used in this study is approximately 1 μm, and concentration of Triton X-100 testing solution is quite low. Triton X-100 molecules, with a maximum length estimated to be 4.5 nm are sufficiently small to pass through the membrane without any significant retention [19]. The microfiltration flux decline of pure Triton X-100 solution is negligible, as presented in Figure 1, compared to the flux decline of the ultrafiltration membrane by Triton X-100 solution reported in the literature [12,20]. The flux decline revealed in

Figure 1 is only marginally larger than the experimental variation. All flux and separation data presented in this section or the following sections are the average of three membrane samples. The detailed experimental results are in Appendix E.

The adsorption of surfactant on the surface of ultrafiltration membranes has generally been examined *via* adsorption kinetics and isotherms. In this Chapter, the Triton X-100 adsorption on the surface of polypropylene microfiltration membranes was examined dynamically. The dynamic adsorption of Triton X-100 is caused by a balance between the adsorption and the desorption of Triton X-100 on the polypropylene membrane surface. The adsorption of Triton X-100 is due to hydrophobic interaction between the hydrophobic tails of Triton X-100 and the membrane surface, and the desorption of the Triton X-100 from the membrane surface is caused by the flow shear stress and/or the back diffusion of Triton X-100 due to concentration gradient adjacent to the membrane surface. After the desired volume of Triton X-100 solution passed through the membrane, the membrane was dried and the mass of Triton X-100 adsorbed on the membrane surface was determined gravimetrically. Results are as presented in Figure 2. The mass gain of Triton X-100 adsorbed on the surface of the polypropylene microporous membranes increased significantly with increasing concentration of Triton X-100 initially, then slowly increased after 400 ml and approached a plateau. The results presented in Figure 2 suggest that the dynamic adsorption of Triton X-100 is quickly established. Initially, the adsorption of Triton X-100 molecules on the membrane surface is dominated by the hydrophobic interaction. After 400 ml Triton X-100 solution had passed through the membrane, a balance of adsorption and desorption of Triton X-100 is approached, which leads to a plateau of Triton X-100 mass gain curve. The desorption was measured by washing the membrane with deionized water when the plateau of the adsorption had been reached. Almost

half the adsorbed Triton X-100 was washed away after 300 ml deionized water had passed through the membrane, as shown in Figure 2.

6.2.2 Membrane surface properties and separation performance

After the adsorption test, with different Triton X-100 concentrations, the through-pore wetting surface energy of the same membranes was determined using a series of mixture solution with various surface tensions. The method used is the same as presented in Chapter 5. The surface wetting energy increased with increasing Triton X-100 concentrations, as shown in Table 2. The nascent membrane became more hydrophillic after the adsorption of Triton X-100 at the membrane surface.

All membranes being tested were pre-compacted by 4 litres of buffer solution at a desired Triton X-100 concentration (0.015, 0.045 or 0.1 mmol/L). The polystyrene latex (PSL) testing solution were made at the same Triton X-100 concentration as the pre-compact buffer solutions. The modification of the membrane surface by the adsorption of Triton X-100 results in a significant change of the polypropylene membrane performance, as presented in Figure 3 The separation of PSL spheres significantly decreases, from 100% to 28%, and PSL solution flux dramatically increases, from 0.38 kg m^{-2} s^{-1} to 0.76 kg $m^{-2}s^{-1}$, with increasing the Triton X-100 concentration from 0 to 0.1 mmol/L in both pre-compacting buffer solution and testing solution. PSL spheres with a hydrophobic nature can adsorb on the hydrophobic surface of nascent membranes much easier than on the hydrophillic surface of modified membranes. The adsorption of Triton X-100 on the nascent membrane surface modified the nascent membrane surface

to be more hydrophillic compared to the untreated nascent membranes, which led to a lower adsorption of PSL on the membrane surface. Less adsorption of PSL on the hydrophillic surface of the MF membrane caused the decrease in separation of PSL spheres and the increase in the solution flux.

Two parallel experiments were designed to clarify the influence of Triton X-100 on the membrane separation performance in the pre-compact buffer solution. First, a nascent membrane was pre-compacted with a buffer solution at 0.1 mmol/L Triton X-100 concentration, and then the membrane separation performance was tested by 100 ppm PSL solution without Triton X-100. The separation and flux of PSL solution is found to be identical to that of the nascent membrane, which was pre-compacted and tested without Triton X-100, as depicted in Table 2. Second, a nascent polypropylene membrane was pre-compacted by deionized water without Triton X-100, and then tested by a PSL solution with 0.1 mmol/L Triton X-100 concentration. The separation performance, separation and flux, as shown in Table 2, is close to that of the membrane treated with 0.1 mmol/L Triton X-100 concentration in both pre-compact and testing solution. These results indicate that including or excluding Triton X-100 in the pre-compact solution does not have any significant influence on the membrane separation performance of a nascent PP microfiltration membrane. This is probably due to the quick desorption of Triton X-100 from the membrane surface into the PSL testing solution if the PSL testing solution is Triton X-100 free. Also, the results confirm that Triton X-100 in the PSL testing solution, and not the precompaction step, cause the change in the membrane separation behaviour.

6.2.3 Mechanism of effects of Triton X-100 on the membrane performance

The effects of Triton X-100 on the membrane performance can be explained as the resultant of two effects as follows. (1) Triton X-100 molecules have a hydrophobic tail and a hydrophillic head. The hydrophobic tails can adsorb on the polypropylene microfiltration membrane surface due to the hydrophobic interaction, and the hydrophillic heads expands toward to aqueous solution. The adsorption of Triton X-100 molecules on the membrane surface caused membrane surface to be more hydrophillic. The separated PSL particle with a hydrophobic nature can be pushed away by a hydrophillic head of Triton X-100 adsorbed on the membrane surface, which reduces the hydrophobic adsorption of PSL. Thus, the separation of PSL particles decreases and flux increases in term of reducing the adsorption of the PSL particle on the membrane surface. (2) The addition of Triton X-100 in the testing solution makes the PSL particles more stable in aqueous solution and prevent PSL spheres from forming clusters or aggregates in the high concentration region, such as the concentration polarization region at the membrane top (feed) surface and/or at the inside of the membrane matrix. Thus, overall performance in the presence of Triton X-100 is probably a combination of both factors.

6.2.4 Membrane fouling analysis

In order to verify the extent of the fouling of the corresponding membranes in the separation of PSL spheres, a resistance-in-series analysis was carried out, as described in Chapter 5. The degree of fouling was found to decrease with increasing Triton X-100 concentration in the testing system, as presented in Figure

4. These results are consistent with the SEMs, in Figure 5, taken on the tested membrane surface after separating 100 ppm PSL solution with different Triton X-100 concentrations. Figure 5(a) shows that the feed side of the membrane pores is completely blocked by a dense packing of PSL spheres after the separation test of PSL solution without Triton X-100. At a low Triton X-100 concentration (0.015 mmol/L) in the testing solution, the adsorption of PSL spheres on the polypropylene membrane surface is reduced and the severe blockage of the membrane pore is greatly alleviated, as shown in Figure 5(b). When the concentration of Triton X-100 reached 0.1 mmol/L, no PSL spheres adsorption is observed on the membrane surface, as shown in Figure 5(d). Few, or no spheres are adsorbed on the bottom surface of any of the membrane (Figure 5(a-d) (bottom)). Obviously, the membrane fouling is decreased by reducing adsorption on the external and/or internal membrane surface.

6.2.5 Polyethylene glycol (PEG) ester membranes

In order to further investigate the impact of physically adsorbed Triton X-100 on the membrane performance, polyethylene glycol ester membranes were examined. These membranes, with pendent polyether moieties, mimic the membrane onto which the Triton X-100 was physically adsorbed. The surface properties of a polyethylene glycol (PEG) ester membrane are compared to nascent and DK membranes in Table 3. The PEG ester membrane is found to be more hydrophillic, by the through-pore penetration method, than the nascent membrane and DK membrane. The PEG ester membrane is also slightly negatively charged because of the formation of carboxylic acid groups caused by the trace amount of water involved in the photochemical reaction system. The reaction conversion of

PEG photochemical transformation is approximately 40% as discussed in Chapter 5. The PEG ester membrane is not a perfect model for the Triton X-100 adsorbed membrane since the polypropylene membrane was coated by a polysulfonamide layer prior to the photochemical transformation with polyethylene glycol. This polysulfonamide coating layer has been shown to modify the membrane performance. The slight negative charge on the PEG ester membrane surface may also have influences on the membrane performance.

In Table 3, the separation of PSL spheres with DK membrane is the same as the nascent membrane and the flux slightly increases. However, SEMs (Figure 6(a)) taken from the tested DK membranes show that the adsorption of PSL spheres on the membrane surface (feed side) is reduced significantly, compared to the nascent membrane (Figure 5(a)), due to the polysulfonamide coating which increases the membrane surface hydrophilicity.

For PEG ester membranes, a significant increase of PSL solution flux and a decrease of separation with PSL spheres are found in Table 3. SEMs in Figure 6(b) taken from the tested PEG ester membrane has an almost clear surface except for a few scattered beads sticking on the membrane surface (feed side). Therefore, the significant change of membrane separation performance can be attributed to the characteristics of the PEG ester functional groups on the membrane surface. PEG molecules attached on the membrane surface do have an impact on the membrane performance. This result indicates that Triton X-100 adsorbed on the nascent membrane surface has a similar impact on the membrane separation performance.

The packing density of PEG ester functional groups, calculated based on the total membrane surface area (15 m^2/g, measured by BET method) and the mass gain of the PEG ester groups, is 0.14 PEG molecules/nm^2. The packing density of adsorbed Triton X-100 molecules at the membrane surface has also been calculated

based on the mass of the Triton X-100 adsorption and membrane surface area, as listed in Table 4; packing density increases with increasing Triton X-100 concentration. Apparently, higher Triton X-100 packing density leads to a lower separation and higher solution flux. However, compared to the membrane with 0.12 Triton X-100 molecules/nm^2, at a Triton X-100 feed concentration of 0.045 mmol/L, the PEG ester membrane with the higher packing density of PEG was found to have a higher separation of PSL spheres and lower flux than that of the Triton X-100 adsorbed membrane if neglecting the influences caused by either polysulfonamide coating layer or the electric charges. SEMs show that the adsorption of PSL at PEG ester membrane surface (Figure 6(b) feed side) was much less than the Triton X-100 adsorbed membrane at a concentration of 0.045 mmol/L (Figure 5(c) feed side). The combination of PEG ester membrane separation performance with SEMs indicates that the severe aggregates of PSL spheres entrapped at the inside of the PEG ester membrane matrix, which caused the increased PSL separation and decreased solution flux. A possible reason for formation of the PSL aggregates at the inside of PEG ester membranes is that the PSL spheres in the absence of Triton X-100 are not very stable and can aggregate at the high concentration region, such as inside of membrane.

The function of Triton X-100 on the membrane separation performance can be to modify the membrane surface to be more hydrophillic and reduce the PSL spheres adsorption at the membrane surface; and prevent the PSL spheres from aggregating, specially in the high concentrated area, such as at the inside of the membrane matrix and/or adjacent to the membrane feed surface. But, PEG ester membrane studied in this chapter only demonstrated the former behaviour.

6.3 Conclusions

The results obtained in this Chapter indicate that the addition of Triton X-100 in the feed solution can significantly influence the polypropylene microfiltration membrane performance. The higher the concentration of Triton X-100 in the testing solution, the lower the separation of PSL spheres with polypropylene MF membranes. The change of membrane performance is directly related to the modification of the membrane surface caused by the physical adsorption of Triton X-100 molecules at the membrane surface. According to the results of the polyethylene glycol ester membrane, which mimic the Triton X-100 adsorbed membrane, the functions of Triton X-100 in the feed solution was not only to temporarily modify the membrane surface, but also to prevent the separated spheres from aggregating at the inside of the membrane matrix. Hence, the addition of Triton X-100 in the feed solution can be considered as an alternative way to temporarily modify the membrane performance without any membrane surface chemical reaction.

References

(1) H. Cheiel, R.M. McDonogh, H. Bauser and N. Stroh, "Aspecific interaction of protein with polymer surface", J. Dispersion Sci. and Tech., 12(2), (1991) 161-177.

(2) B. Hallstrom, Surface properties of ultrafiltration membranes, Proc. of the 8th ESMST Summer School, Gargnano, Italy, September 1990, M. Pegoraro (Ed.), Politecnico di milano 1990.

(3) A.S. Jonsson and G. Trägårdh, Ultrafiltration applications, Desalination, 77 (1990) 135-179.

(4) D. Doulia, V. Gekas and G. Trägårdh, Interaction behaviour in ultrafiltration of non-ionic surfactants. Part 1. Flux behaviour, J. Membrane Sci., 69 (1992) 251-258.

(5) E. Matthiasson, The role of macromolecular adsorption in fouling of ultrafiltration membranes, J. Membrane Sci., 16 (1983) 23-26.

(6) A.G. Fane and C.D.J. Fell, A review of fouling and fouling control in ultrafiltration, Desalination, 62 (1987) 117-136.

(7) A.S. Jonsson, Y. Blomgren and E. Petersson, Influence of pH and surfactant on ultrafiltration membranes during the treatment of bleach plant effluent, Nord. Pulp Paper Res. J., 3(4) (1988) 159-165.

(8) A.D. Marshall, P.A. Munro and G. Trägårdh, The effect of protein fouling in microfiltration and ultrafiltration on permeate flux, protein retention and selecivity: A literature review, Desalination, 91 (1993) 65-108.

(9) H. Attia, M. Bennasar and B. Tarodo de la Fuente, Study of the fouling of inorganic membrane by acidified milks using scanning electron-microscopy and electrophoresis. 2. Membrane with pore diameter 0.8 μm, J. Dairy Res., 55 (1991) 51-65.

(10) W. Pusch and A. Walch, Membrane structure and its correlation with membrane permeability, J. Membrane Sci., 40 (1989) 189-197.

(11) G. Morel, A. Graciaa and J. Lachaise, Enhanced nitrate ultrafiltration by cationi surfactant, J. Membrane Sci., 56 (1991) 1-12.

(12) J.A. Palmer, H.B. Hopfenberg and R.M. Felder, Effects of solute-membrane interaction on flux-limiting concentration polarization in ultrafiltration processing, J. Colloid and Interface Sci., 45 (2) (1973) 223-234.

(13) T. Swaminathan, M. Chaudhuri and K.K Sirkar, Flux enhancement in ultrafiltration by detergent treatment of membrane, J. Colloid and Interface Sci., 76(2), (1980) 573-579.

(14) Standard methods for the examination of water and wastewater, M.A. Franson (Ed.), Fourth Edition, John Wiley & Sons, New York, 1975.

(15) P. Mukerjee and K.J. Mysels, Critical micelle concentration of aqueous surfactant systems, Nat. Stand. Ref. Data Ser. (U.S. Nat. Bur. Stand.), NSRDS-NBS-36, 1971.

(16) A.G. Fane, C.J.D. Fell and K.J. Kim, The effect of surfactant pretreatment on the ultrafiltration of proteins, Desalination, 53 (1985) 37-55.

(17) R.B. Grieves, D. Bhattacharyya, W.G. Schomp and J.L. Bewley, Membrane ultrafiltration of a nonionic surfactant, AIChE J , 19(4) (1973) 766-774.

(18) D. Bargman and F. van Voorst Vader, Effect of surfactants on contact angles at nonpolar solids, J. Colloid and Interface Sci., 42(3) (1973) 467-472.

(19) L.M. Kushner and W.D. Hubbard, Viscometric and turbidimetric measurements on dilute aqueous solutions of nonionic detergent, J. Phys. Chem. 58 (1954) 1163-1167.

(20) A. Jonsson and B. Jonsson, The influence of nonionic and ionic surfactants on hydrophobic and hydrophilic ultrafiltration membranes, J. Membrane Sci., 56 (1991) 49-76.

Table 1. Characteristics of Triton X-100[a]

Surfactant	<mm>[b] (g/mol)	hlb[c]	CMC[d] (mmol/L)	Solubility
Triton X-100	645	13.5	0.25	Soluble in Water

[a] Formula: $C_{18}H_{17}(C_6H_4)O(CH_2CH_2O)_{10}H$

[b] Mean molar mass

[c] Hydrophilic lipophilic balance

[d] Critical micelle concentration

Table 2. Surface properties and separation performance of polypropylene nascent membranes treated with various concentrations of Triton X-100.

Triton X-100 (mmol/L)	γ_w [a] (dyne/cm)	Separation (%)	Solution flux (kg/m^2 s)	R_{if} [b] (10^6 m^{-1})
0	35.0 ±0.025	99.5 ±0.5	0.38 ±0.04	245 ±33.3
0.015	36.0 ±0.025	79.9 ±0.4	0.63 ±0.01	99.3 ±9.9
0.045	37.0 ±0.025	41.0 ±1.1	0.74 ±0.03	28.4 ±1.1
0.10	37.5 ±0.025	27.5 ±1.2	0.77 ±0.03	8.5 ±2.7
Pretreatment solution (0.1 mmol/L) Testing PSL solution (0 mmol/L)	37.5 ±0.025	99.9	0.34 ±0.02	256 ±17.3
Pretreatment solution (0 mmol/L) Testing PSL solution (0.1 mmol/L)	35.0 ±0.025	30.0 ±1.4	0.75 ±0.03	15.2 ±2.4

[a] γ_w is through-pore wetting surface tension measured by a surface penetration method with 2-ethoxy-ethanol and formamide mixtures.

[b] R_{if} is the resistance of internal fouling of membranes analyzed by a resistance-in-series model.

Table 3. Surface properties and separation performance of polypropylene nascent membranes, DK[a] and polyethylene glycol ester membranes without Triton X-100.

Name	γ_w[b] (dyne/cm)	Separation (%)	Solution flux (kg/m^2 s)	Pure Buffer Flux (kg/m^2 s)
Nascent	35.0 ±0.02	99.5 ±0.5	0.38 ±0.04	0.99 ±0.03
DK	36.0 ±0.025	99.2 ±0.7	0.42 ±0.04	1.11 ±0.02
PEG Ester	37.5 ±0.025	67.8 ±3.9	0.68 ±0.04	1.16 ±0.02

[a] DK is defined as polysulfonamide coated membrane.

[b] γ_w is through-pore wetting surface tension measured by a surface penetration method with 2-ethoxy-ethanol and formamide mixtures.

Table 4. Triton X-100 molecular packing density on the polypropylene membrane internal surface and polyethylene glycol molecules packing density on the PEG ester membrane internal surface[a].

Triton X-100 Concentration (mmol/L)	Mass Gain (%)	Triton molecule adsorption (molecules/nm^2)
0	0	0
0.015	2.4	0.09
0.045	3.0	0.12
0.10	4.1	0.16
PEG Ester membrane	N/A	0.14 (PEG molecules/nm^2)

[a] Assuming membrane surface area is 15 m^2/g.

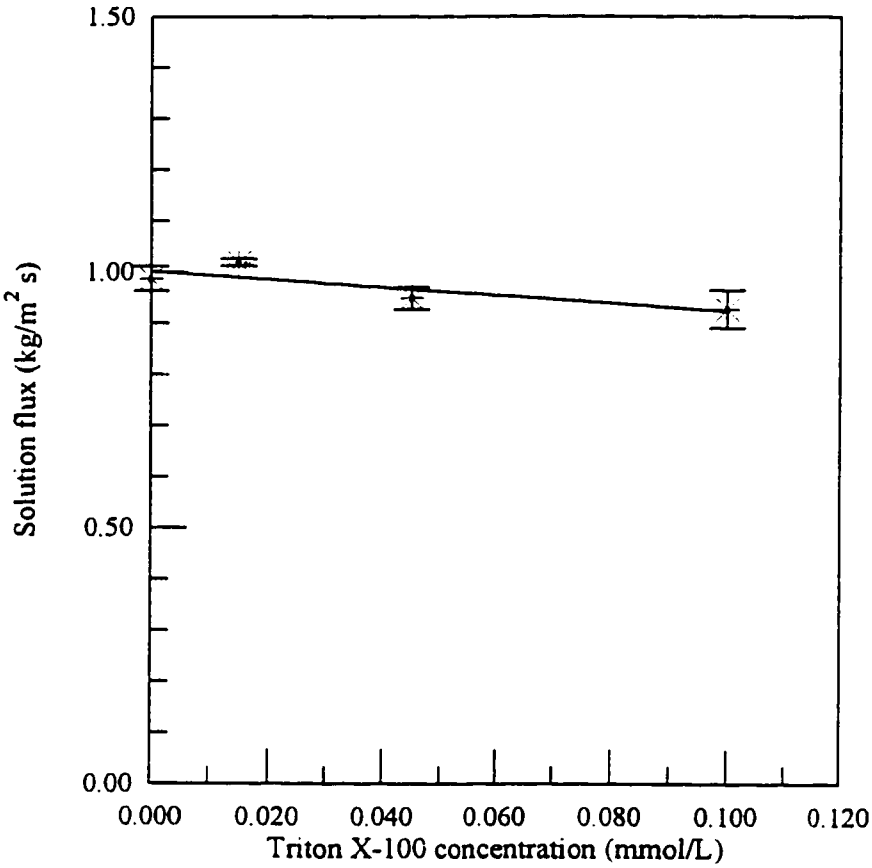

Figure 1. Water solution flux with different Triton X-100 concentrations.

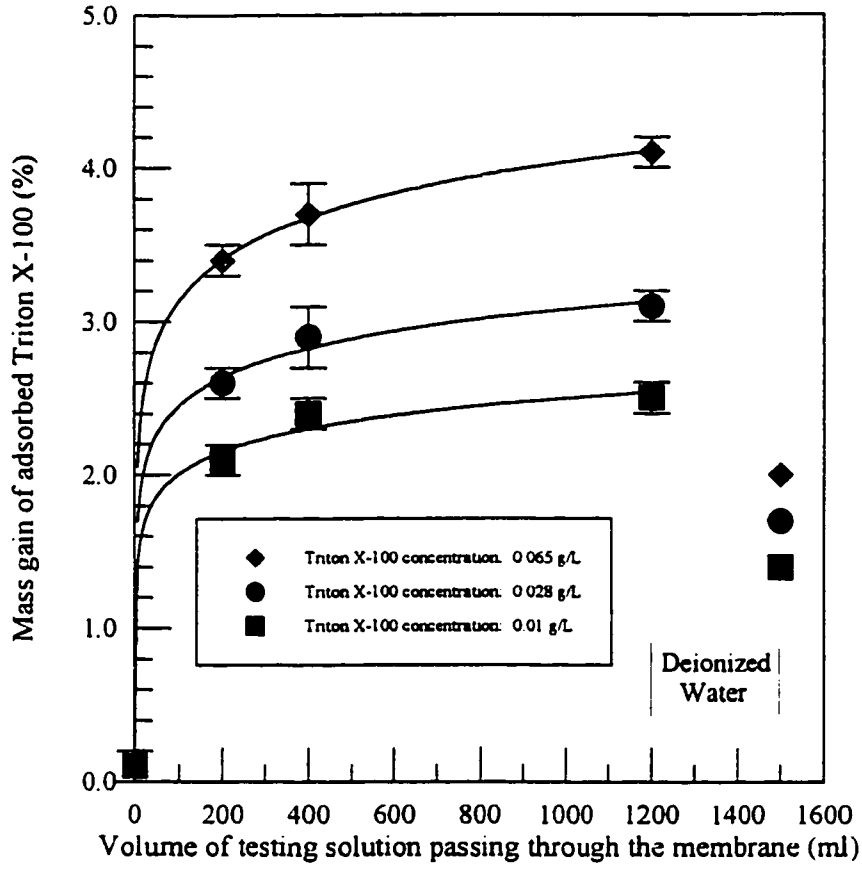

Figure 2. Dynamic equilibrium of Triton X-100 adsorption at membrane surface when the membrane was treated with different Triton X-100 concentrations.

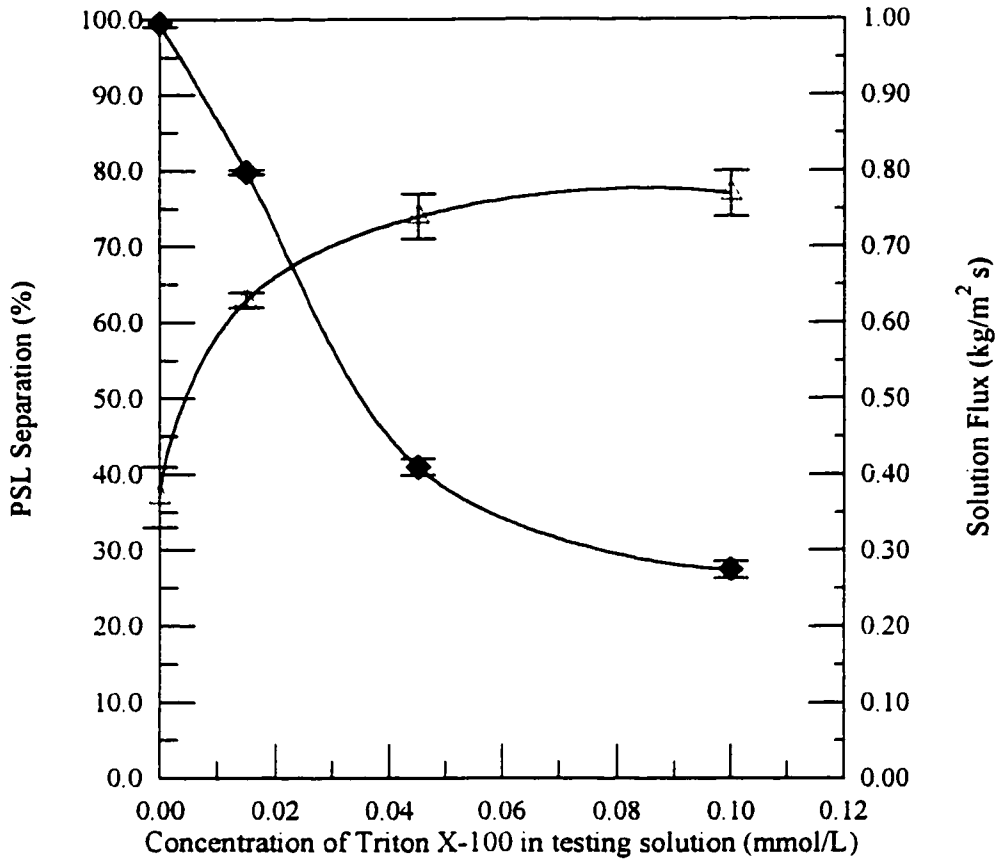

Figure 3. Flux and separation performance of polypropylene membranes in 100 ppm PSL solution and different Triton X-100 concentrations.

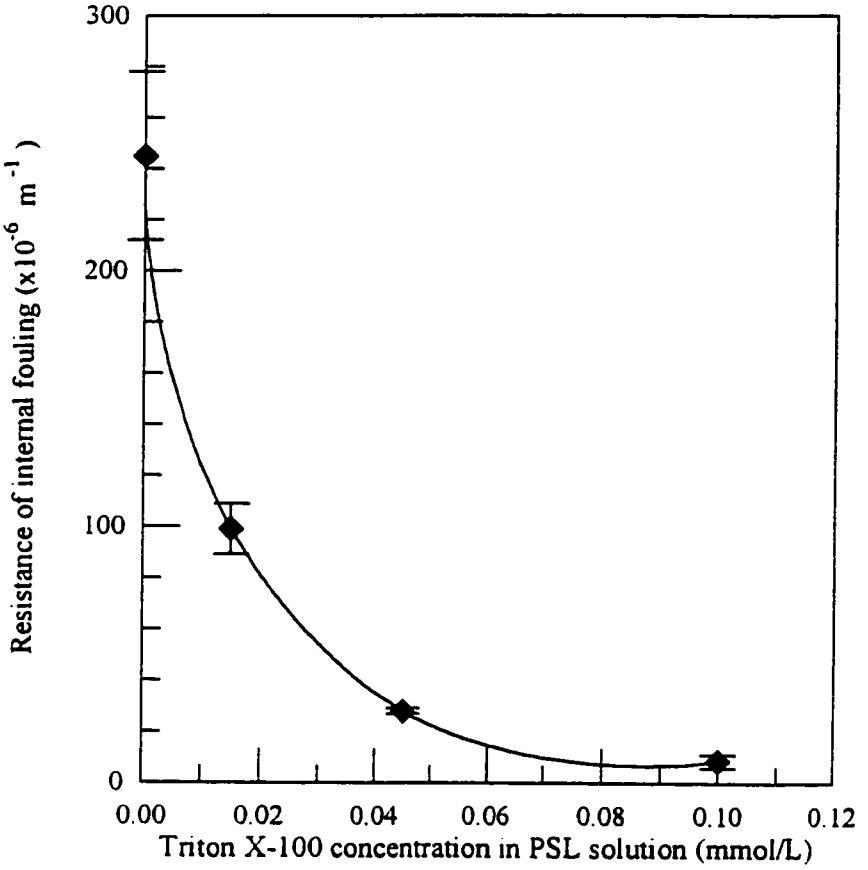

Figure 4. Internal fouling resistance of polypropylene membranes after separation of PSL solution with various Triton X-100 concentrations.

(a) (Top)

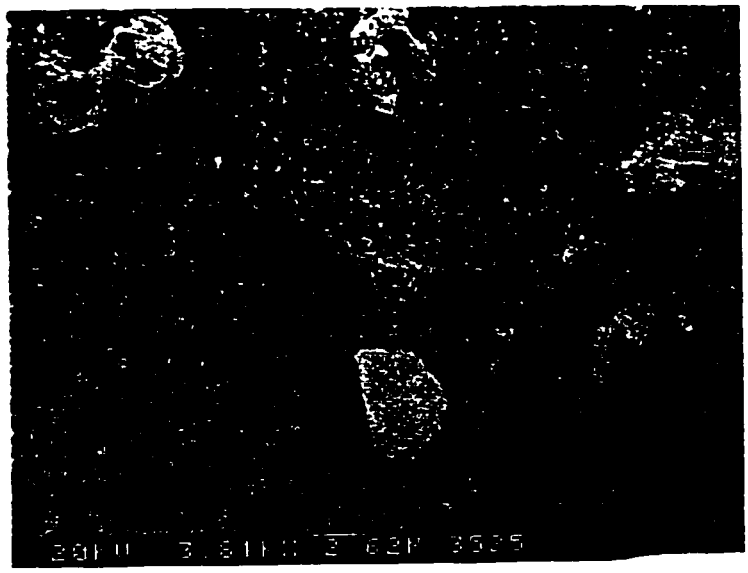

(a) (Bottom)

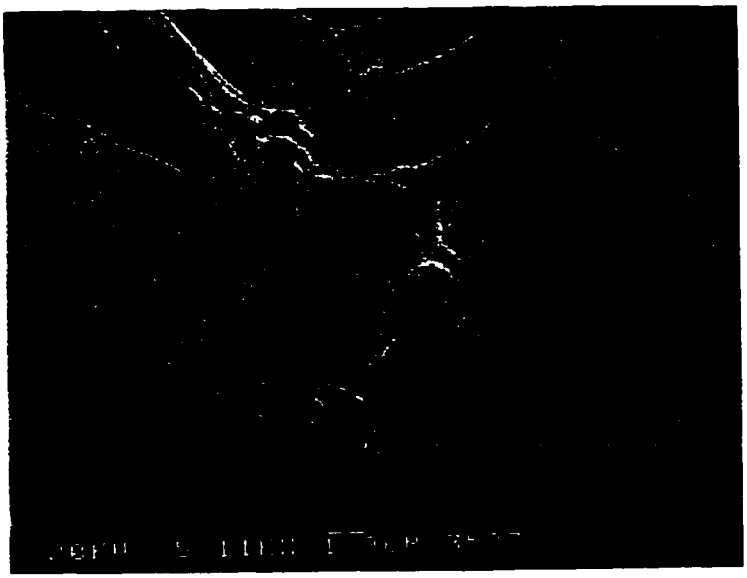

Figure 5. SEMs of polypropylene membrane surfaces after separation of 100 ppm PSL solution with different Triton X-100 concentrations. (a) Triton X-100 concentration: 0; (b) Triton X-100 concentration: 0.015 mmol/L; (c) Triton X-100 concentration: 0.045 mmol/L; (d) Triton X-100 concentration: 0.1 mmol/L.

(b) (Top)

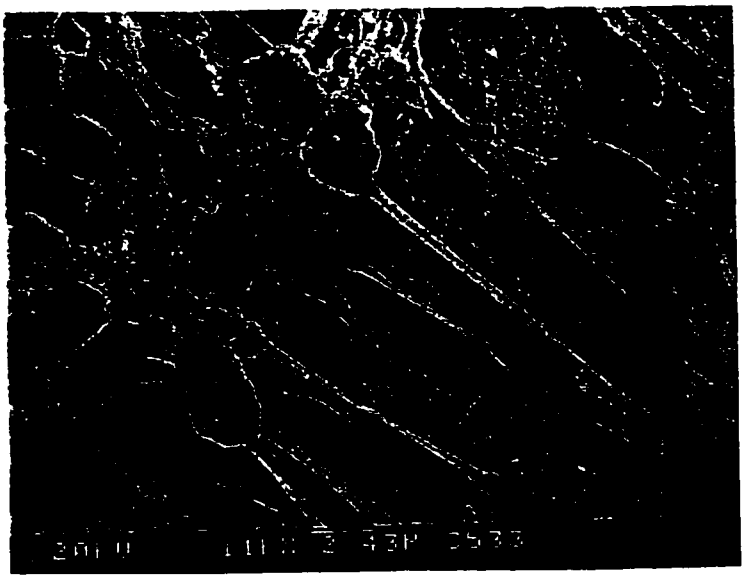

(b) (Bottom)

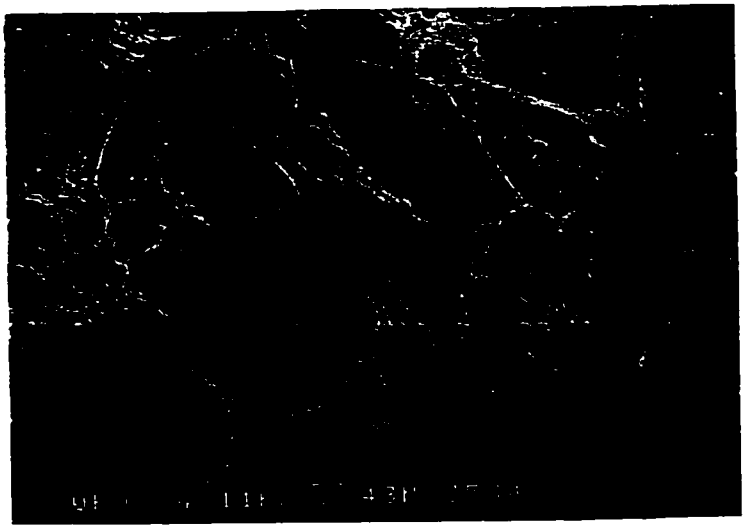

(c) (Top)

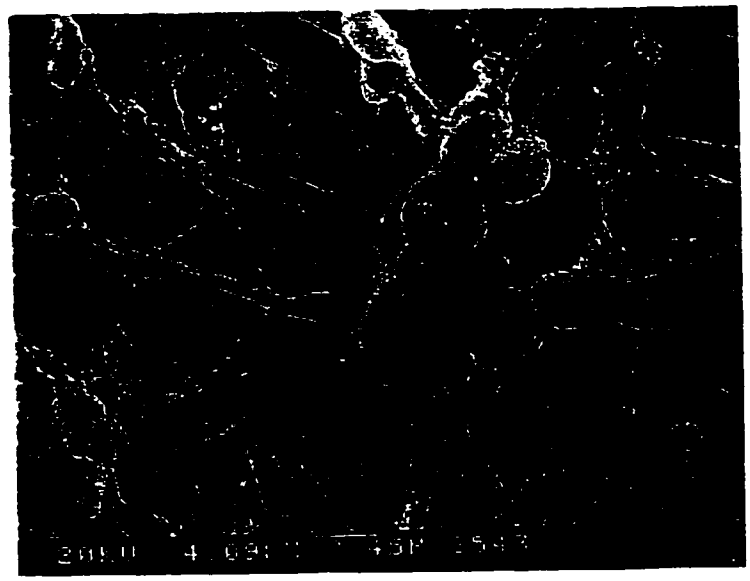

(c) (Bottom)

(d) (Top)

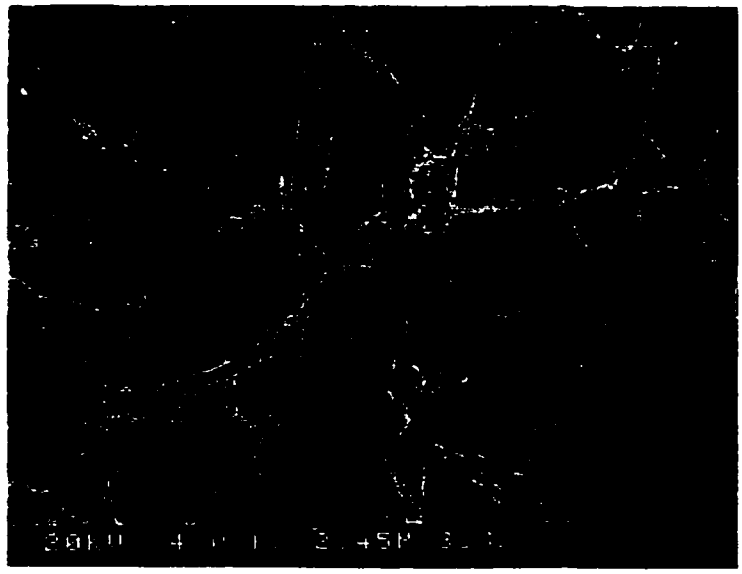

(d) (Bottom)

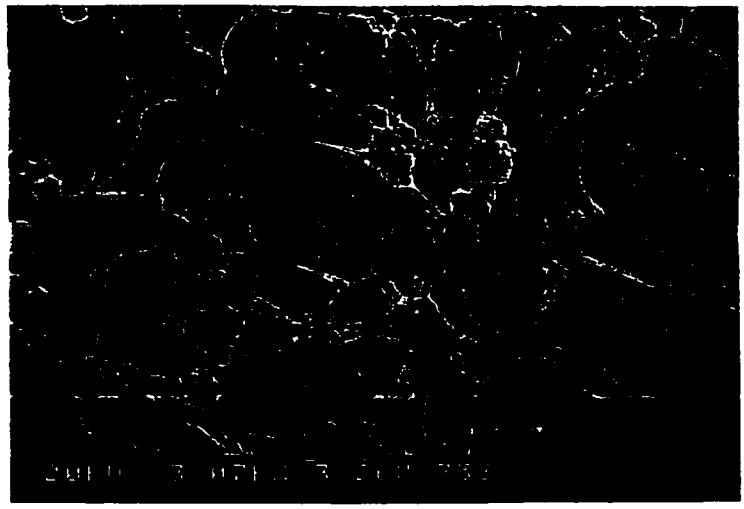

(a) (Top)

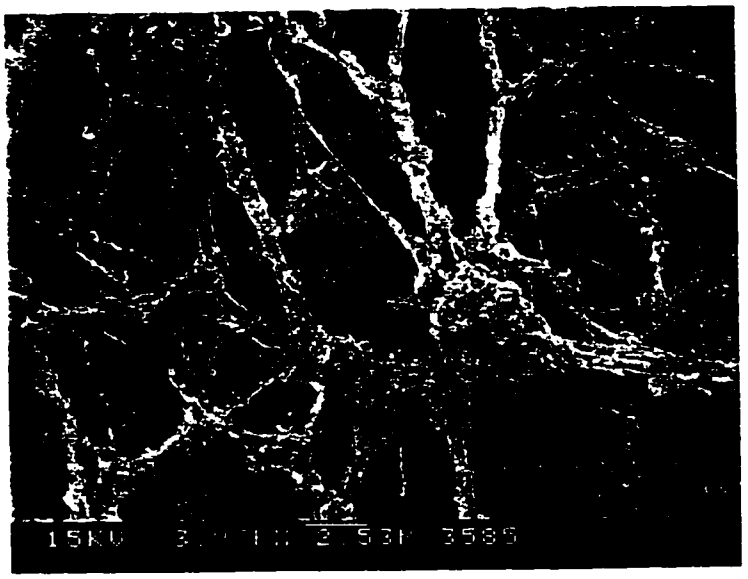

(a) (Bottom)

Figure 6. SEMs of surface of DK and polyethylene glycol ester (PEG) membranes after separation of 100 ppm PSL solution without Triton X-100. (a) DK membrane; (b) PEG ester membrane,

(b) (Top)

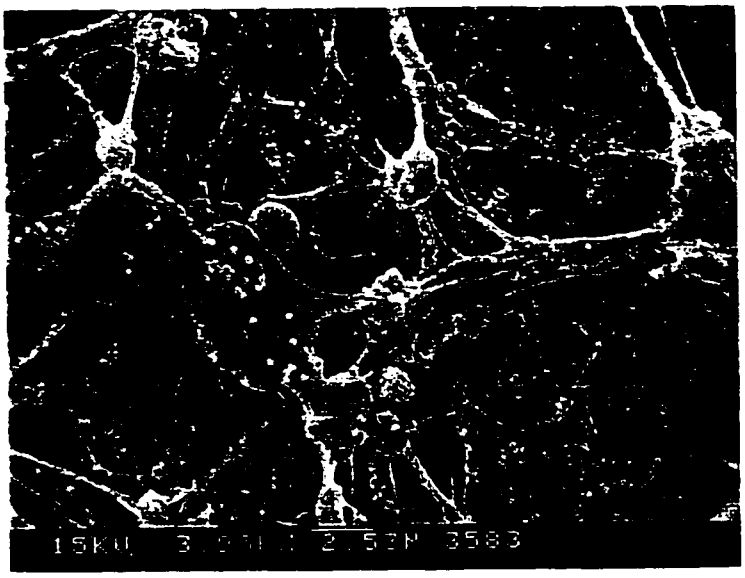

(b) (Bottom)

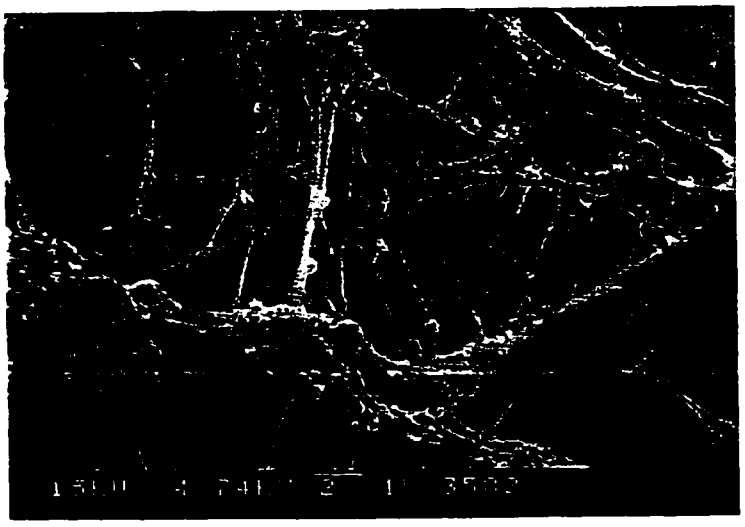

Chapter 7

Conclusions and Recommendations

This thesis examines the surface coating, photochemical modification, characterization and membrane performance of polypropylene microfiltration membranes. Aspects involved in this study are: (i) further development of the internal surface coating technology based on 1,6-naphthalene disulfonylchloride containing a photoactive diazoketone group, as a pendent group, and octanediamine; (ii) proposal and qualitative investigation of the coating mechanism; (iii) demonstration of the general applicability of this new coating technology; (iv) photochemical transformation of diazoketone groups into different functionalities; (v) permeability properties of the membranes and the effect of surfactant on the membrane performance.

The major conclusions can be drawn as follows:

(1) A photoactive thin film coating for the internal surface of polypropylene microfiltration membrane has been successfully made by a modified interfacial polymerization of 1,6-naphthalene disulfonylchloride containing a diazoketone (DK) group on the side chain and 1,8-octanediamine. Various fabrication conditions including concentration of monomers, organic solvent selection, crosslinking agent, selection of acid acceptor and reaction time were investigated. The choice of organic solvent was found to be the key factor for obtaining an even, smooth coating layer without significantly changing the membrane morphology. Mass of the coating layer was typically 10%-15% of the mass of the base membrane, but depended on the amount of crosslinking agent and the acid acceptor.

(2) The coating technology has been evaluated in various ways. The solid evidence coming from FT-IR and SEM/EDS indicated that the polysulfonamide coating layer has an even distribution covering the whole membrane internal surface. Also, the coating layer at the internal membrane surface demonstrated a high stability to Soxhlet extraction with $CHCl_3$ for 48 hours, implying a long operating life time of the coating.

(3) A mechanism of this new type of interfacial polymerization is qualitatively proposed, and investigated experimentally. Most results from experiments, including end-group analysis for the molecular weight measurement of coating polysulfonamide by neutron activation technique, either strongly support the proposed mechanism or can be reasonably interpreted by the proposed mechanism. The mechanistic study defines the most important principles of this new type of interfacial polymerization which can be varied to control the coating process, and gives researchers a better understanding of this new type of interfacial polymerization.

(4) General applicability of this new type of coating technology has been demonstrated by applying this technology to coat other polymers (a polyester and a polyamide) onto internal surface of polypropylene microfiltration membrane. The polyester and polyamide were found to be successfully coated on the internal surface of polypropylene membranes based on the results of mass gain and SEMs. The mass gain of polyester coating layer can be up to 120% and the mass gain of polyamide coating layer is approximately 15% of the base membrane.

(5) The chemical functionality of the polysulfonamide coated membrane surface could be further modified *via* photochemical reaction in the presence of an appropriate medium. Membranes containing indene acid, glycolic acid,

bromoethyl ester, and polyethylene glycol ester functionalities were fabricated and confirmed by FT-IR and neutron activation analysis, and the efficiency of those photochemical reactions was approximately 80%. The charge density of DK control and corresponding functionalized membranes was determined. The highest charge density (0.097 meq/g) could be achieved on the glycolic acid ester membranes. The wetting surface tension, γ_w, was determined using a series of wetting solutions of different surface tension. The hydrophilicity of the membrane surface is increased by polysulfonamide coating and further increased by photochemical functionalization.

(6) The microfiltration flux and separation performance of these membranes with polystyrene latex (PSL) and carboxylate modified latex (CML) spheres, were examined. The extent of fouling of the membranes was studied by SEM. A lower separation of PSL was found for the functionalized membrane compared to the DK control membrane. Pure water flux was increased after photochemical modification. The decreased separation was due to decreased blockage of the membranes by decreasing the physical adsorption of the separated spheres to the coated membranes compared to the nascent membranes. These results suggest that the increase of hydrophilicity of the photochemically modified membranes was the dominated factor affecting the membrane separation performance. The degree of fouling of the functionalized membranes was significantly decreased and should lead to an improvement of the membrane effective life-time.

(7) The influence of a non-ionic surfactant, Triton X-100, on the polypropylene microfiltration membrane performance has also been investigated using 100

ppm polystyrene latex (PSL) testing solution in a dead-end stirred test cell. A remarkable decrease of separation and a significant increase of solution flux was found after the addition of Triton X-100 in the feed solution. The degree of fouling of each tested membrane was examined by SEM and also analyzed by a resistance-in-series model. It was found that fouling of the tested membrane caused by the adsorption of PSL spheres was significantly reduced by increasing Triton X-100 concentration in the testing solution; at concentrations far below the critical micelle concentration of Triton X-100. In order to clarify the function of Triton X-100 in the membrane separation performance, polyethylene glycol ester membranes were fabricated to mimic the membrane passively adsorbed with Triton X-100. The results suggested that the Triton X-100 in the testing solution not only temporarily modified the membrane surface properties to be more hydrophilic, thus reducing physical adsorption of PSL spheres, but also prevented the PSL particles from aggregating, particularly in the membrane matrix.

Recommendations for further study of this project are as follows.

(1) In order to further expand the application of this new coating technology, other condensation polymers, such as polyurea, polyurethane or polycarbonate, should be tested for coating the internal surface of both polypropylene and polyethylene microfiltration membranes with different pore sizes. Although polyester and polyamide have been reported to be successfully coated on the PP microfiltration membrane surface in this thesis, further investigations are needed, particularly, in terms of permeability properties.

(2) A qualitative mechanism for the modified interfacial polymerization has been hypothesized and is supported by the experimental results. Further experimental studies of the mechanism standing behind this new type of interfacial polymerization are needed.

(3) To modify the microfiltration membrane surface with different functionalities using the same precursor is a desired technology for most membrane scientists. However, the photochemical transformation of diazoketone group into various functionalities on the membrane surface is hindered by the side competing reaction with water, as reported in this thesis. Other active groups contained in the coating polymer backbone or side chain may be worthwhile to develop in order to overcome this shortcoming of the diazoketone photochemistry. The relatively low charge density of the functionalized membrane is another obstacle encountered, which is mainly due to the relative small amount of diazoketone group incorporated into the coating polymer layer. Increasing the amount of active group incorporated in the coating polymer and increasing the efficiency of the transformation of the functionalities onto the membrane surface can be the subject of further study.

Appendix A

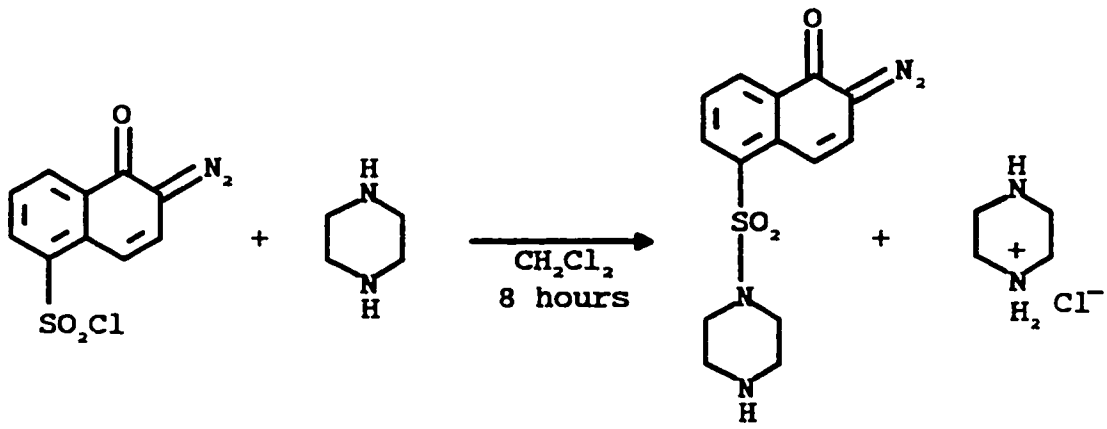

(A)

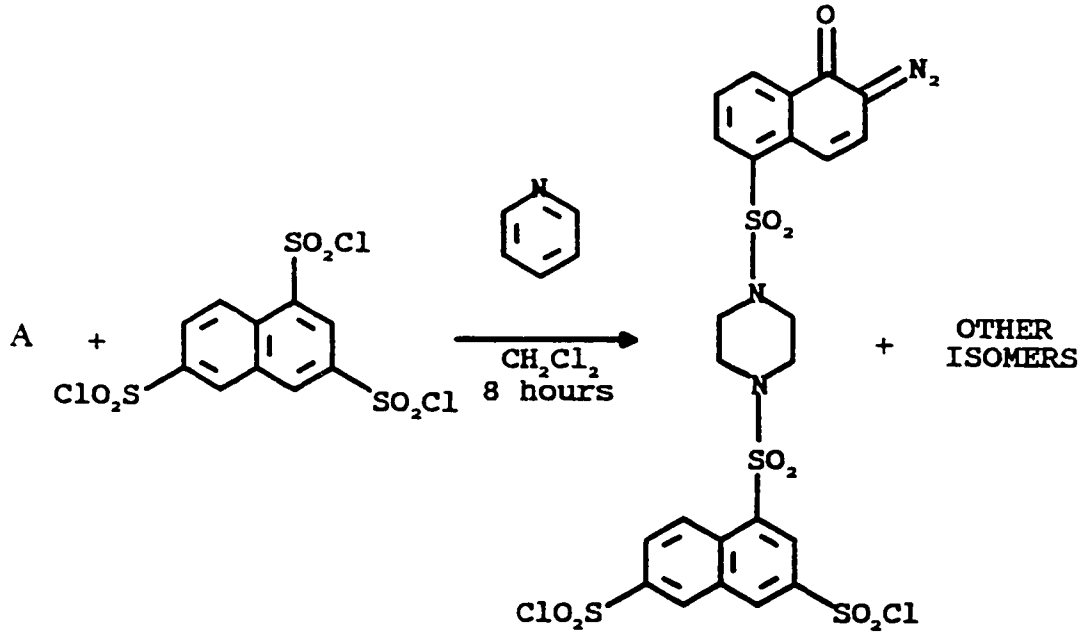

Monomer I

Figure A-1. Synthesis of monomer I

Appendix A

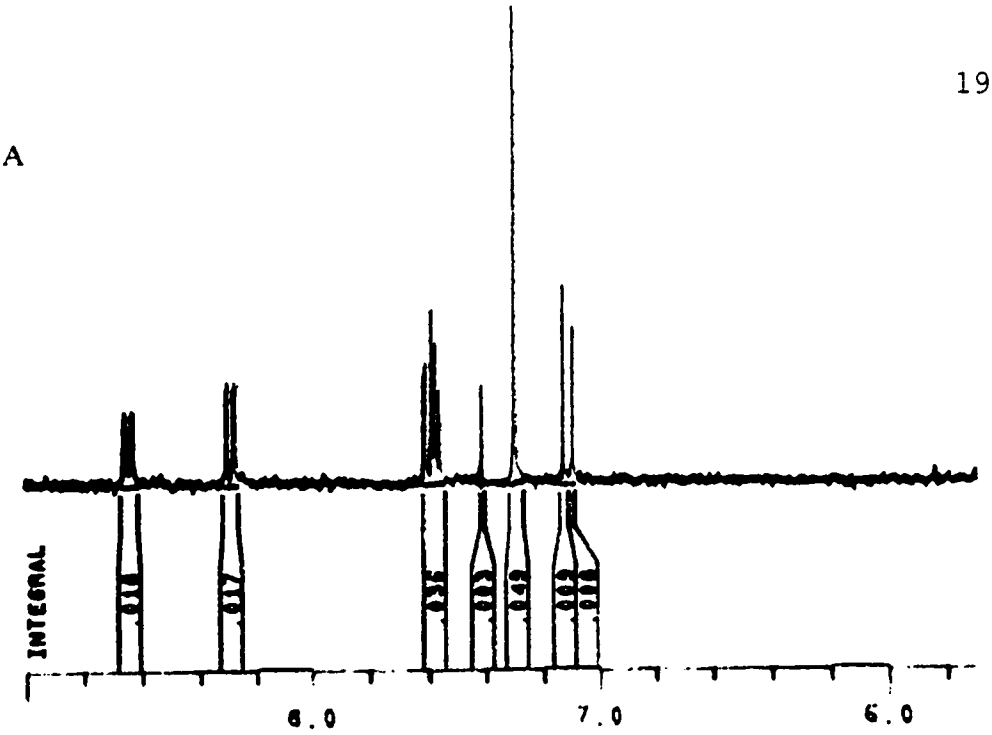

(a)

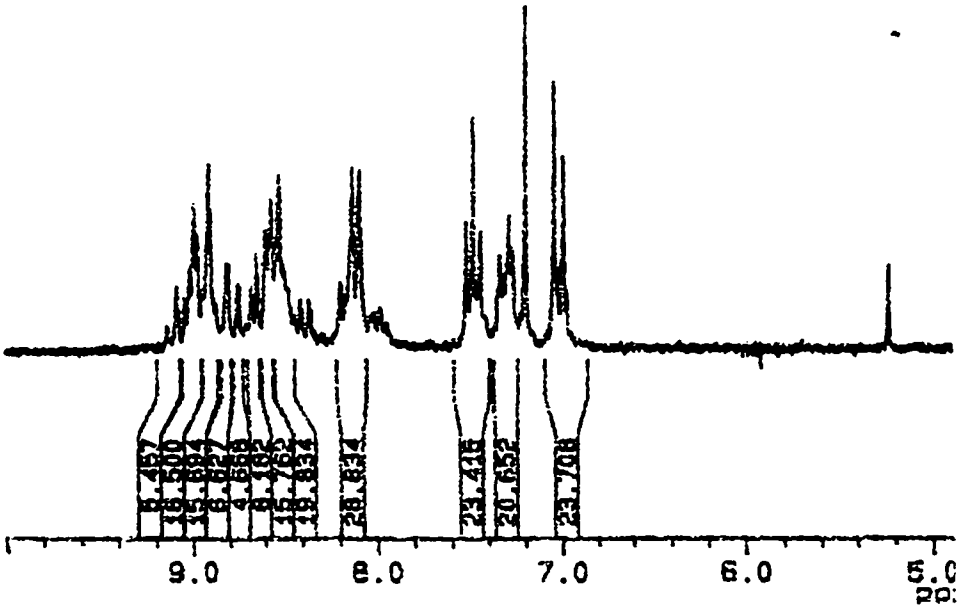

(b)

Figure A-2. ^{1}H NMR spectra of product A and monomer I. (a) NMR of product A; (b) NMR of monomer I

Appendix A

A-3 Coating polymerization procedure for polysulfonamide coated membranes.

Circular nascent membrane samples for coating polymerization were made using a die. The die has two bored cutting edges, one on each end of the 3.5 inch cylinder. For dead-end cell, the cutter diameter were 3.375 inch with 0.125 inch edge. The membrane samples were cut with a press, pressure applied approximately 3000 pounds. The membrane sample was placed on a nylon board (1 inch thick), Whatman filter paper was also placed between the membrane sample and nylon board to prevent the damage of the membrane sample.

The membrane sample was washed with methanol three times, five minutes each, then, soaked in 20 wt% diamine solution (methanol used as a solvent) five minutes, removed from the solution and then dried at room temperature for 60 minutes to evaporate the methanol. The membrane was immersed in 50 ml of disulfonyl chloride solution (1 g/L) contained in a 300 ml wild mouth jar with a threaded lid, for one hour. The jar was placed into a water bath to keep a constant polymerization temperature.

After polymerization, the membrane was removed from the jar and washed with CH_2Cl_2 twice, 5 minutes each, and then with methanol for 5 minutes. The membrane sample was dried for 60 minutes and weighed to give the mass gain of the membrane sample.

Appendix A.

A-4. Sample preparation and scanning electron microscope/energy disperse spectrum.

The scanning electron microscope (SEM) used was a ISI model DS-130 and the energy disperse analysis (EDS) was performed with a PGT Model System 4000 having a standard beryllium detector. The top and bottom surface view of membrane was obtained by cutting a square of size (15 mm by 10 mm) with scissors to fit on the aluminum stub (sample platform). The membrane sample was fixed on the stub for the surface view with silver paint.

The membrane cross section was obtained by fracturing the membrane along with grain. The membrane samples held by forceps was immersed into liquid nitrogen for 5 min. Then, remove the sample from liquid nitrogen, make a nick at the edge of the membrane sample with a razor blade. The membrane sample was immersed into liquid nitrogen again for 5 min. After the membrane was removed from the liquid nitrogen, a second pair of forceps was used to pull apart the sample where the nick was made. Since the sample was flimsy, the fractured sample supported by a small toothpick was glued on the stab with 5 minutes epoxy, so that the fractured edge of the membrane sample can be face up to obtain the required angle to the detector. A light microscope with 10 times magnification was used to confirm visually that the required position of the sample was obtained. If only SEM was performed on the sample, the fractured edge can be grounded to the stub by silver paint.

The mounted samples were placed in a desiccator under low vacuum and for SEM were sputter coated with a minimum of 15-20 nm thick layer of gold. The maximum accelerating voltage of the electron beam was 15 kV, to prevent deterioration of the sample. The mounted sample for EDS measurement was coated with chromium. The conditions applied for EDS analysis were 256 channels, dwell time 0.1 and 10 passes.

Appendix A

A-5. Sample preparation for FT-IR analysis

To increase the translucency of the membrane sample, a circular piece of membrane sample (Diameter: 0.6 cm) was compressed with 10,000 pounds force by a press. A solid steel cylinder 1 inch diameter and 1 inch length was used to concentrate the loading on the sample. To obtain an evenly compressed sample, the pressure was applied for 1 min and 3 times rotating the steel cylinder a few degrees each time. Forceps were used to remove the sample from the press and put the sample into a sample holder for FT-IR analysis.

A-6. Stability study

The method applied to evaluate the durability of coated membranes (Soxhlet extration) was that three coated membranes were placed into a 500 ml flask with 300 ml $CHCl_3$. The flask connected to a reflux condenser, was heated by an electric bowl to keep temperature at 61°C ($CHCl_3$ boiling point) for 48 hours. The membrane sample was removed from the flask and the sample dried at room temperature for one hour, then weighed to give the mass loss of the sample.

Appendix B

Table B-1. Mass gain of polysulfonamide at different monomer I concentrations. (Reaction conditions are listed in Figure 3 at Chapter 2).

Monomer I concentration (mmol/L)	Mass Gain (%)			Average (%)	Standard deviation
	Sample 1	Sample 2	Sample 3		
0	0	0	0	0	0
1.4	7.8	6.4	7.1	7.1	0.7
2.8	7.5	8.5	8.9	8.3	0.7
3.5	8.5	9	9.7	9.1	0.6
7.1	16.7	14.9	15.6	15.7	0.9
14.2	23.4	21.9	23.1	22.8	0.8

Appendix B

Table B-2. Mass gain of coating polysulfonamide at different solvent mixtures. (Reaction conditions are listed in Figure 5 at Chapter 2).

CCl_4 /CH_2Cl_2 (v/v)	Mass Gain (%)			Average (%)	Standard deviation
	Sample 1	Sample 2	Sample 3		
0/100	7.4	7.3	6.7	7.1	0.4
30/70	7.8	8.6	8.3	8.2	0.4
40/60	9.8	9.3	9.6	9.6	0.3
45/55	10.5	11.0	10.1	10.5	0.5
50/50	12.6	13.7	13.4	13.2	0.6
55/45	15.6	15.5	16.2	15.8	0.4
60/40	17.6	19.0	18.3	18.3	0.7
80/20	17.8	16.7	18.1	17.5	0.7

Appendix B

Table B-3. Mass gain of coating polysulfonamide at different octanediamine depositions. (Reaction conditions are listed in Figure 8 at Chapter 2).

Octanediamine deposition (%)	Mass Gain (%)			Average (%)	Standard deviation
	Sample 1	Sample 2	Sample 3		
0	0	0	0	0	0
10	4.5	4.1	4.0	4.2	0.3
19.7	10	10.7	9.9	10.2	0.4
27.8	15.3	14.6	14.2	14.7	0.6
36.8	15.0	15.7	14.9	15.2	0.4

Appendix B

Table B-4. Mass gain of coated polysulfonamide at different polymerization time. (Reaction conditions are listed in Figure 10 at Chapter 2)

Polymerization time (min)	Mass Gain (%)			Average (%)	Standard deviation
	Sample 1	Sample 2	Sample 3		
0	0	0	0	0	0
20	1.2	1.8	1.7	1.6	0.3
40	7.2	6.3	6.5	6.7	0.5
60	9.2	10.6	9.4	9.7	0.8
90	11.2	11.9	11.4	11.5	0.4
120	13.4	12.4	12.1	12.6	0.7
180	14.7	13.9	13.6	14.1	0.6
240	15.6	14.3	13.8	14.6	0.9

Appendix B

Table B-5. Mass gain of coated polysulfonamide at different amounts of crosslinking agent (NTSC). (Reaction conditions are listed in Figure 12 at Chapter 2).

NTSC/monomer I (mol/mol)	Mass Gain (%)			Average (%)	Standard deviation
	Sample 1	Sample 2	Sample 3		
0	11.4	10.6	11.1	11.0	0.4
2	11.5	11.8	11.0	11.4	0.4
9	14.5	13.6	13.3	13.8	0.6

Appendix B

Table B-6 Mass gain of coated polysulfonamide at different acid acceptors. (Reaction conditions are listed in Figure 14 at Chapter 2).

Pyridine/ monomer I (mol/mol)	Mass Gain (%)			Average (%)	Standard deviation
	Sample 1	Sample 2	Sample 3		
0	11.4	11.0	10.8	11.1	0.3
1	11.4	11.7	12.2	11.8	0.4
4	11.1	11.9	11.1	11.4	0.5
10	11.0	11.4	11.2	11.2	0.2
Triethylamine/ monomer I (mol/mol)	Mass Gain (%)			Average (%)	Standard deviation
	Sample 1	Sample 2	Sample 3		
0	11.8	11.8	11.2	11.6	0.3
1	13 8	14.1	14.6	14.2	0.4
4	15.9	16.3	15.3	15.8	0.5
10	16.0	17.1	16.2	16.4	0.6

Appendix C

Table C-1 Solubility of octanediamine and monomer I in different solvent mixtures

CCl_4/CH_2Cl_2 (v/v)	Solubility of monomer I (mol/L)	Solubility of octanediamine (mol/L)
0/100	0.0525	1.16
10/90	0.0326	N/A
30/70	0.0073	0.76
40/60	0.0046	0.58
50/50	0.0029	0.52
60/40	0.0021	0.48
80/20	0.0006	0.4
100/0	0.0001	0.38

Appendix C

Table C-2 Dissolving of loaded octanediamine on the membrane surface into different solvent mixtures at different time.

CCl_4/CH_2Cl_2 (v/v)	Remaining mass gain (%) of octanediamine on the membrane surface after immersing the membrane into solvent for a certain minutes							
	0	5	10	15	20	30	50	60
0/100	19.5	9.6	6.1	4.3	N/A	2.2	0.3	0
30/70	19.7	11.3	8.5	6.8	N/A	4.0	2.3	1.8
40/60	19.9	12.4	9.6	8.6	N/A	6.0	4.2	4.0
50/50	19.5	13.4	11.5	10.2	N/A	8.2	6.2	5.8
80/20	19.8	14.9	14.5	N/A	12.8	N/A	12.3	12.0
100/0	19.8	15.6	15.2	N/A	14.0	N/A	13.5	13.1

Appendix C

Table C-3 Turbidity of reaction medium after the coating polymerization.

Polymerization time (min)	Turbidity (NTU)			Average (NTU)	Standard deviation
	Sample 1	Sample 2	Sample 3		
0	0	5	10	5	5
20	155	170	150	158	10
40	250	220	240	237	15
60	365	375	355	365	10
90	435	425	415	425	10
120	535	530	515	527	10

Appendix C

Table C-4 Average molecular weight of coating polysulfonamide at different octanediamine loading

Octanediamine loading (%)	Average molecular weight			Average	Standard deviation
	Sample 1	Sample 2	Sample 3		
10	25300	24300	21800	23800	1800
20	See Table 1 in Chapter 3			21800	2180
37.6	21300	18800	18400	19500	1570

Appendix D

Table D-1 Experimental results of photochemical conversion of indene acid, glycolic acid ester, PEG ester and bromoethyl ester membranes.

	Indene acid membranes				
	Sample 1	Sample 2	Sample 3	Average	STD
DK (μmol)	4.88	5.29	4.69	4.95	0.31
Na (μmol)	3.60	3.61	2.83	3.35	0.45
Conversion (%)	73.8	68.2	60.5	67.5	6.7
	Glycolic acid ester membranes				
DK (μmol)	5.58	5.49	5.53	5.53	0.05
Na (μmol)	4.69	4.83	4.73	4.75	0.07
Conversion (%)	84.1	88.1	85.6	85.9	2.0
	Bromoethyl ester membranes				
DK (μmol)	8.62	8.36	8.29	8.42	0.17
Br (μmol)	7.20	6.79	6.60	6.86	0.31
Conversion (%)	83.6	81.3	79.6	81.5	2.0
	Conversion of indene acid on PEG ester membranes				
DK (μmol)	8.59	8.09	8.96	8.55	0.44
Na (μmol)	3.08	2.94	3.73	3.20	0.4
Conversion (%)	35.8	36.4	41.6	37.9	3.2
	Conversion of PEG ester measured gravimetrically				
Conversion (%)	40.1	42.7	38.2	40.3	2.3

Appendix D

Table D-2 Pure buffer flux and separation performance of nascent, DK, indene acid and glycolic acid ester membranes at separation of PSL 204. (Separation conditions are already listed in Figure 3 in Chapter 5)

	Pure buffer flux (kg m^{-2} s^{-1})				
	Sample 1	Sample 2	Sample 3	Average	STD
Nascent	1.52	1.45	1.39	1.45	0.07
DK	1.53	1.61	1.49	1.54	0.06
I-CON	1.58	1.50	1.53	1.54	0.04
G-CON	1.59	1.49	1.52	1.53	0.05
I-ACID	1.67	1.65	1.66	1.66	0.01
G-ACID	1.61	1.64	1.61	1.62	0.02
	Solution flux (kg m^{-2} s^{-1})				
Nascent	0.86	0.77	0.72	0.78	0.07
DK	0.96	0.92	0.91	0.93	0.03
I-CON	0.97	0.99	0.91	0.96	0.04
G-CON	0.97	0.94	0.92	0.94	0.03
I-ACID	1.10	1.09	1.08	1.09	0.01
G-ACID	1.15	1.10	1.08	1.11	0.04
	Separation of PSL 204 solution (%)				
Nascent	72.1	64.9	61.2	66.1	5.5
DK	41.9	39.9	34.1	38.6	4.1
I-CON	41.0	33.6	36.2	36.9	3.8
G-CON	36.3	44.7	42.3	41.1	4.3
I-ACID	21.6	18.6	16.2	18.8	2.7
G-ACID	13.2	14.9	18.7	15.6	2.8

Appendix D

Table D-3 Pure buffer flux and separation performance of nascent, DK, indene acid and glycolic acid ester membranes at separation of CML 203. (Separation conditions are already listed in Figure 3 in Chapter 5).

	Pure buffer flux (kg m^{-2} s^{-1})				
	Sample 1	Sample 2	Sample 3	Average	STD
Nascent	1.47	1.49	1.48	1.48	0.01
DK	1.54	1.62	1.52	1.56	0.05
I-CON	1.56	1.52	1.56	1.55	0.02
G-CON	1.58	1.49	1.55	1.54	0.05
I-ACID	1.69	1.64	1.67	1.67	0.03
G-ACID	1.70	1.62	1.64	1.65	0.04
	Solution flux (kg m^{-2} s^{-1})				
Nascent	0.86	0.77	0.83	0.82	0.05
DK	0.94	0.90	0.89	0.91	0.03
I-CON	0.95	0.98	0.91	0.95	0.04
G-CON	0.99	0.93	0.91	0.94	0.04
I-ACID	1.37	1.38	1.34	1.36	0.02
G-ACID	1.17	1.22	1.15	1.18	0.04
	Separation of CML 203 solution (%)				
Nascent	61.5	68.9	65.7	65.4	3.7
DK	42.6	45.6	47.8	45.3	2.6
I-CON	38.8	46.2	40.8	41.9	3.8
G-CON	43.9	41.8	48.2	44.6	3.3
I-ACID	9.9	9.2	9.7	9.6	0.4
G-ACID	15.5	14.2	10.1	13.3	2.8

Appendix D

Table D-4 Chlorine and bromine standard solution measurement by NAA

	Chlorine Measurements		
No.	Standard (μg)[a]	Measured value	Deviation (%)
1	47.9	53.3 ±2.3	10.1
2	191.5	192.8 ±8.0	0.7
	Bromine Measurements		
	Standard (μg)[b]	Measured value	Deviation (%)
1	75.0	76.9 ±1.0	2.5
2	301.3	307.7 ±3.6	2.1
3	600.3	574.8 ±7.0	4.2

[a] Chlorine standard solution was made by diluting HCl standard solution.

[b] Bromine standard solution was made by dissolving KBr (99.99%) in deionized water

Appendix E

Table E-1 Pure buffer flux and separation performance of membranes at different Triton X-100 concentrations[a].

Conc. of Triton X-100 (mmol/L)	Pure buffer flux (kg m^{-2} s^{-1})				
	#1	#2	#3	Average	STD
0	1.01	0.99	0.96	0.99	0.03
0.015	1.02	1.01	1.01	1.01	0.01
0.045	0.96	0.93	0.97	0.95	0.02
0.10	0.91	0.95	0.92	0.93	0.02
	Solution flux (kg m^{-2} s^{-1})				
0	0.41	0.34	0.39	0.38	0.04
0.015	0.65	0.64	0.63	0.64	0.01
0.045	0.75	0.71	0.76	0.74	0.03
0.10	0.81	0.75	0.76	0.77	0.03
Trial 1[b]	0.37	0.34	0.31	0.34	0.03
Trial 2[b]	0.78	0.74	0.73	0.75	0.03
	Separation of PSL 304 (%)				
0	99.9	99.7	99.0	99.5	0.5
0.015	80.4	79.6	79.8	79.9	0.4
0.045	42.1	40.1	40.8	41.0	1.0
0.10	28.8	26.6	27.1	27.5	1.2
Trial 1[b]	100	99.9	99.9	99.9	0
Trial 2[b]	31.6	29.5	28.9	30.0	1.4

[a] Separation conditions: 100 ppm PSL 304 nm solution, buffer pH=9.0, pressure: 13.8 kPa, temperature: 25°C±1°C@ 450 rpm.

b Trial 1 and 2 are Designed experiments (see 6th and 7th row in Table 2 in Chapter 6).

Appendix E

Table E-2 Pure buffer flux and separation performance of DK and PEG-ester membranes[a]

Membrane	Pure buffer flux (kg m^{-2} s^{-1})				
	Sample 1	Sample 2	Sample 3	Average	STD
DK	1.13	1.09	1.10	1.11	0.02
PEG-ester	1.18	1.16	1.14	1.16	0.02
	Solution flux (kg m^{-2} s^{-1})				
DK	0.46	0.41	0.38	0.42	0.04
PEG-ester	0.71	0.70	0.64	0.68	0.04
	Separation of PSL 304 (%)				
DK	99.9	99.0	98.6	99.2	0.7
PEG-ester	71.3	68.4	63.6	67.8	3.9

[a] Separation conditions: 100 ppm PSL 304 nm solution, buffer pH=9.0, pressure: 13.8 kPa, temperature: 25°C±1°C@ 450 rpm.

IMAGE EVALUATION
TEST TARGET (QA-3)

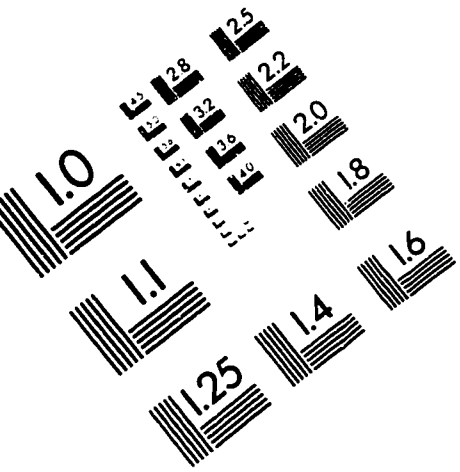

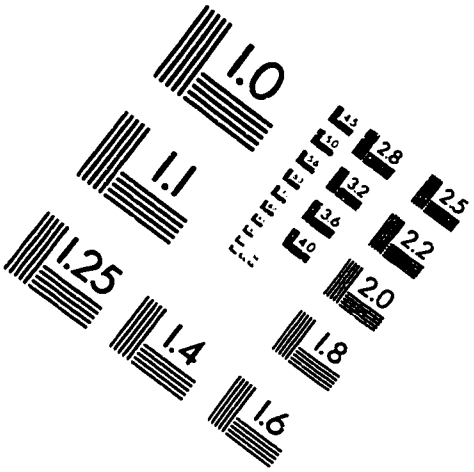

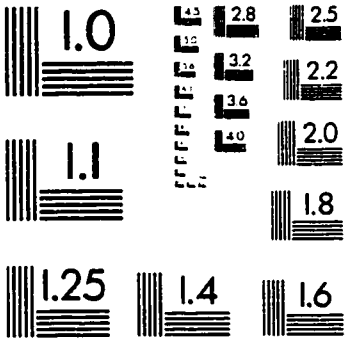

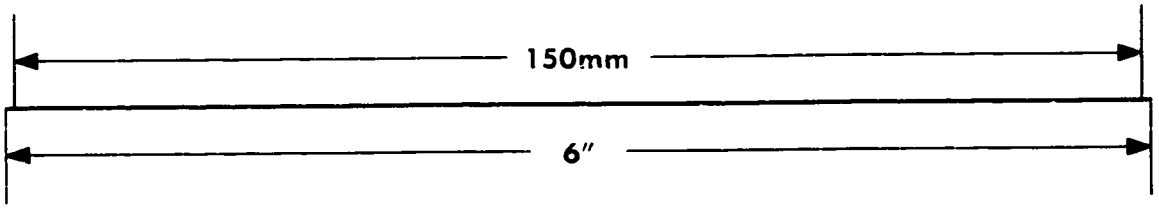

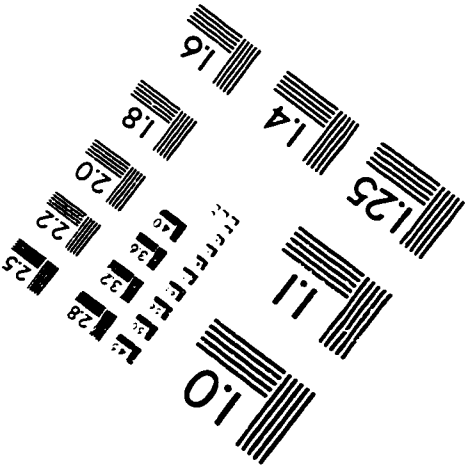

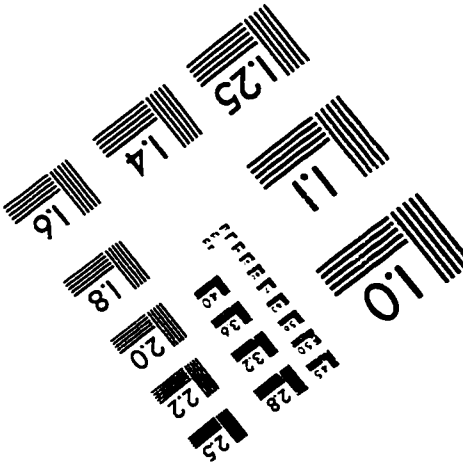

APPLIED IMAGE, Inc
1653 East Main Street
Rochester, NY 14609 USA
Phone: 716/482-0300
Fax: 716/288-5989